Conducting an Integrated Experimental Modeling Program

Steve Zinkle
Materials Science & Technology Div.

ATR National Scientific User Facility
Users Week
Idaho Falls, Idaho
June 1-5, 2009

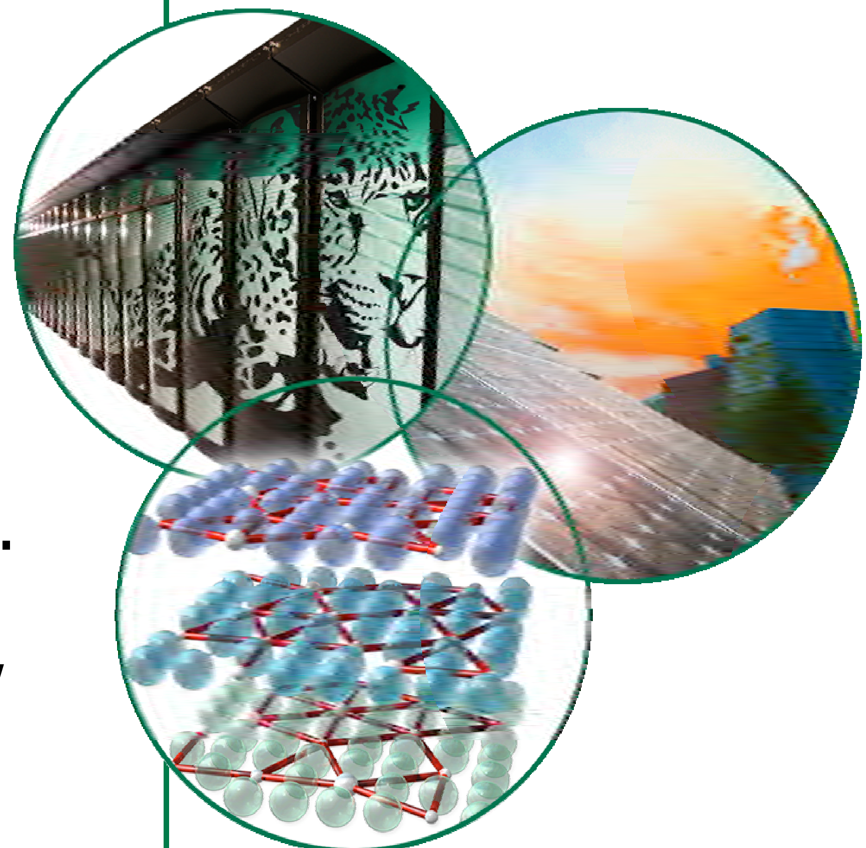

U.S. DEPARTMENT OF ENERGY

OAK RIDGE NATIONAL LABORATORY
MANAGED BY UT-BATTELLE FOR THE DEPARTMENT OF ENERGY

Outline

- Examples of structural materials design data
- Overview of key temperature regimes for radiation damage
  - Amorphization, point defect swelling, void swelling
  - (corresponds to immobile SIAs, immobile vacancies, and fully mobile defects, respectively)
- Radiation hardening fundamentals
- Design strategy for radiation resistance

Development of structural materials for applications involving public safety is historically a long process

- **"When you hear something about a new material, write it down because it will be the best thing you'll ever hear about it"** (Jim Williams, paraphrasing Bob Sprague of General Electric)
- **Aerospace structural materials**
  - Over 50 years to develop TiAl intermetallics from initial studies in 1950s
  - Design cycle times have been reduced to 3-5 years, but development and qualification of new materials still requires >7 years
    - Qualification time dominated by creep and fatigue testing
- **Structural materials for nuclear reactors**
  - Qualification requires all of the mechanical property testing on unirradiated material, plus neutron irradiation and testing of irradiated material
    - Sequential approach would lead to unacceptably long qualification times

History of improvement in temperature capability of Ni-base superalloys

- **Historical rate of improvement is ~5°C/year**

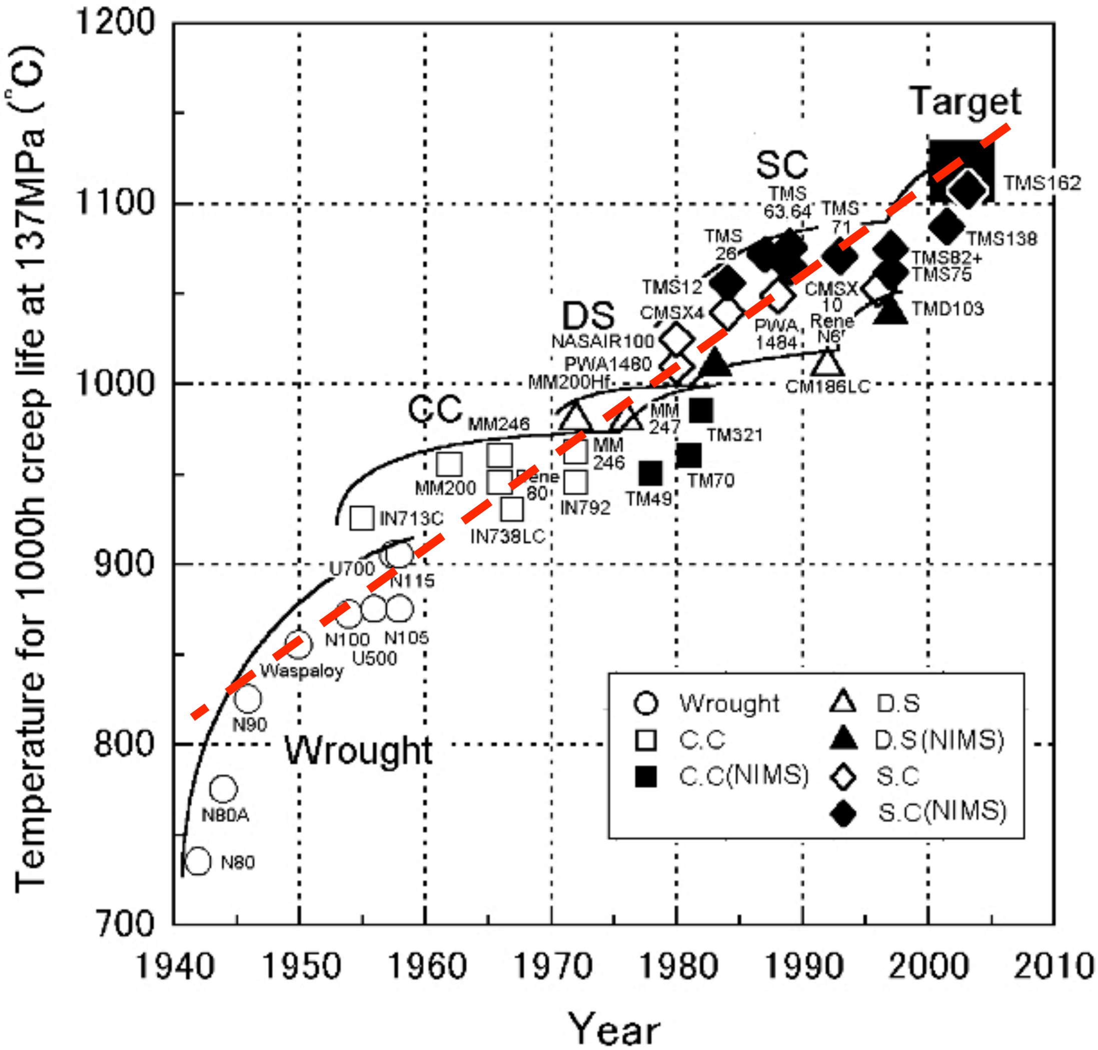

Y. Koizumi et al., Proc. Int. Gas Turbines Conf., 2003, paper TS-119

Qualification of new structural materials involves two considerations based on safety and financial protection

- **Cognizant licensing authority**
  - Considers public safety aspects
  - Generally requires the structural material to be evaluated by an appropriate independent engineering society (e.g., ASME, ASTM, etc.)
- **Capital investment organization (federal government, utility, etc.)**
  - Considers potential risk to their investment if a structural material fails
  - Generally requires the structural material to qualified using well-established engineering procedures (e.g., ASME, RRC-MR, JSME, etc.)

Determination of design curves

- **Tensile strength**
  - If large number of test data are available, then design curve can be set at a value equal to two standard deviations below the mean value (represents 97.5% confidence limit)
  - Alternatively, the design curve can be set at the minimum strength values in the data base
- **Fatigue data**
  - Strain range vs. fatigue cycle design curve is determined by the minimum of either $\varepsilon_t/2$ or $N_f/20$

Mean tensile strengths for Type 316 stainless steel

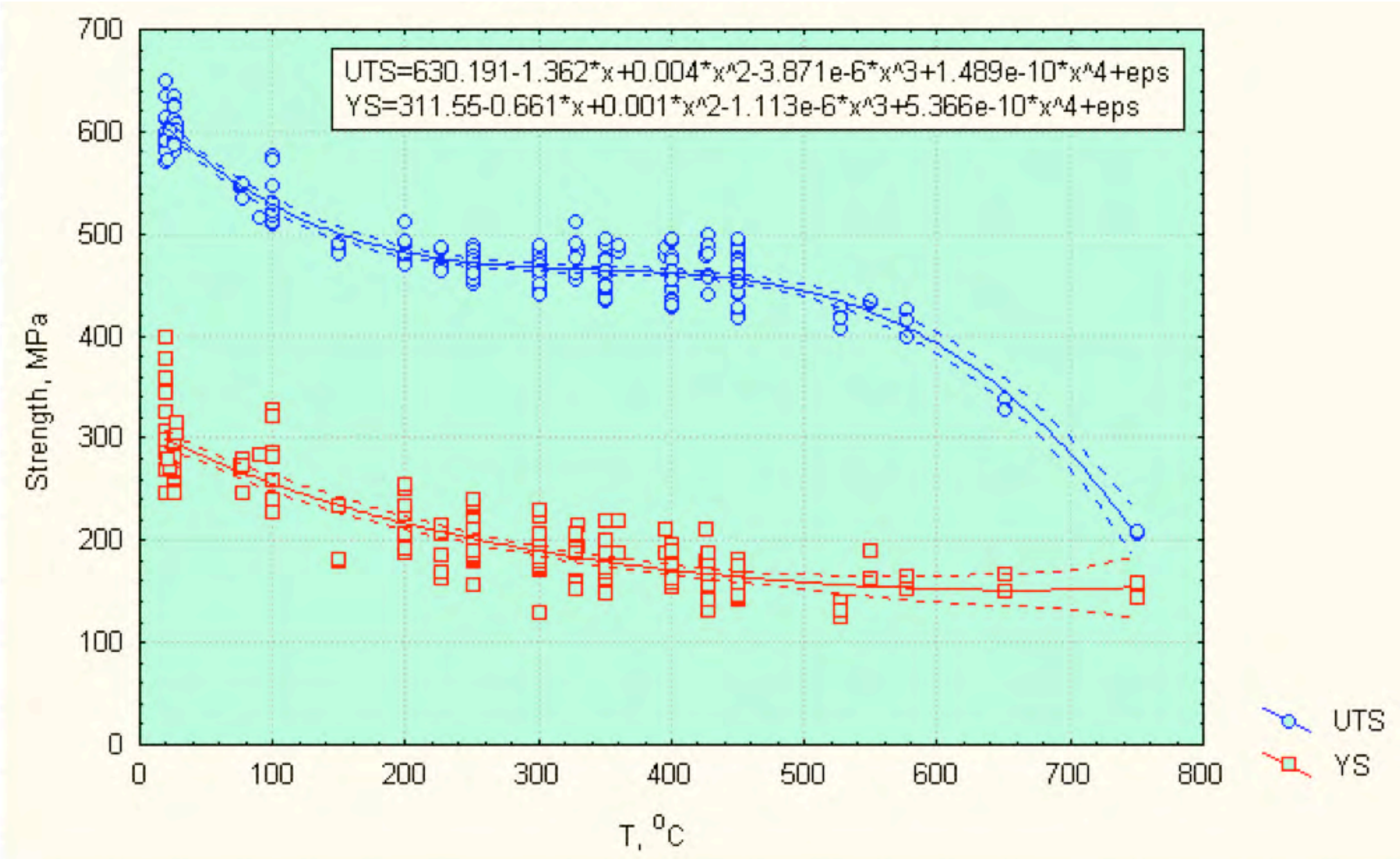

G.M. Kalinin

Design tensile strengths for Type 316 stainless steel

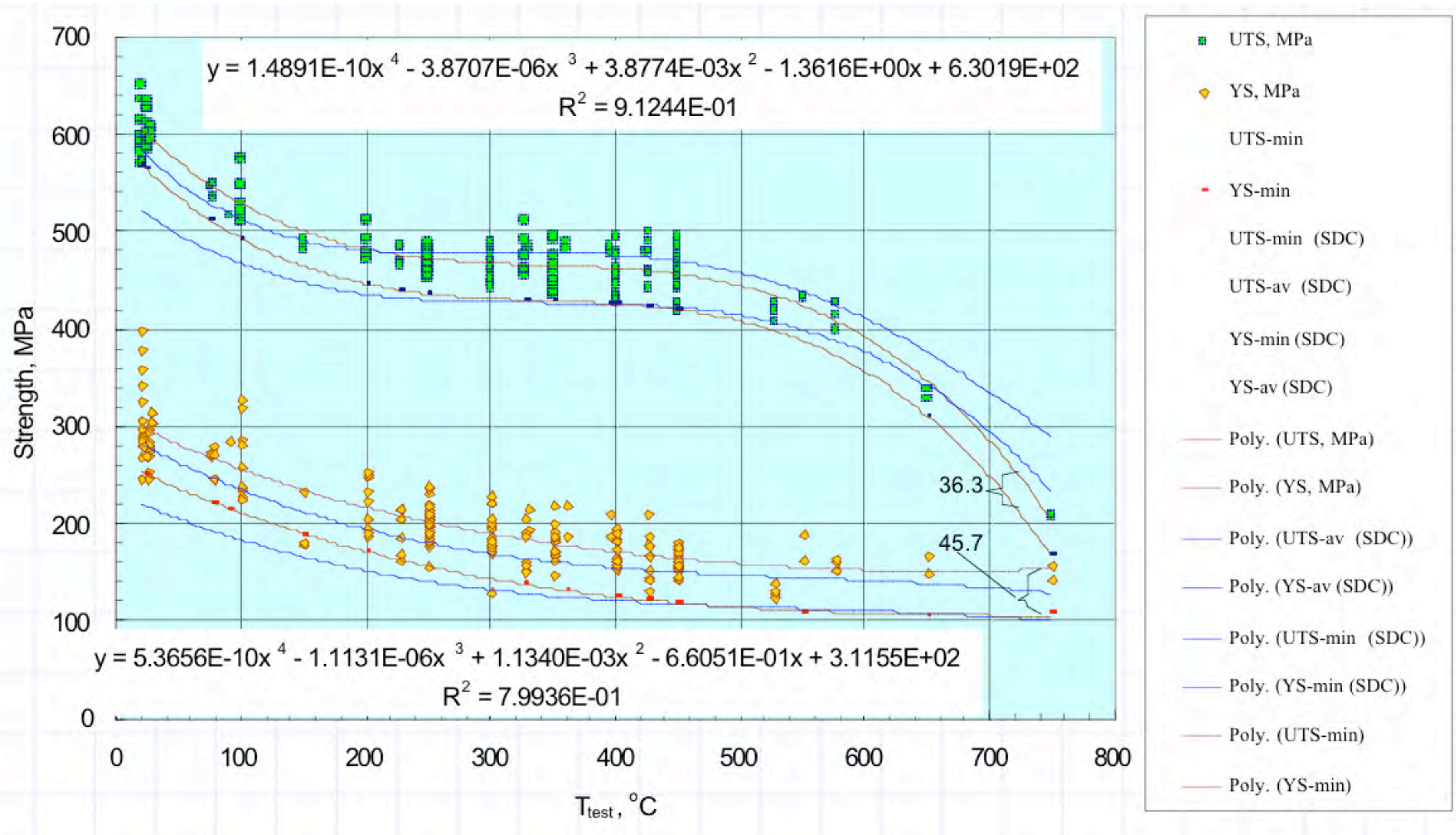

G.M. Kalinin

Design tensile strengths for Type 316 stainless steel

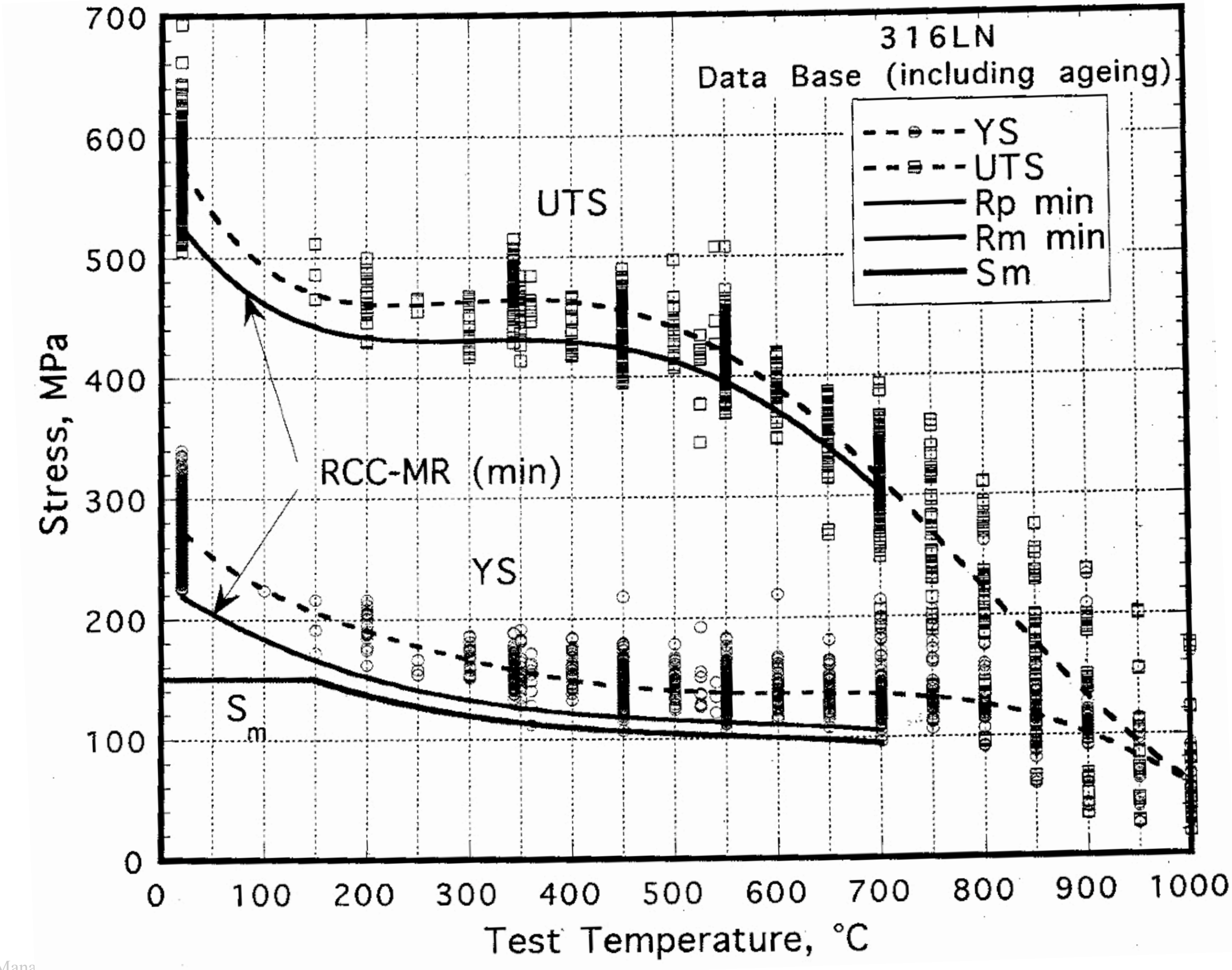

A.A.F. Tavassoli

Summary of design and mean fitted fatigue curve

- **Unirradiated Cu**

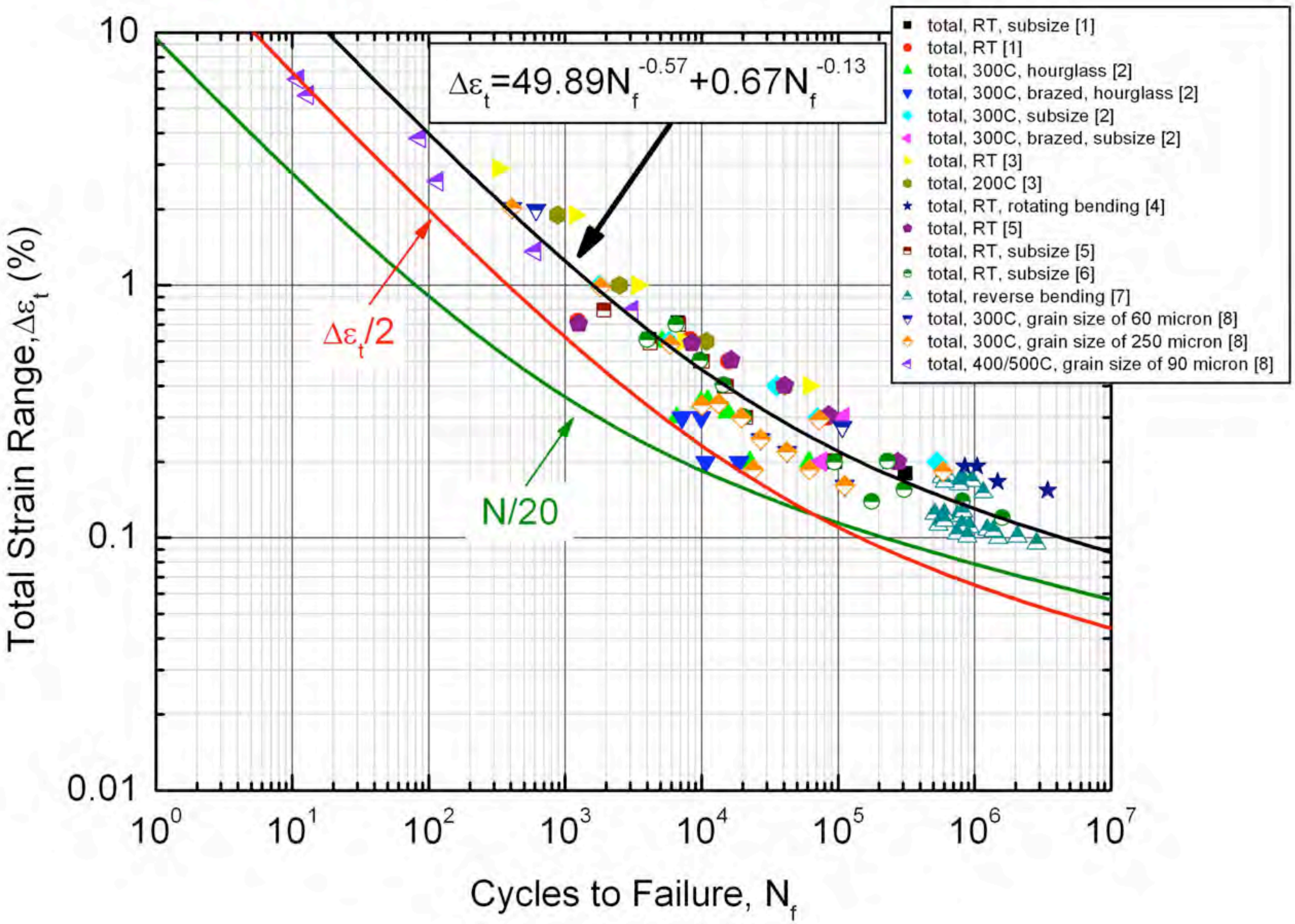

Large variability in thermal creep behavior for three heats of nominally identical Nb-1Zr

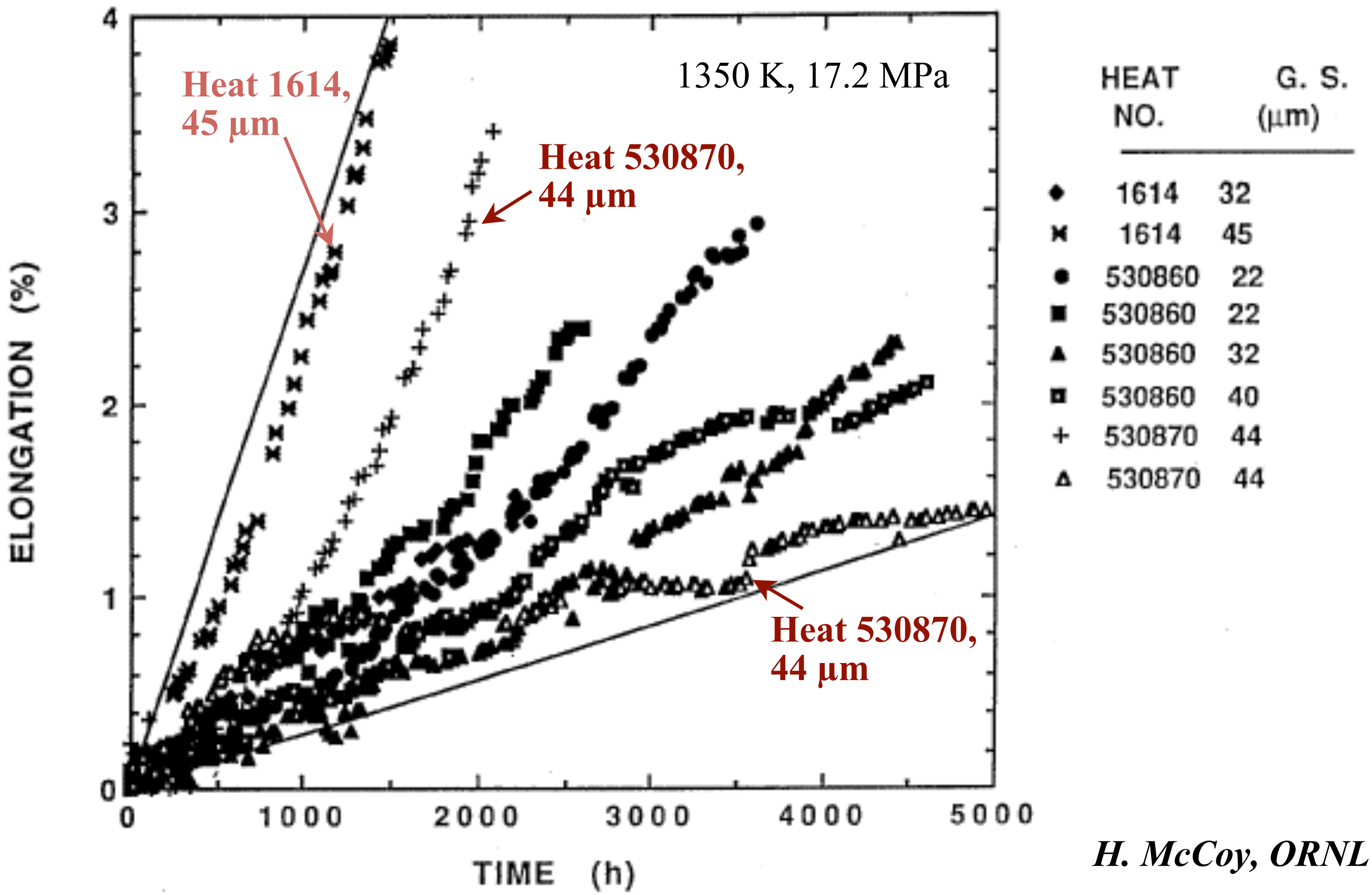

H. McCoy, ORNL

- *In addition to grain size, these results show that **other microstructural inhomogeneities** can also affect the thermal creep behavior of Nb-1Zr*

Development of Texture in Annealed Nb-1Zr

- **Texture pattern in recrystallized Nb-1Zr is strongly dependent on annealing conditions**

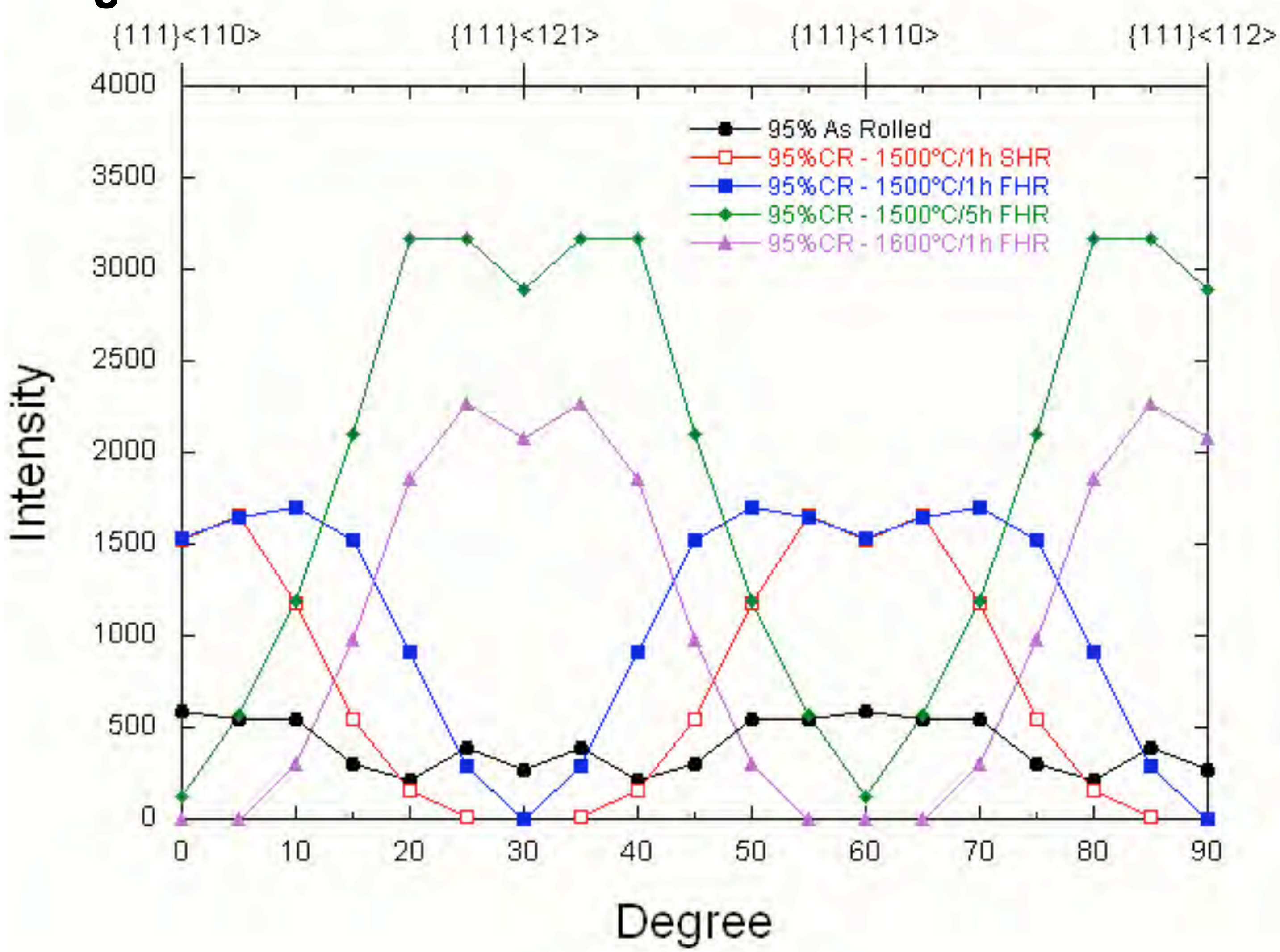

FHR: fast heating rate (>1000˚C/min)
SFR: slow heating rate (10˚C/min)

Overview of Radiation Damage Recovery Stages

- **Originally based on electrical resistivity measurements**
  - **Stage I: self-interstitial atom migration (correlated and uncorrelated)**
  - **Stage II: long-range migration of SIA clusters and SIA-impurity complexes**
  - **Stage III: longstanding controversy; near universal agreement that it is associated with vacancy migration**
  - **Stage IV: migration of vacancy clusters and vacancy-solute complexes**
  - **Stage V: thermal dissociation of (displacement cascade-produced) vacancy clusters**
- **Note: recovery stage temperatures are not unique; they depend on annealing time (e.g., displacement damage rate)**

Al_2O_3 Swelling

- 3 distinct swelling regimes are observed in irradiated Al_2O_3

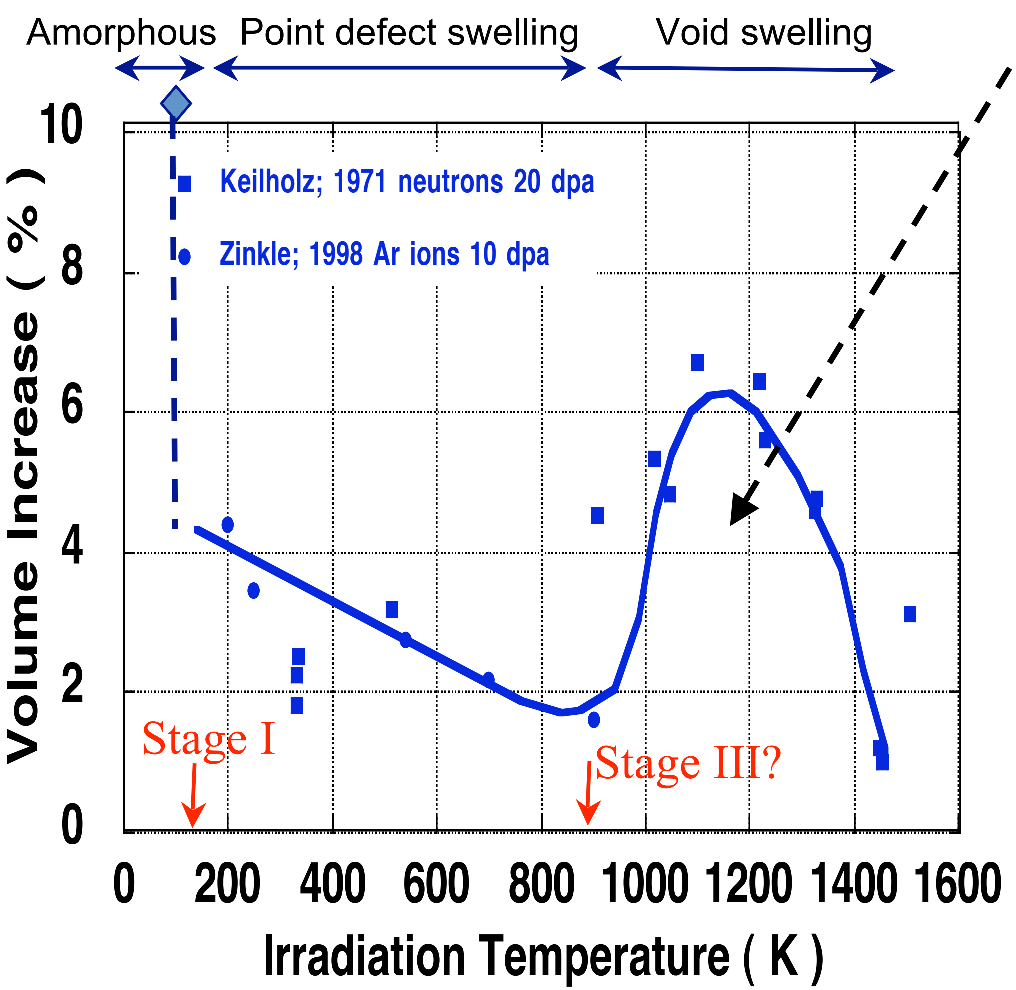

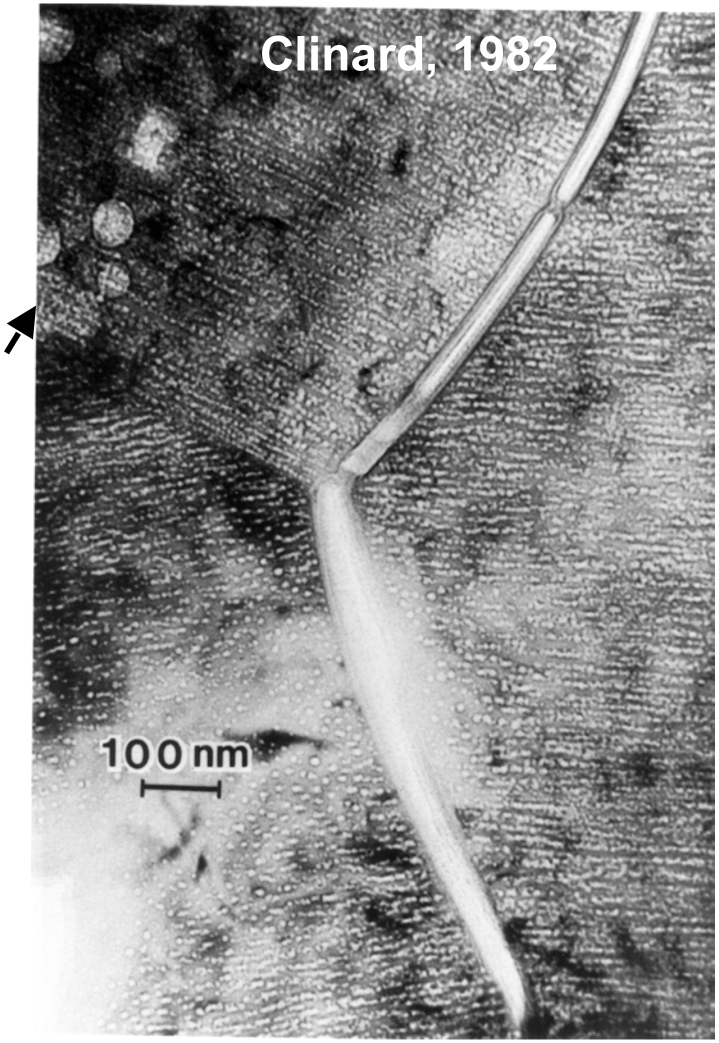

- Activation Energies:
  - Al vacancy; 1.8-2.1 eV
  - O vacancy; 1.8-2 eV
  - Al, O interstitial; 0.2-0.8 eV

Irradiation-induced swelling in SiC

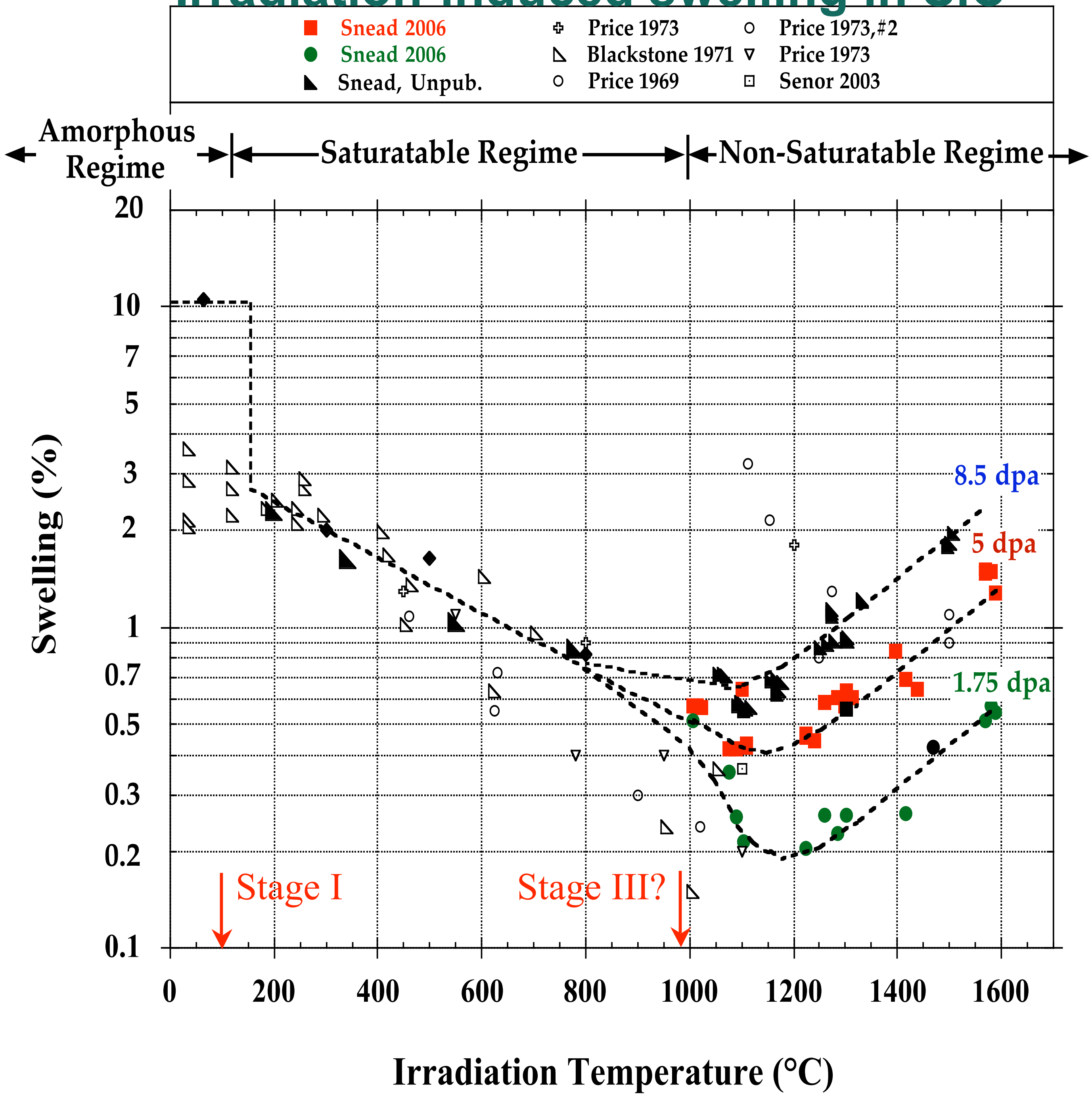

SiC Amorphization

3 recovery substages are observed below 320 K

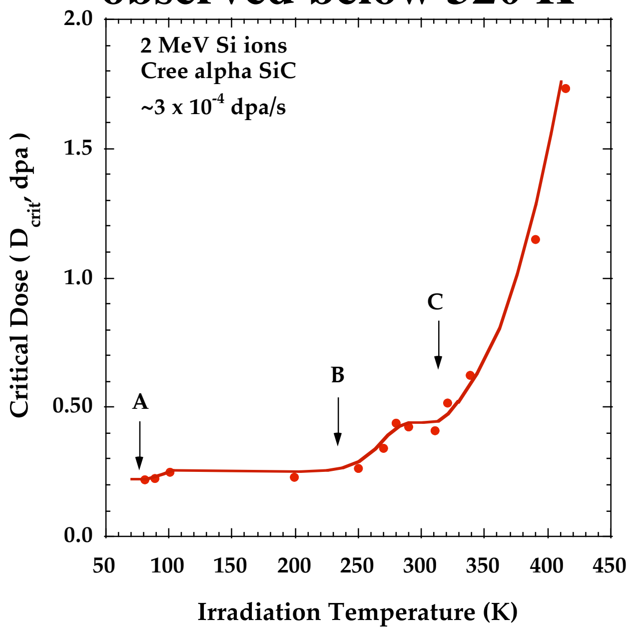

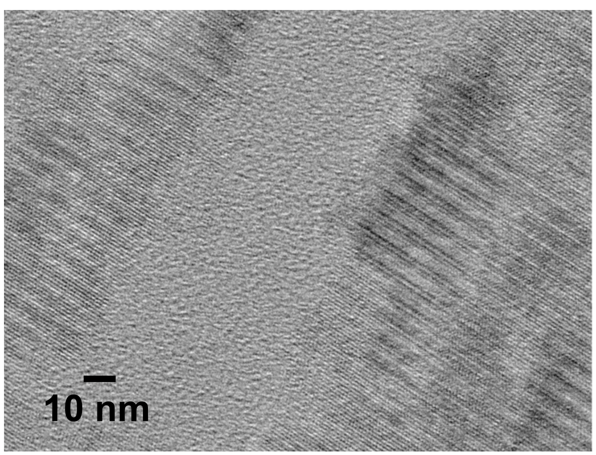

Analysis of flux dependence shows recovery substages are not associated with long range point defect migration (F<0.5 up to 380 K)

D_{crit}-D_o (DPA) = $(A\Phi^F)e^{(-Em/2kT)}$

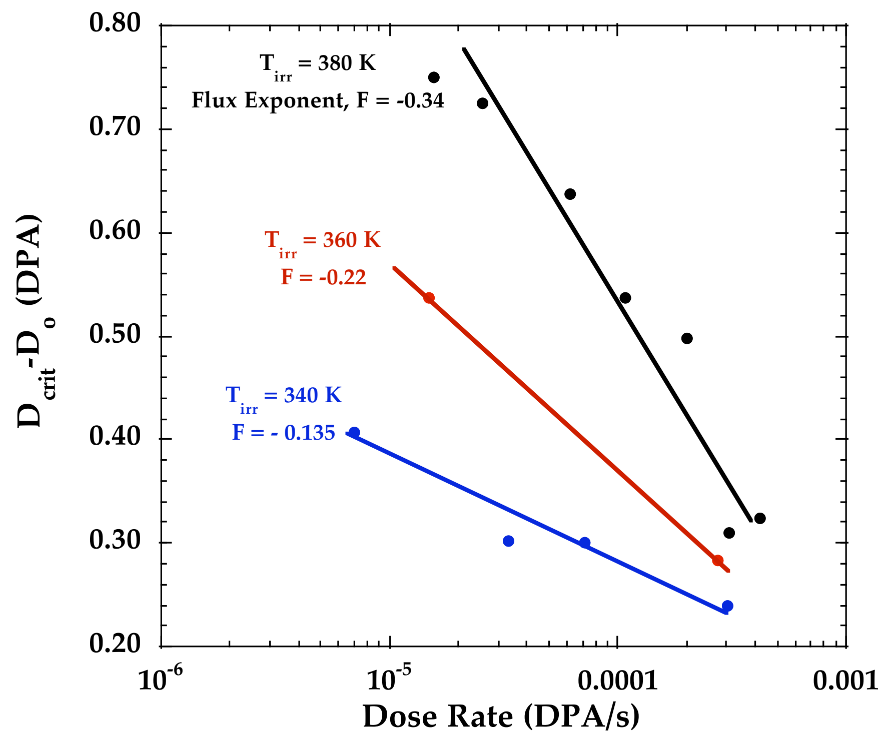

Implies that both vacancies and interstitials are immobile in SiC up to 100˚C (interstitials are mobile in many other ceramics at room temperature)

Comparison of Stage I recovery behavior in Cu after electron and neutron irradiation

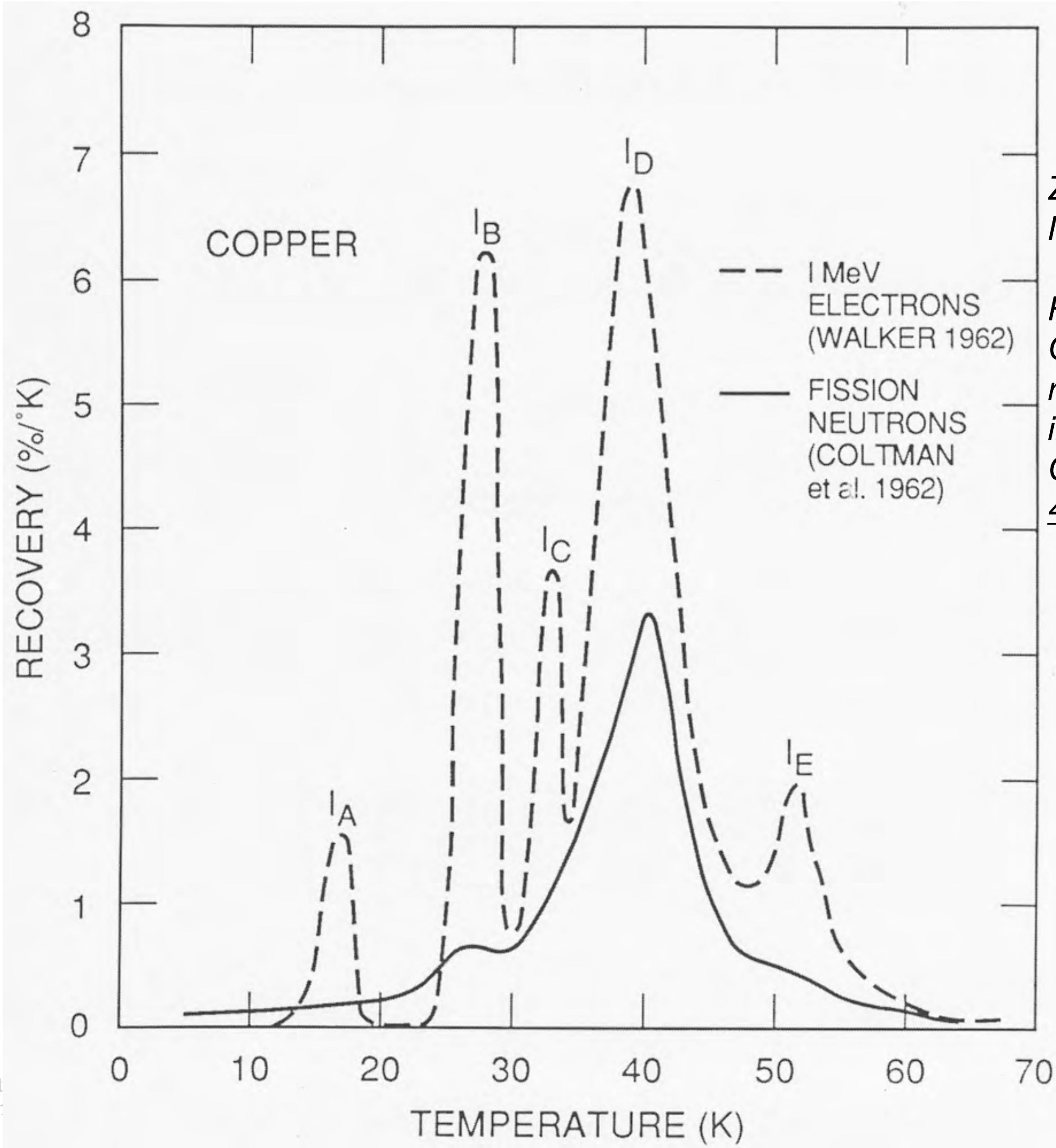

Zinkle and Singh,J. Nucl. Mater. 199 (1993) 173

Recent kinetic Monte Carlo validation of recovery stages in irradiated Fe: C.C. Fu et al., Nature Mat. 4 (2005) 68

Defect Production in Irradiated Materials

- Transition from linear to square root defect accumulation behavior is a characteristic feature of any pure material irradiated at temperatures where point defects are mobile
  - Location of transition is dependent on purity and recombination X-section

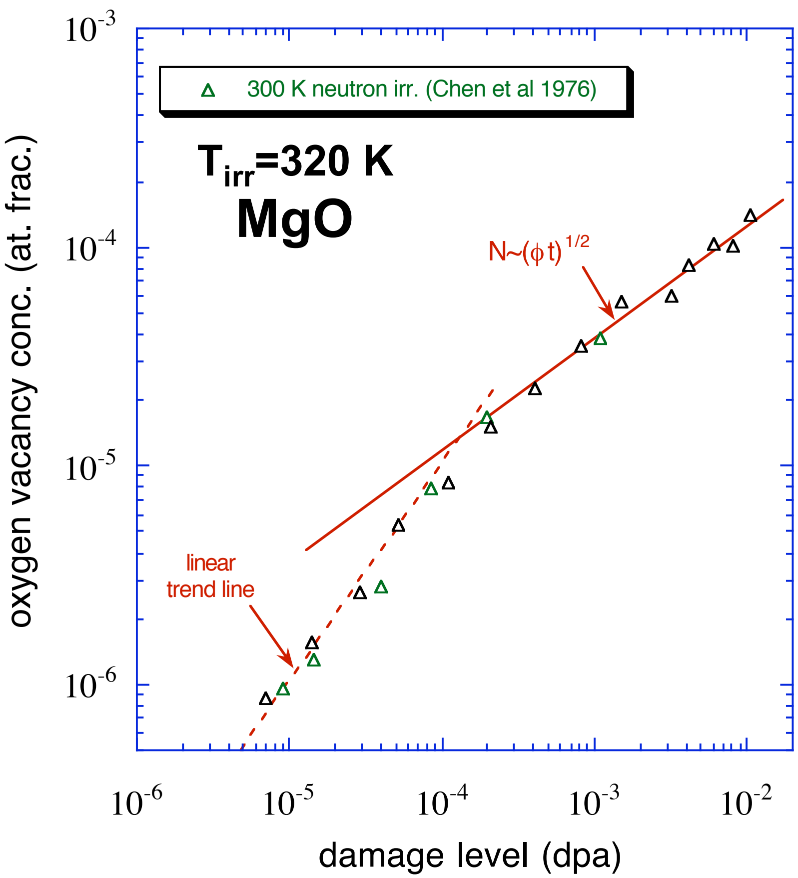

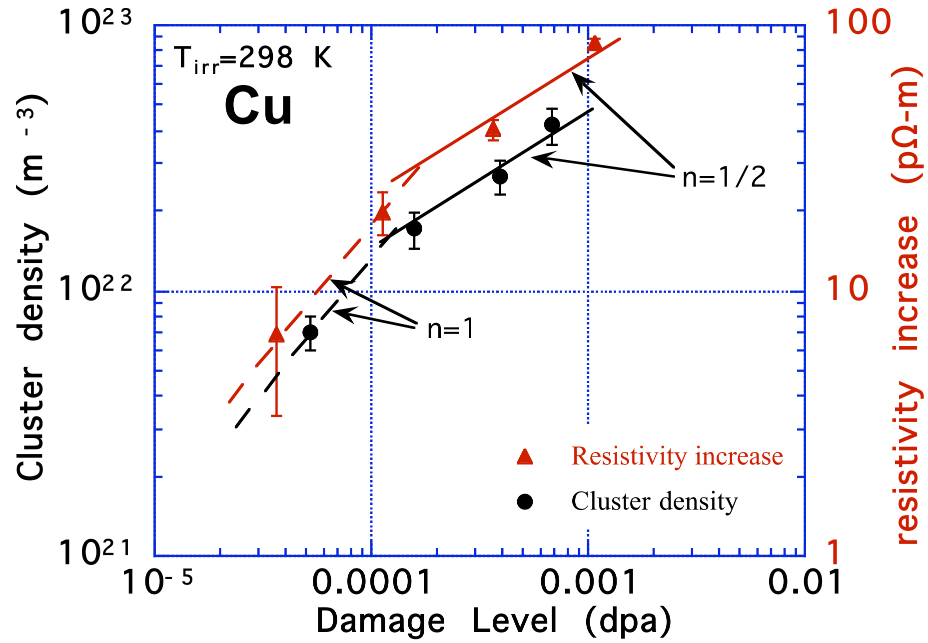

•Data analysis indicates freely migrating interstitial fraction is f_i~11% dpa$_{NRT}$ (good agreement with MD)

Zinkle, JNM 150 (1987) 140

Square root fluence dependence of defect accumulation is an indication of uncorrelated point defect recombination

- **Ionizing radiation may induce athermal point defect recombination in some ceramics (!)**

Sublinear F center accumulation in neutron irradiated MgO (Chen et al 1975)

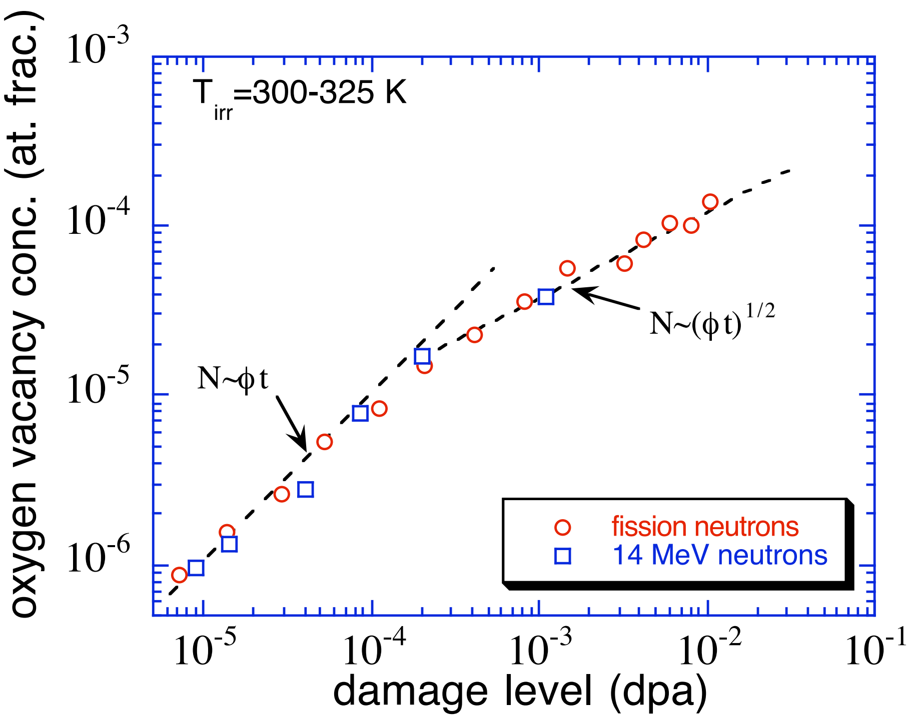

Sublinear F center accumulation in electron irradiated MgO (Scholz & Ehrhart 1993)

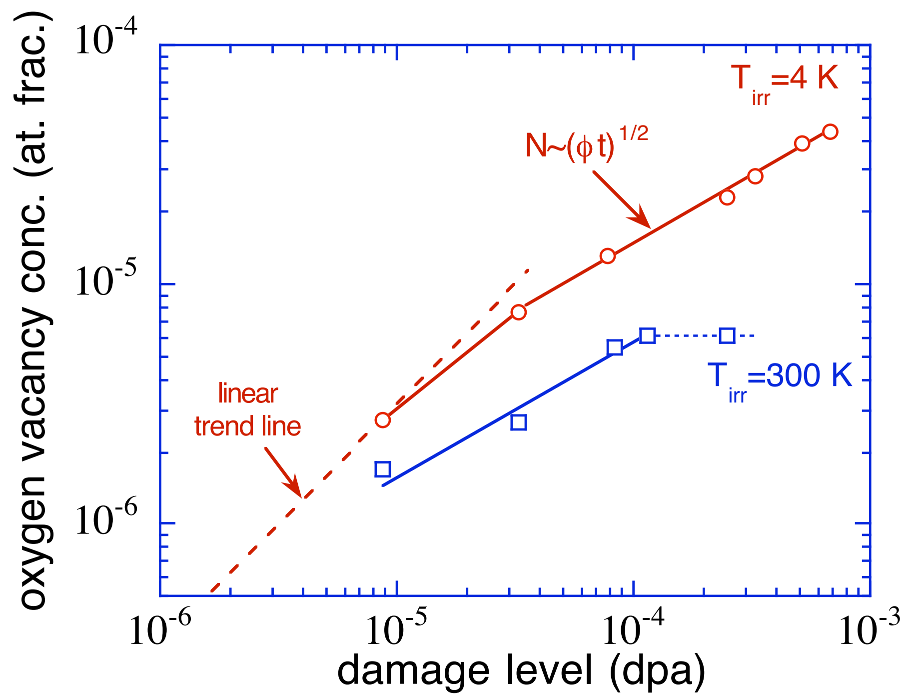

Radiation Hardening in Copper: Seeger vs. Friedel relationships

- **Two general models are available to describe radiation hardening ($\Delta\sigma$) in metals:**
  - **Dispersed barrier model (Seeger, 1958)--valid for strong obstacles**

$$\Delta\sigma = M\alpha\mu b\sqrt{Nd}$$

Where M=Taylor factor

α=defect cluster barrier strength

μ=shear modulus

b=Burgers vector of glide dislocation

N, d=defect cluster density, diameter

  - **Friedel 1963 (also Kroupa and Hirsch 1964) weak barrier model:**

$$\Delta\sigma = \frac{1}{8} M\mu b d N^{2/3}$$

$$\Delta\sigma = M\alpha\mu b\sqrt{Nd}$$

vs.

$$\Delta\sigma = \frac{1}{8}M\mu bdN^{2/3}$$

Shear Strength of Cu Single Crystals Irradiated and Tested Near Room Temperature

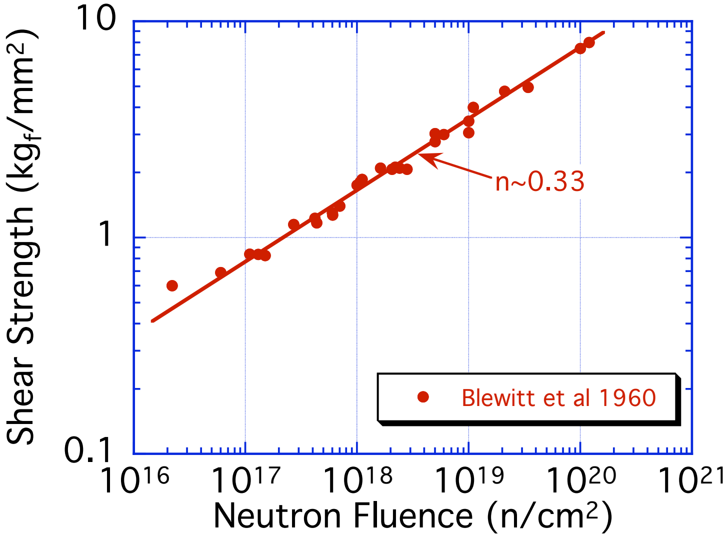

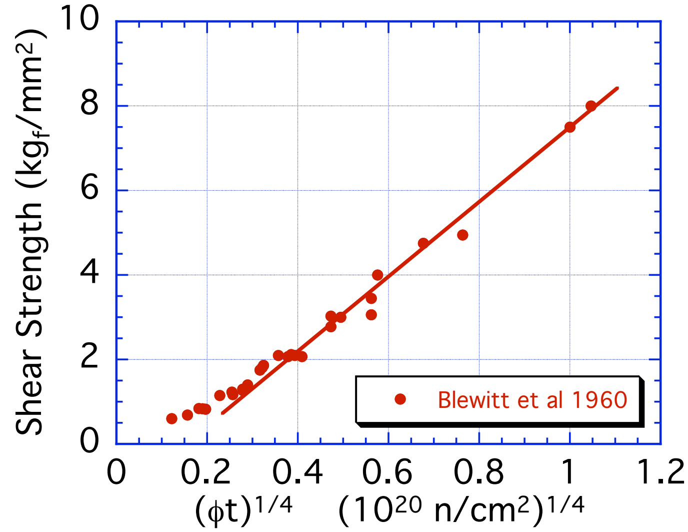

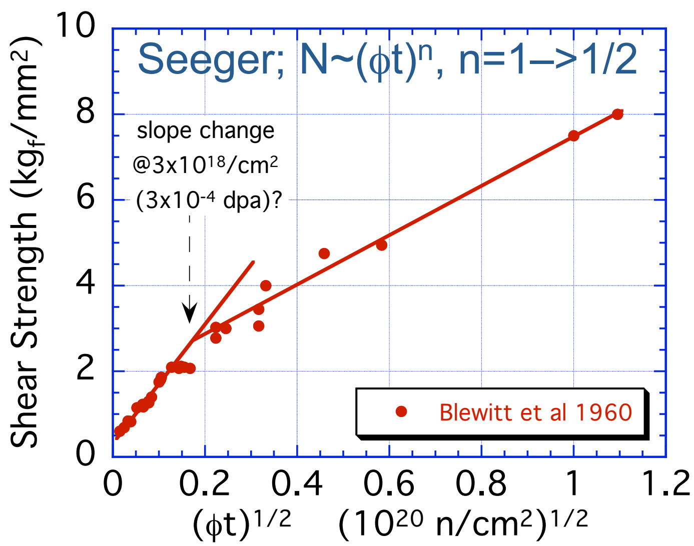

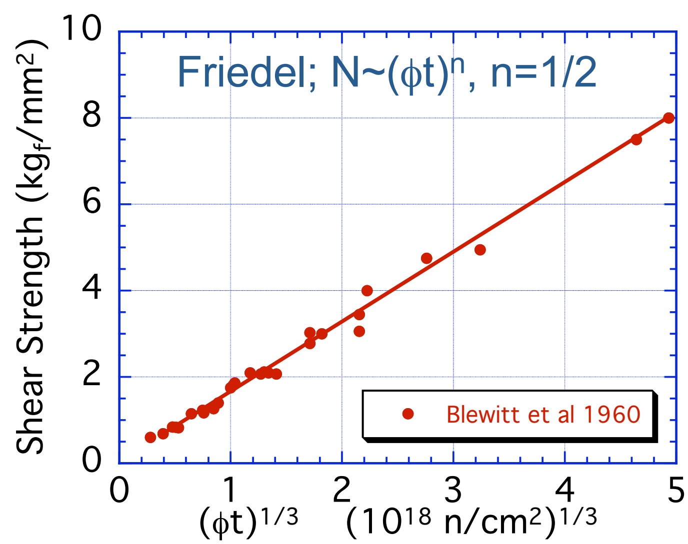

Effect of test temperature on irradiated strength

What is the effect of irradiation on the yield strength test temperature dependence (athermal and thermal components)?

BCC metals: large $\tau_{thermal}$ component

FCC metals: small $\tau_{thermal}$ component

Hardening models (Seeger, Fleisher, etc.): Thermal component of flow stress is controlled by radiation-induced hardening centers

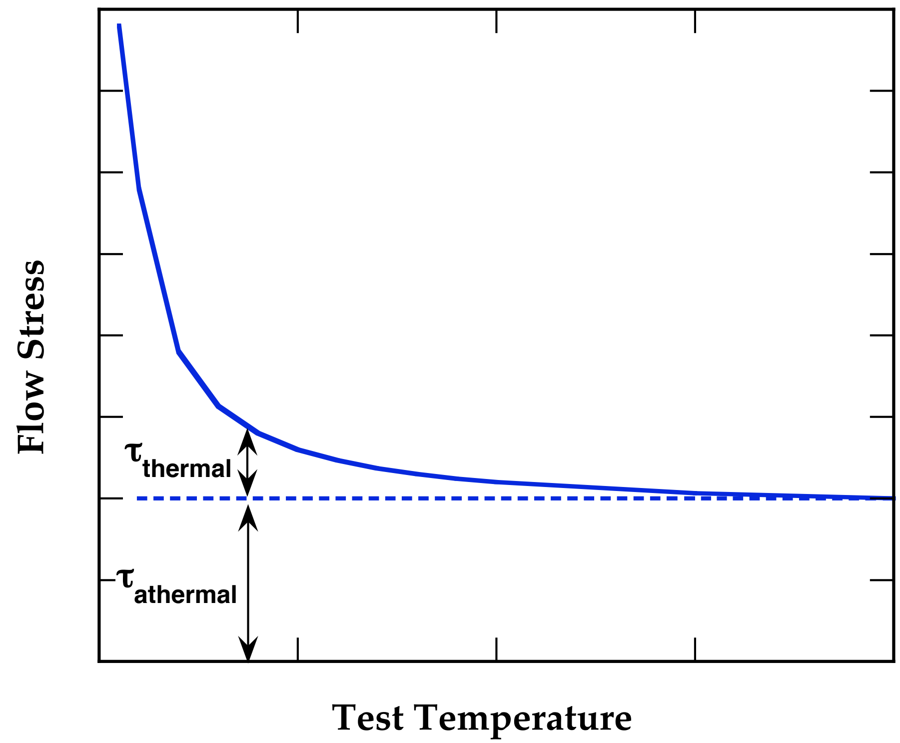

Comparison of the Yield Strength Behavior of Annealed and Irradiated Iron at Higher Doses

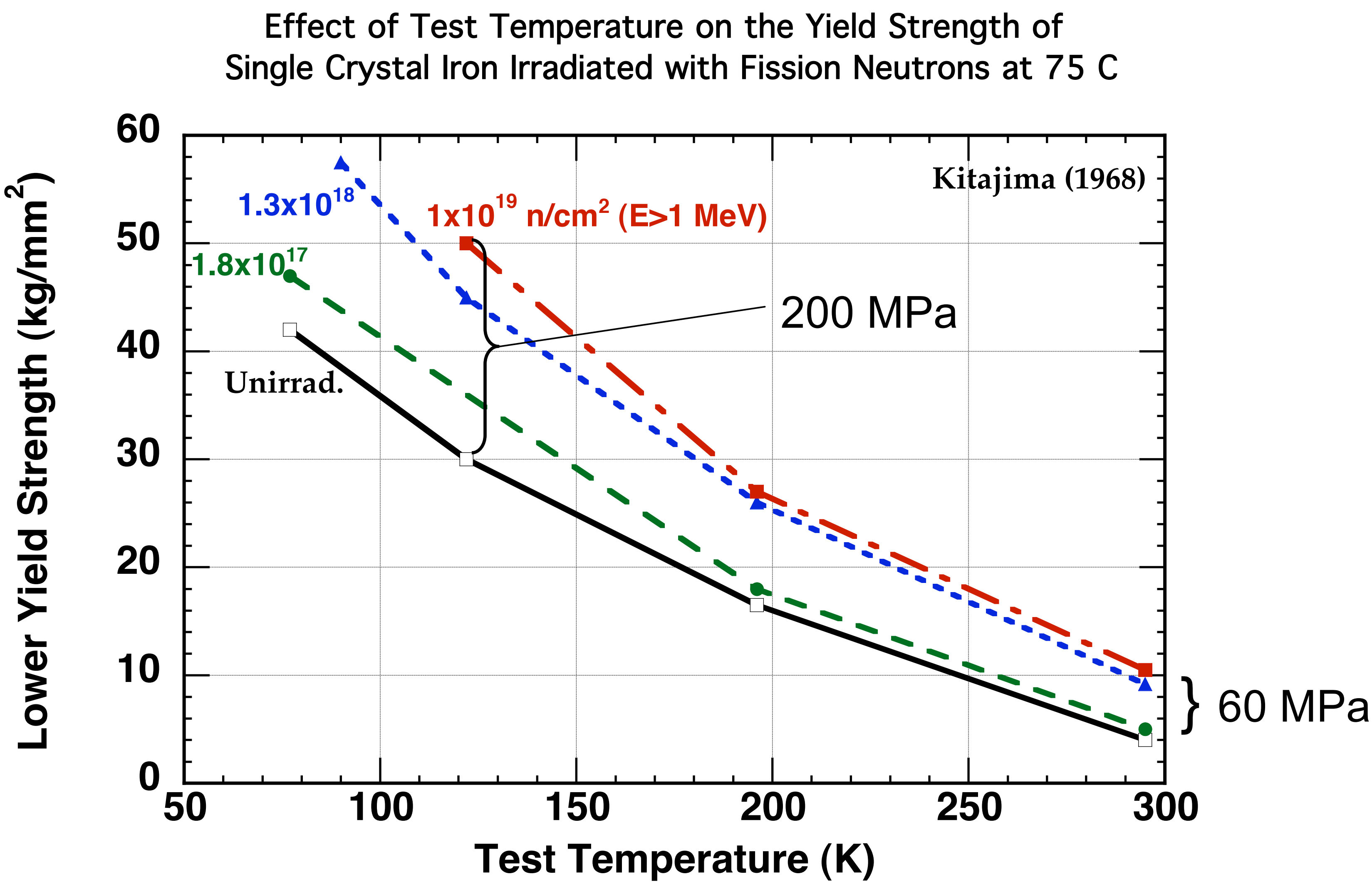

Molecular Dynamics Simulations of the Effect of Temperature on Obstacle Strength

Understanding dislocation-obstacle interaction mechanisms is central to learning how to engineer materials with better low-temperature ductility and fracture toughness.

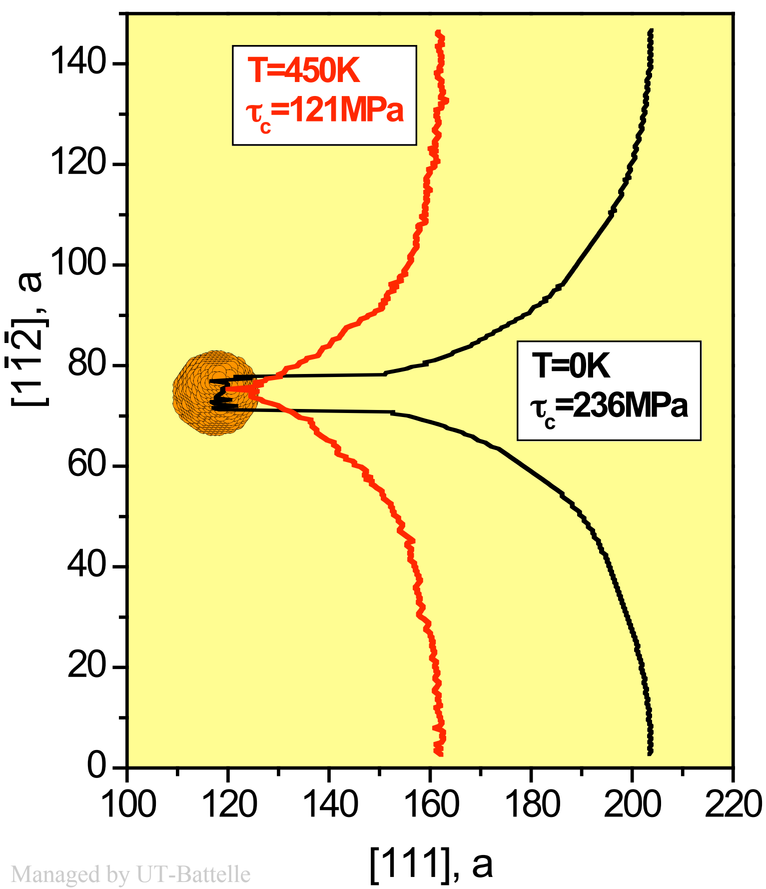

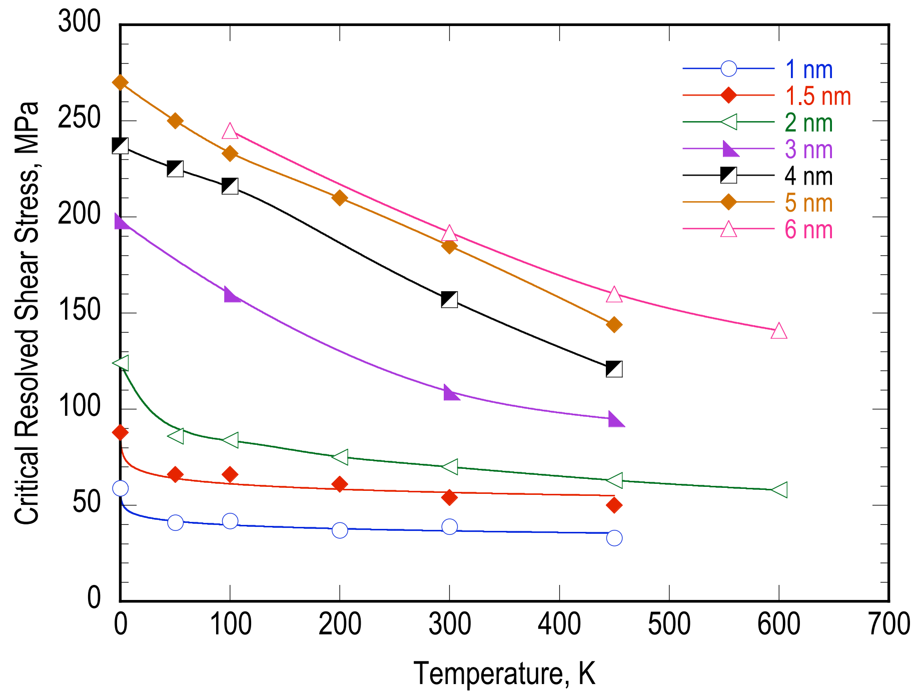

Y.N. Osetsky

Advanced nuclear energy systems impose harsh radiation damage conditions on structural materials

- 1 displacement per atom (dpa) corresponds to stable displacement from their lattice site of <u>all</u> atoms in the material during irradiation near absolute zero (no thermally-activated point defect diffusion)
  - Initial number of atoms knocked off their lattice site during fast reactor neutron irradiation is ~100 times the dpa value
    - Most of these originally displaced atoms hop onto another lattice site during "thermal spike" phase of the displacement cascade (~1 ps)

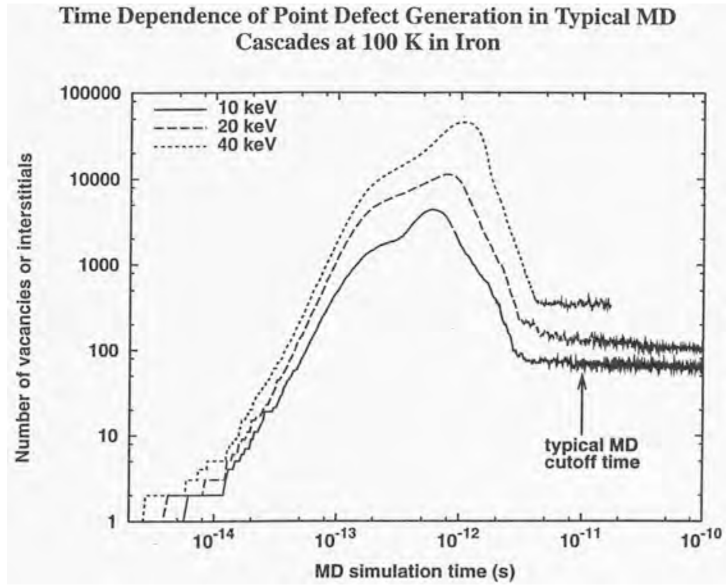

R.E. Stoller

- Requirement for structural materials in advanced nuclear energy systems (~100 dpa exposure):
  - ~99.95% of "stable" displacement damage must recombine
    - ~99.9995% of initially dislodged atoms must recombine
- Two general strategies for radiation resistance can be envisioned:
  - Noncrystalline materials
  - Materials with a high density of nanoscale recombination centers

after S.J. Zinkle, Phys. Plasmas <u>12</u> (2005) 058101

Recent Molecular Dynamics simulations have provided key fundamental information on defect production

- Effect of knock-on atom energy and crystal structure on defect production
- subcascade formation leads to asymptotic surviving defect fraction at high energies

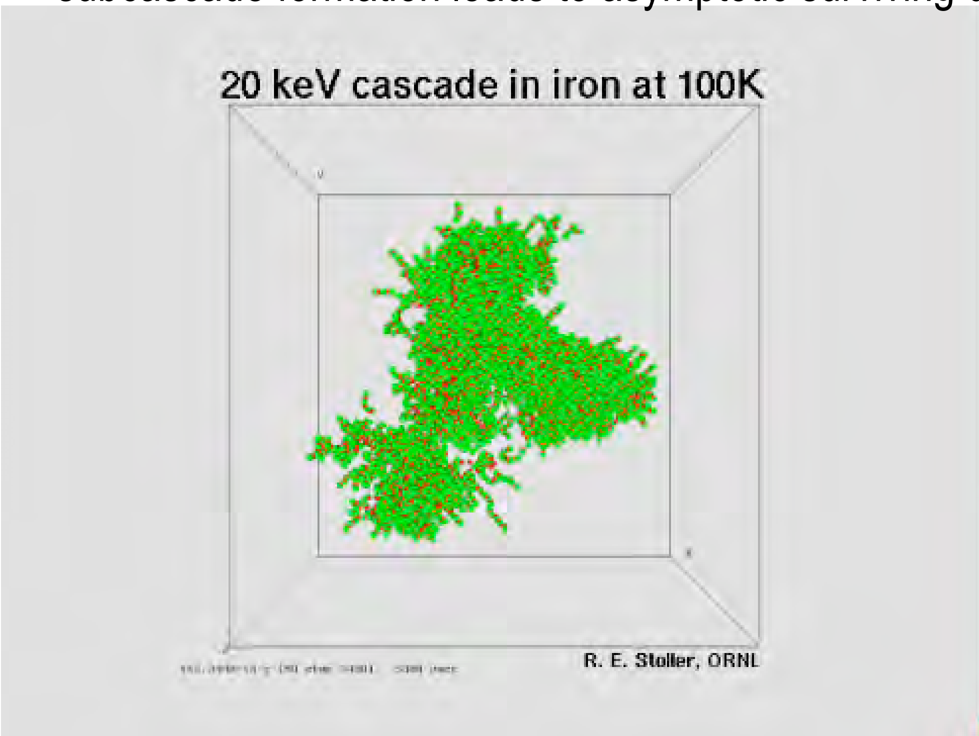

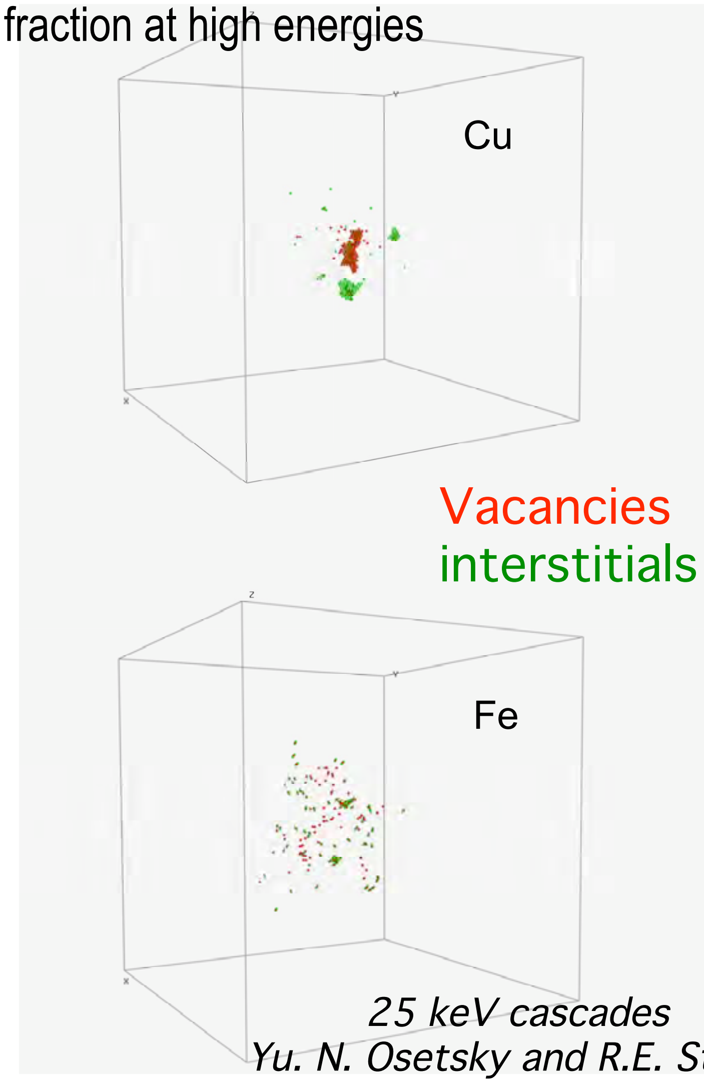

25 keV cascades
Yu. N. Osetsky and R.E. Stoller

Large vacancy clusters are not directly formed in BCC metal displacement cascades

after S.J. Zinkle, Phys. Plasmas 12 (2005) 058101

Correlated in-cascade recombination reduces surviving defect fraction due to freely migrating interstitials

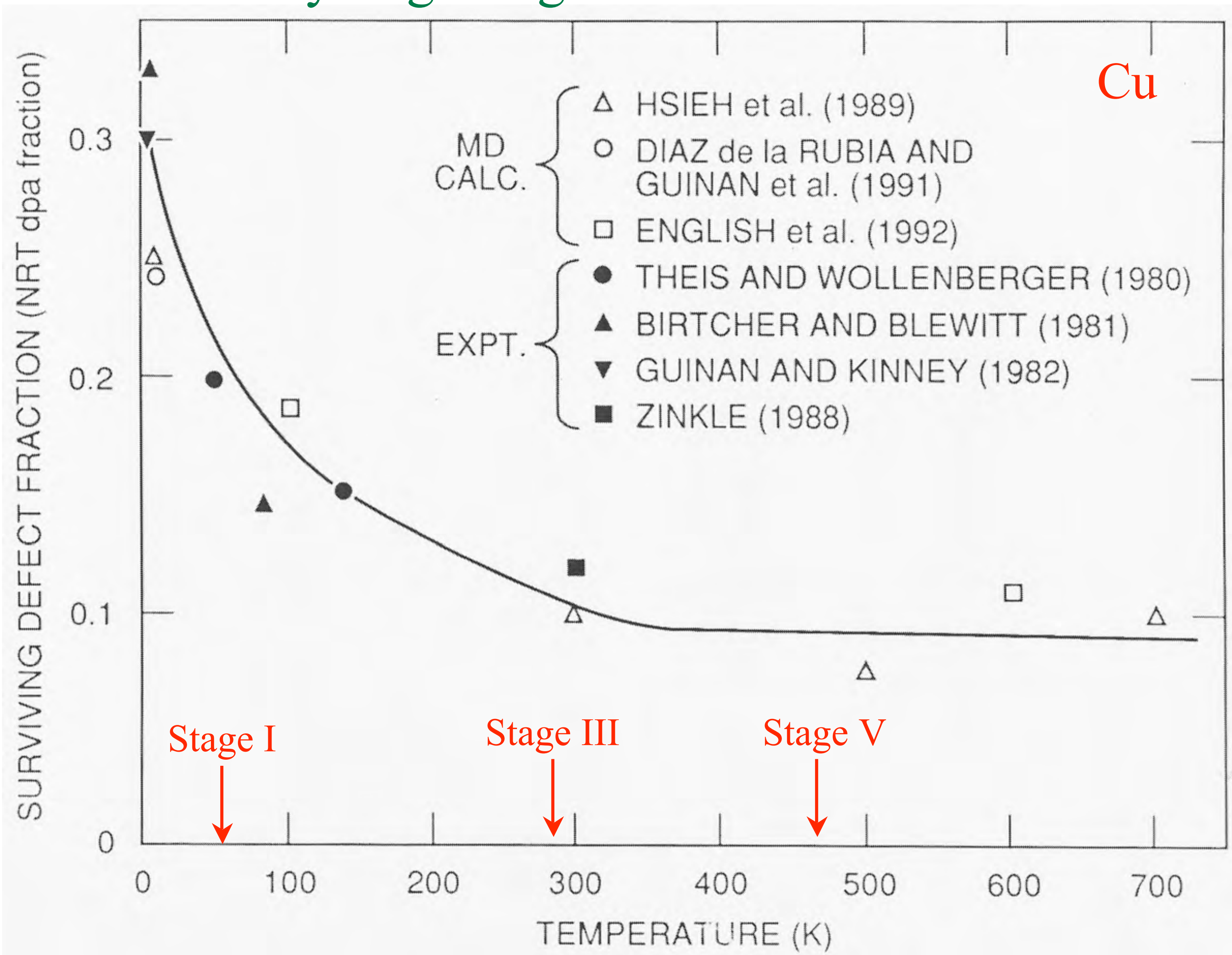

Zinkle and Singh, J. Nucl. Mater. 199 (1993) 173

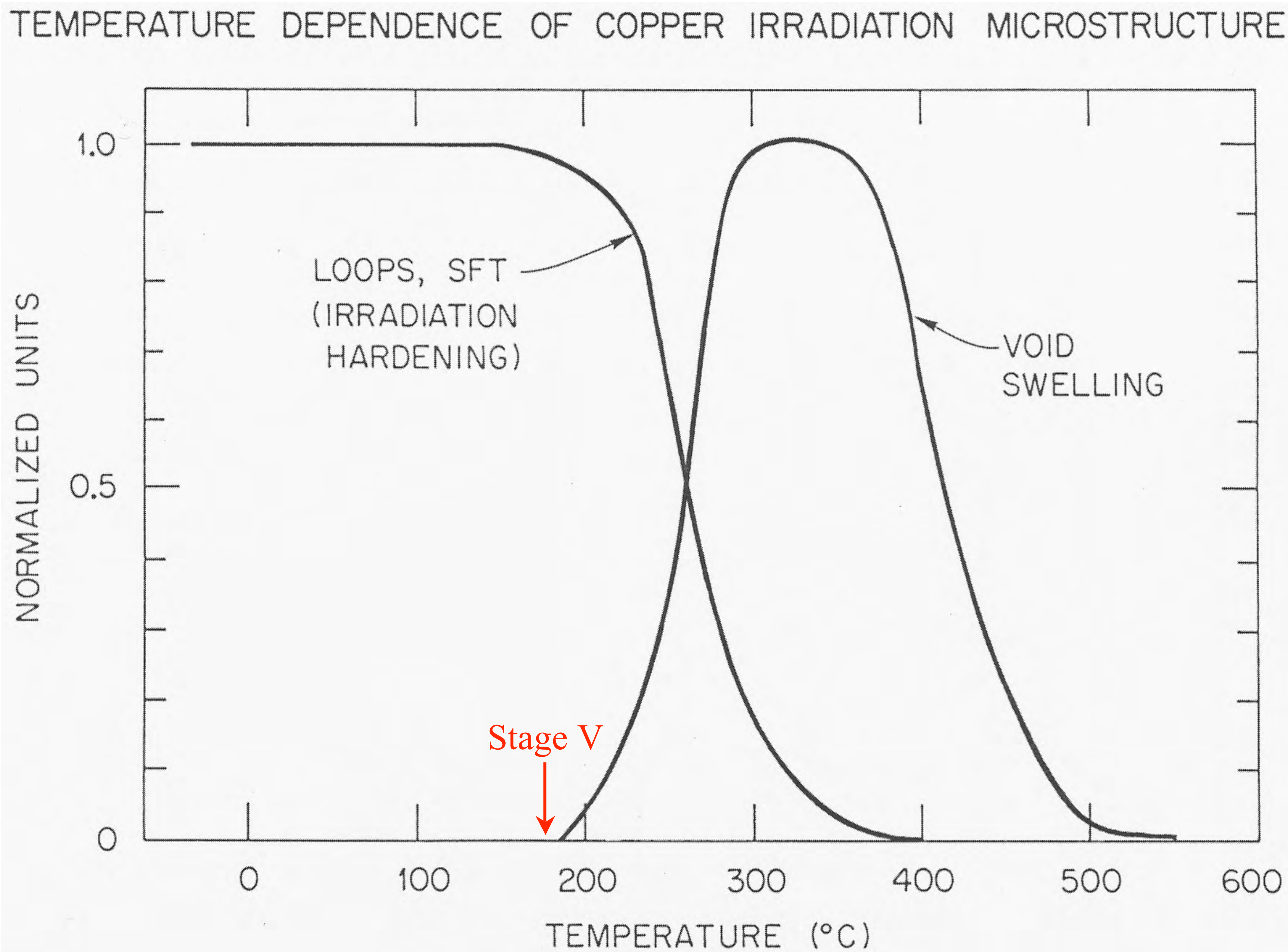
TEMPERATURE DEPENDENCE OF COPPER IRRADIATION MICROSTRUCTURE
NORMALIZED UNITS
1.0
0.5
0
LOOPS, SFT
(IRRADIATION
HARDENING)
VOID
SWELLING
Stage V
0
100
200
300
400
500
600
TEMPERATURE (°C)

Volumetric Swelling in Pure Copper and Cu-B Irradiated with Fission Neutrons to ~1.1 dpa

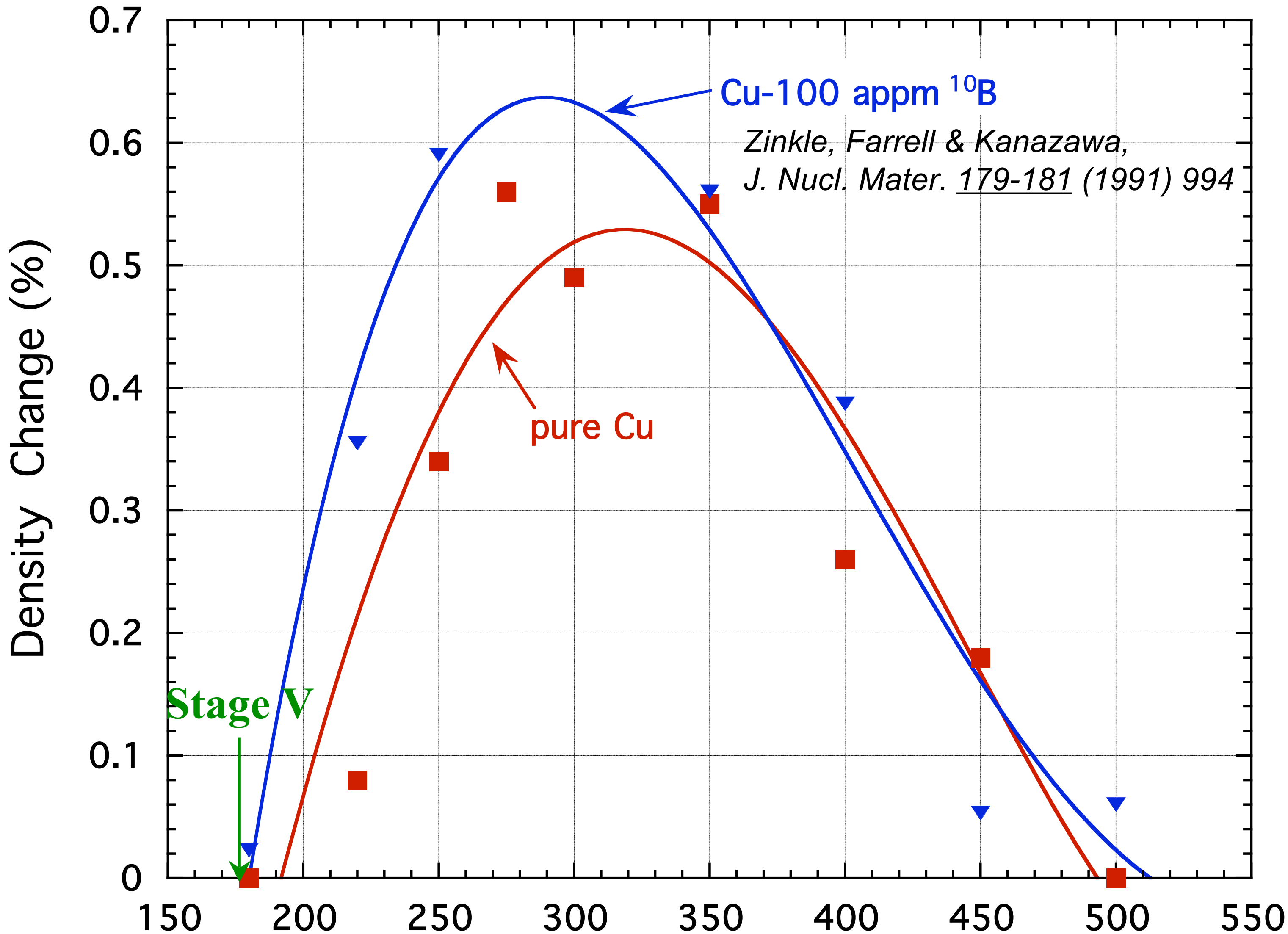

Cavity formation in austenitic stainless steel

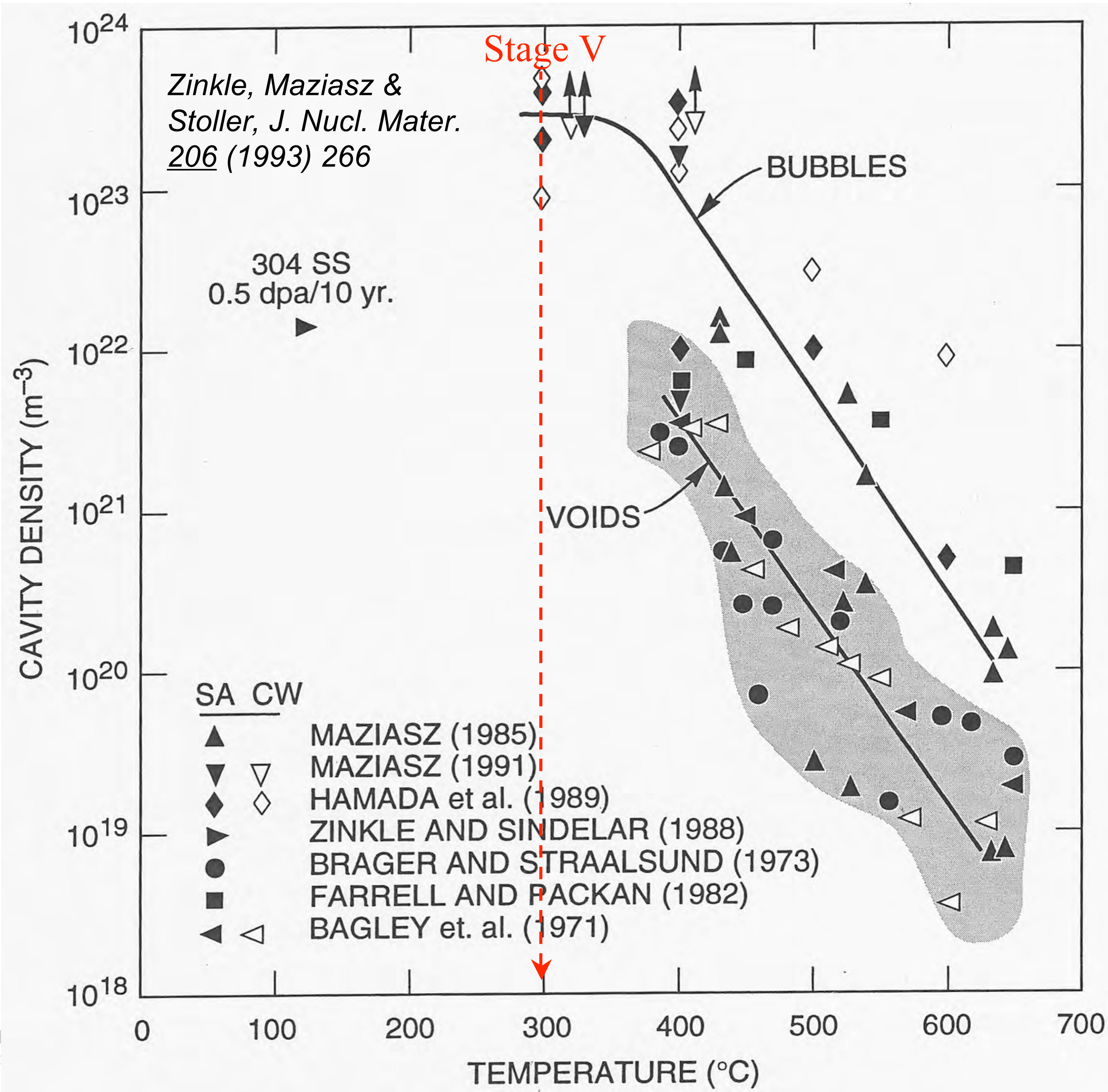

Determination of interstitial migration energies in ceramics

Defect-free zones in ion-irradiated $MgAl_2O_4$

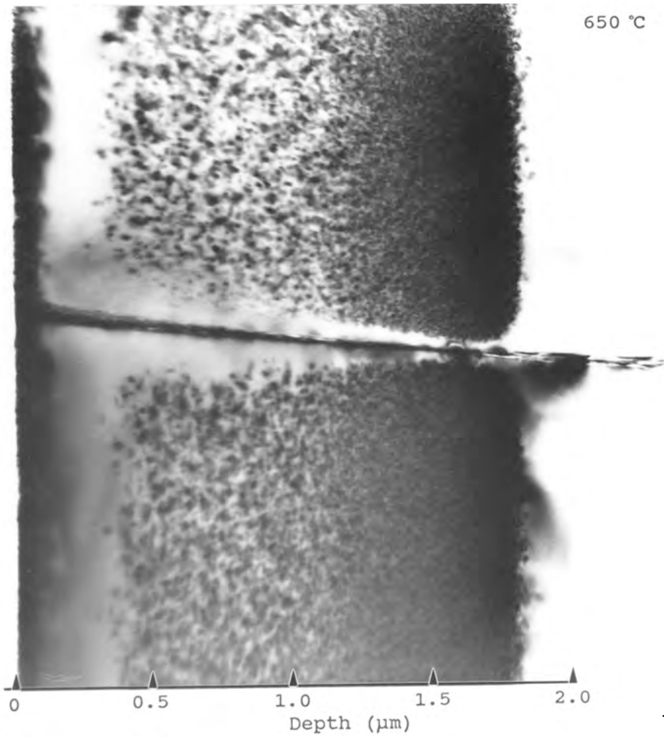

- Solve steady state rate eqns:

$$D_i \frac{d^2 C_i}{dx^2} - \alpha C_i C_v - D_i C_i C_s + P = 0$$

$$D_v \frac{d^2 C_v}{dx^2} - \alpha C_i C_v - D_v C_v C_s + P = 0$$

- For sink-dominant conditions ($C_S > 10^{14}/m^2$), the defect-free zone width is related to the diffusivity (D_i) and damage rate (P) by:

$$D_i = \frac{L\ P}{C_i^{crit} \sqrt{C_s}}$$

Defect-free grain boundary zones in ion-irradiated Al_2O_3

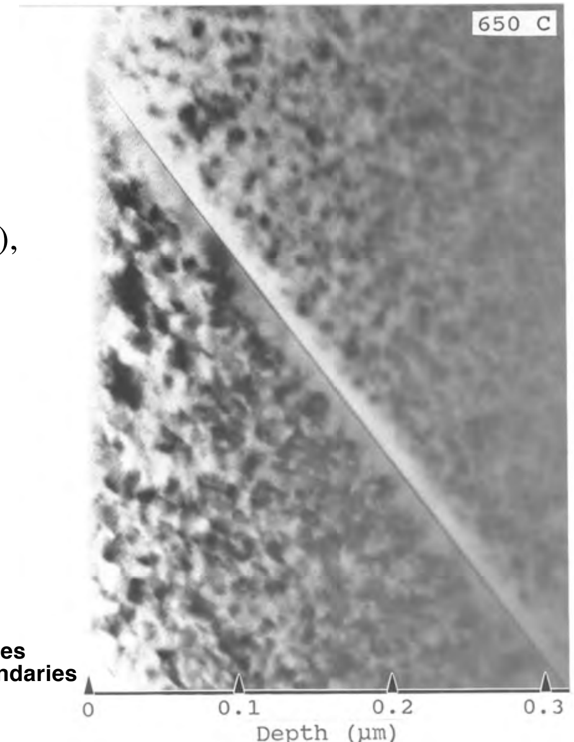

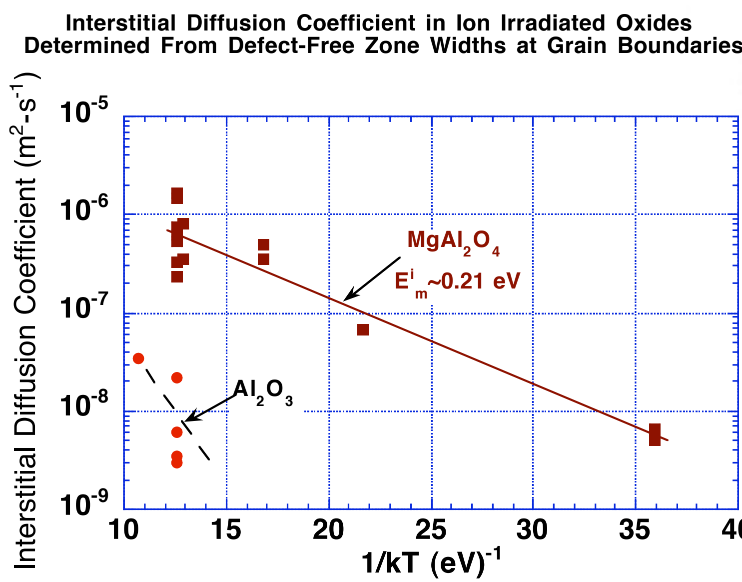

Effect of grain size on cavity swelling

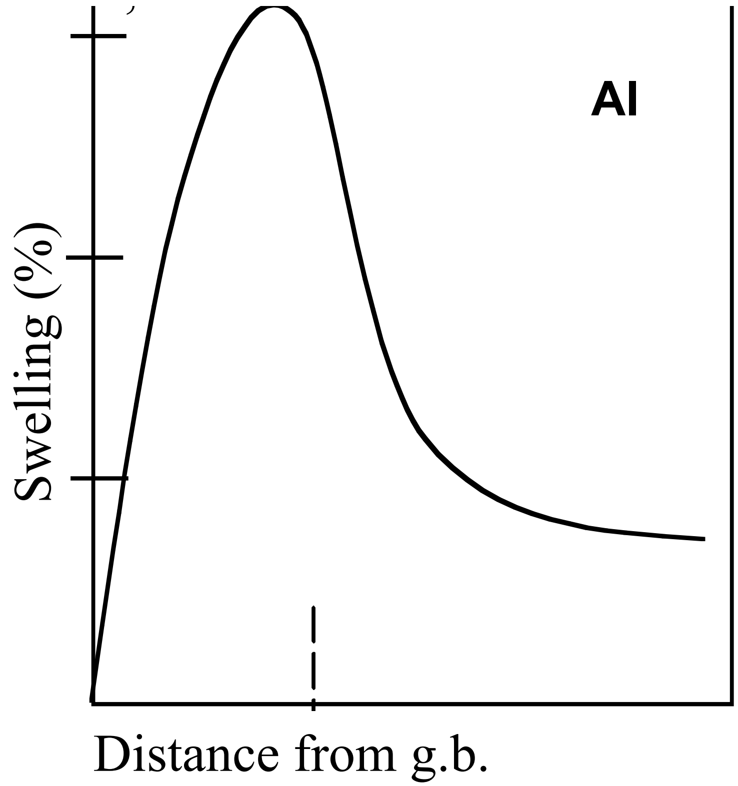

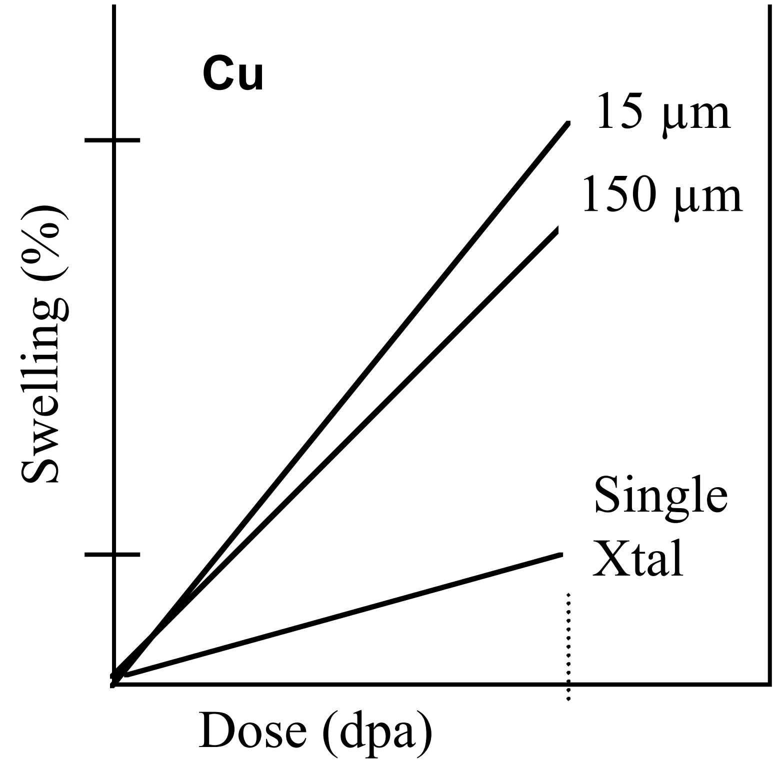

Singh et al., Phil.Mag.A 82(2002)1137

Variation of void swelling vs. distance from grain boundaries in pure well-annealed Al irradiated with fission neutrons at 120°C. Note enhancement in swelling in a relatively wide zone near the grain boundaries (after Singh 1999).

Dose dependence of void swelling for three different grain sizes (Singh 1999). All specimens were irradiated in the same capsule at 350°C to a dose level of ~0.3dpa

Swelling peak occurs at ~10λ from g.b. (λ=void spacing)

λ(Cu)~200nm @250°C, ~1 μm @400°C

λ(SS)~10nm @300°C (He bubbles), ~60 nm @400°C (voids)

Enhanced void swelling next to grain boundary in neutron-irradiated Cu-Ni alloys

420^{o}C, 14 dpa

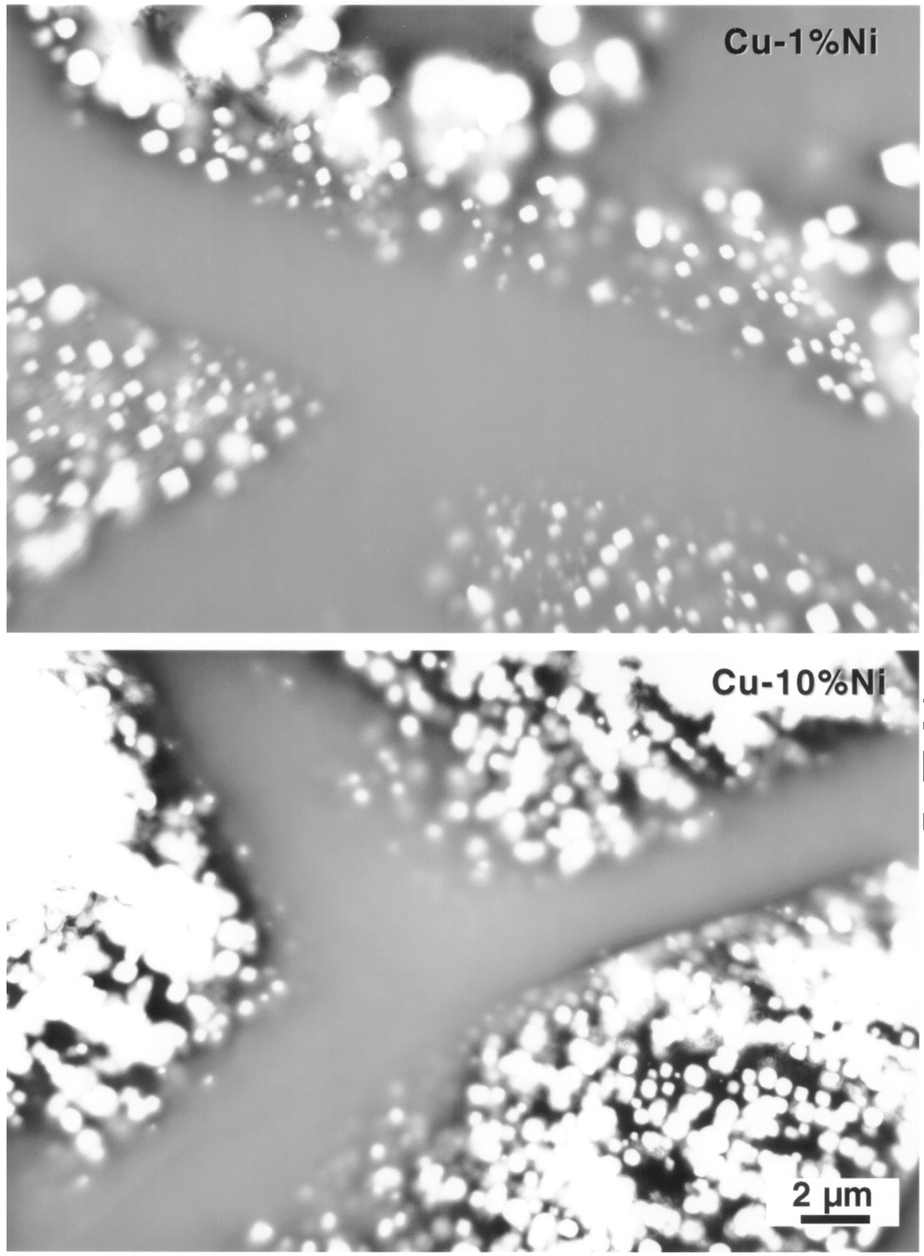

Zinkle and Singh, J. Nucl. Mater. 283-287 (2000)306

Radiation Damage can Produce Large Changes in Structural Materials

- **Radiation hardening and embrittlement (<0.4 T_M, >0.1 dpa)**

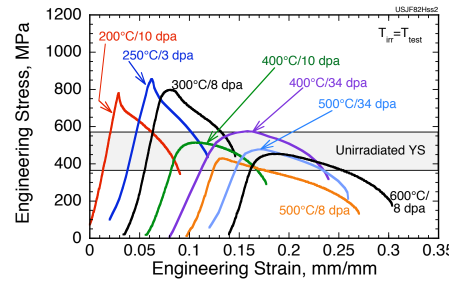

- **Phase instabilities from radiation-induced precipitation (0.3-0.6 T_M, >10 dpa)**

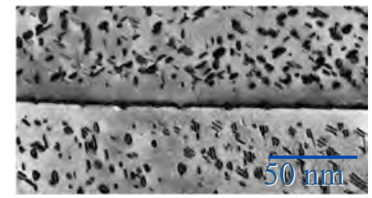

- **Irradiation creep (<0.45 T_M, >10 dpa)**

- **Volumetric swelling from void formation (0.3-0.6 T_M, >10 dpa)**

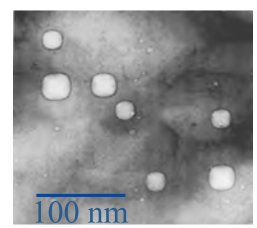

- **High temperature He embrittlement (>0.5 T_M, >10 dpa)**

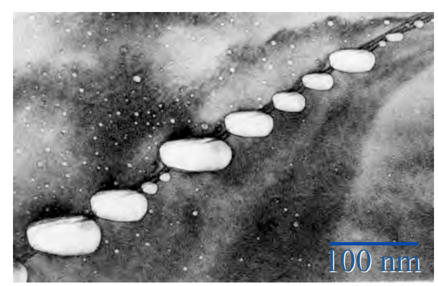

after S.J. Zinkle, Phys. Plasmas 12 *(2005) 058101*

Defect clusters in neutron irradiated copper (low T)

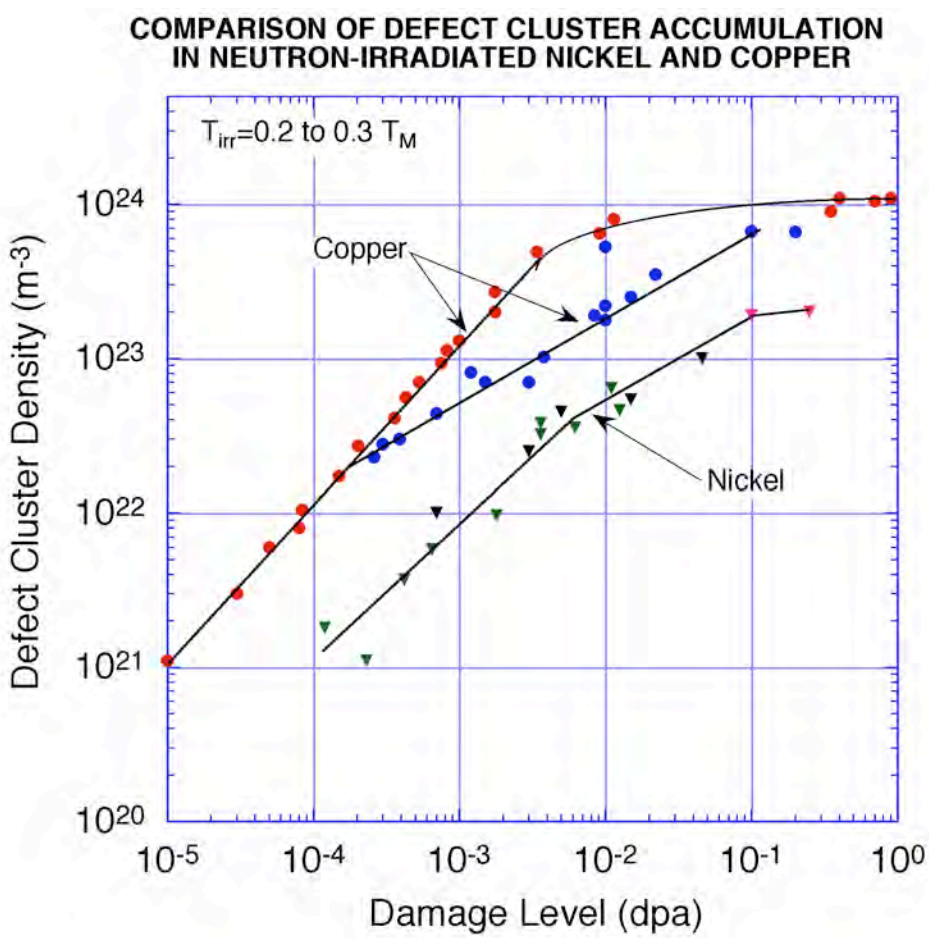

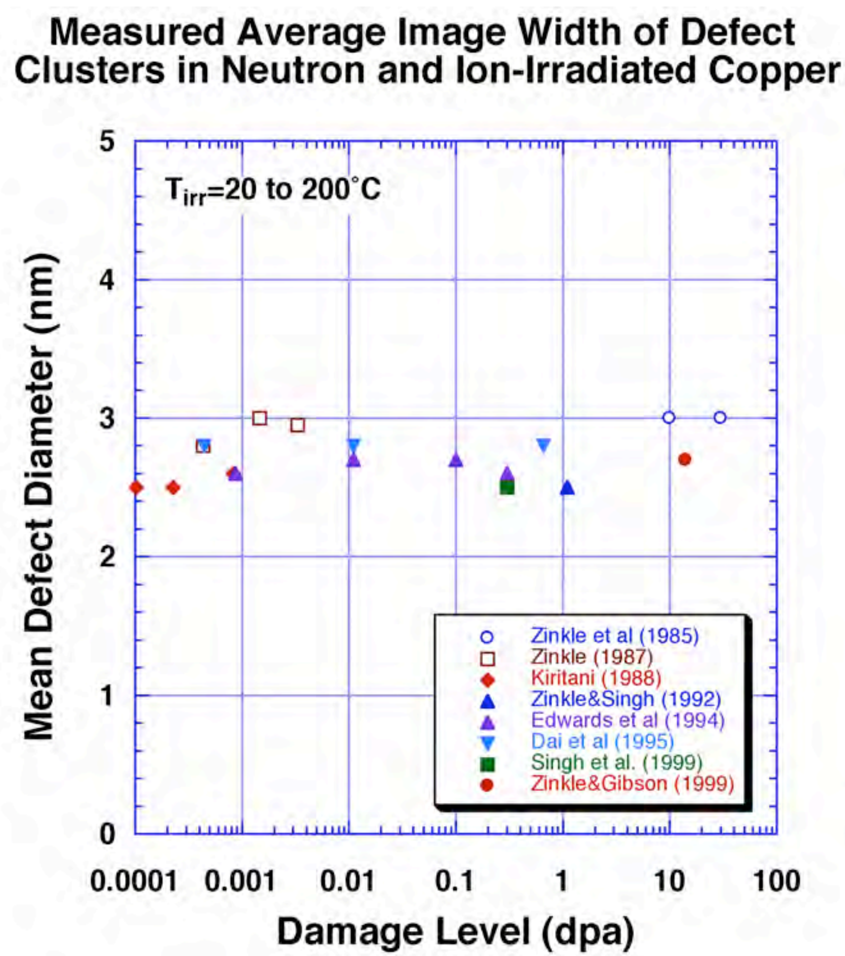

Comparison of defect cluster evolution in neutron irradiated Cu and Ni (low T)

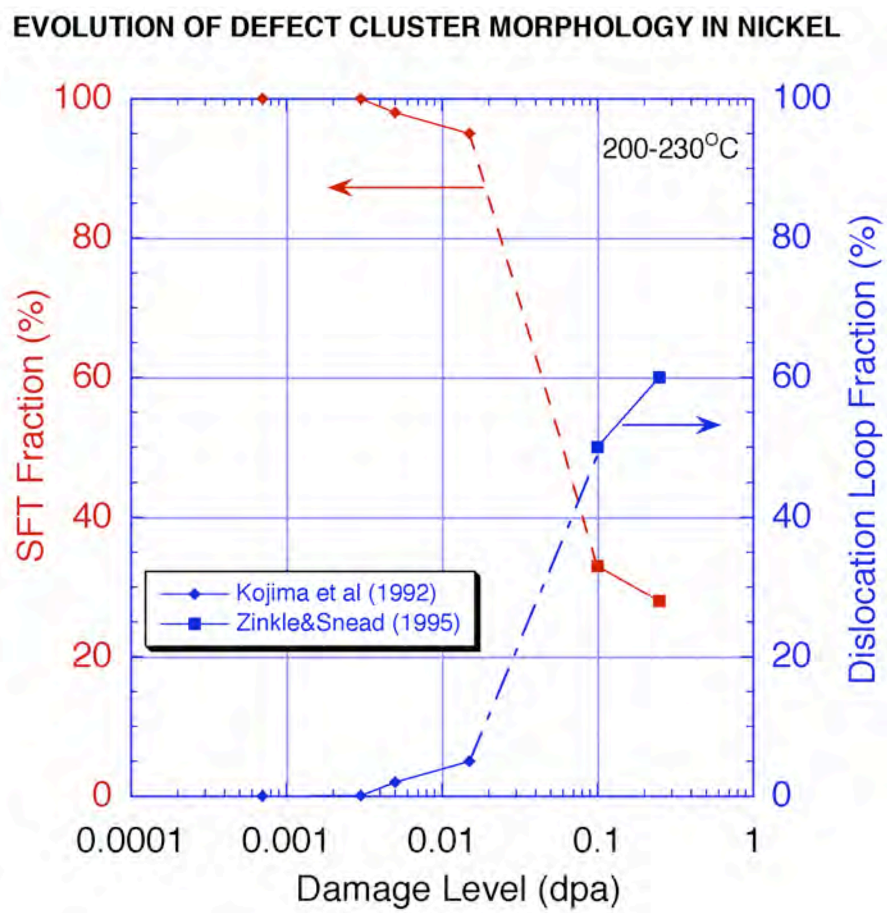

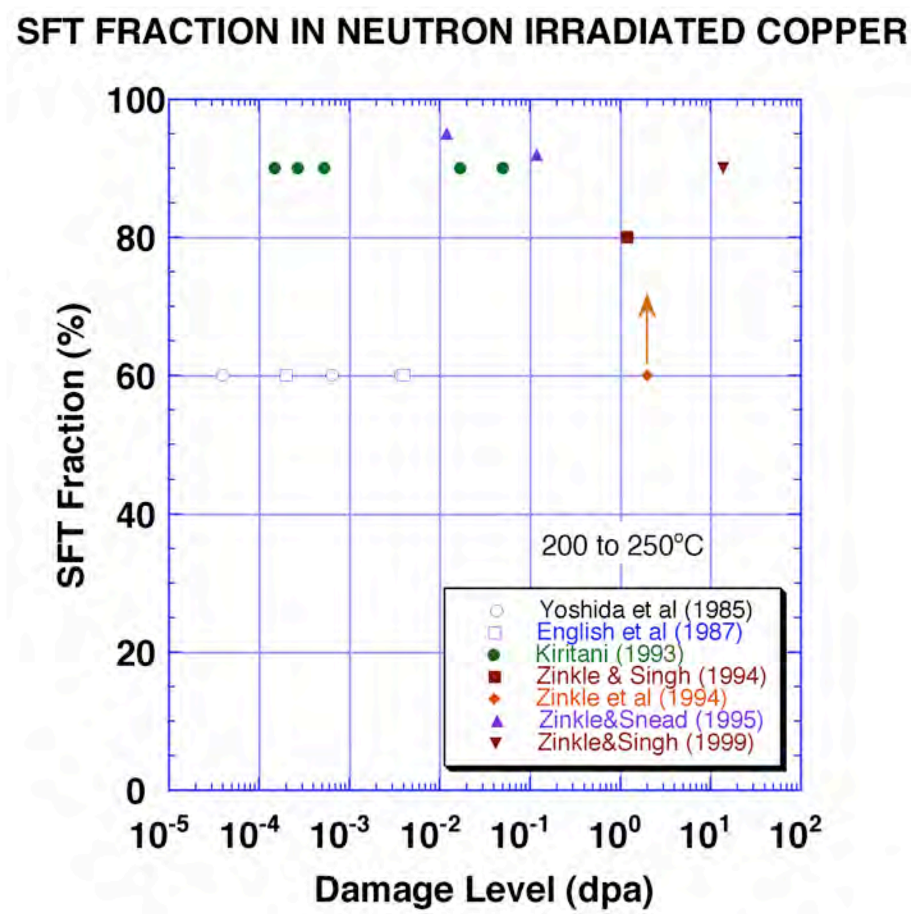

Zinkle and Snead,J. Nucl. Mater. 225 (1995) 123
Zinkle and Singh, J. Nucl. Mater. 283-287 (2000) 306

Dislocation loop evolution in neutron-irradiated Cu at 70˚C

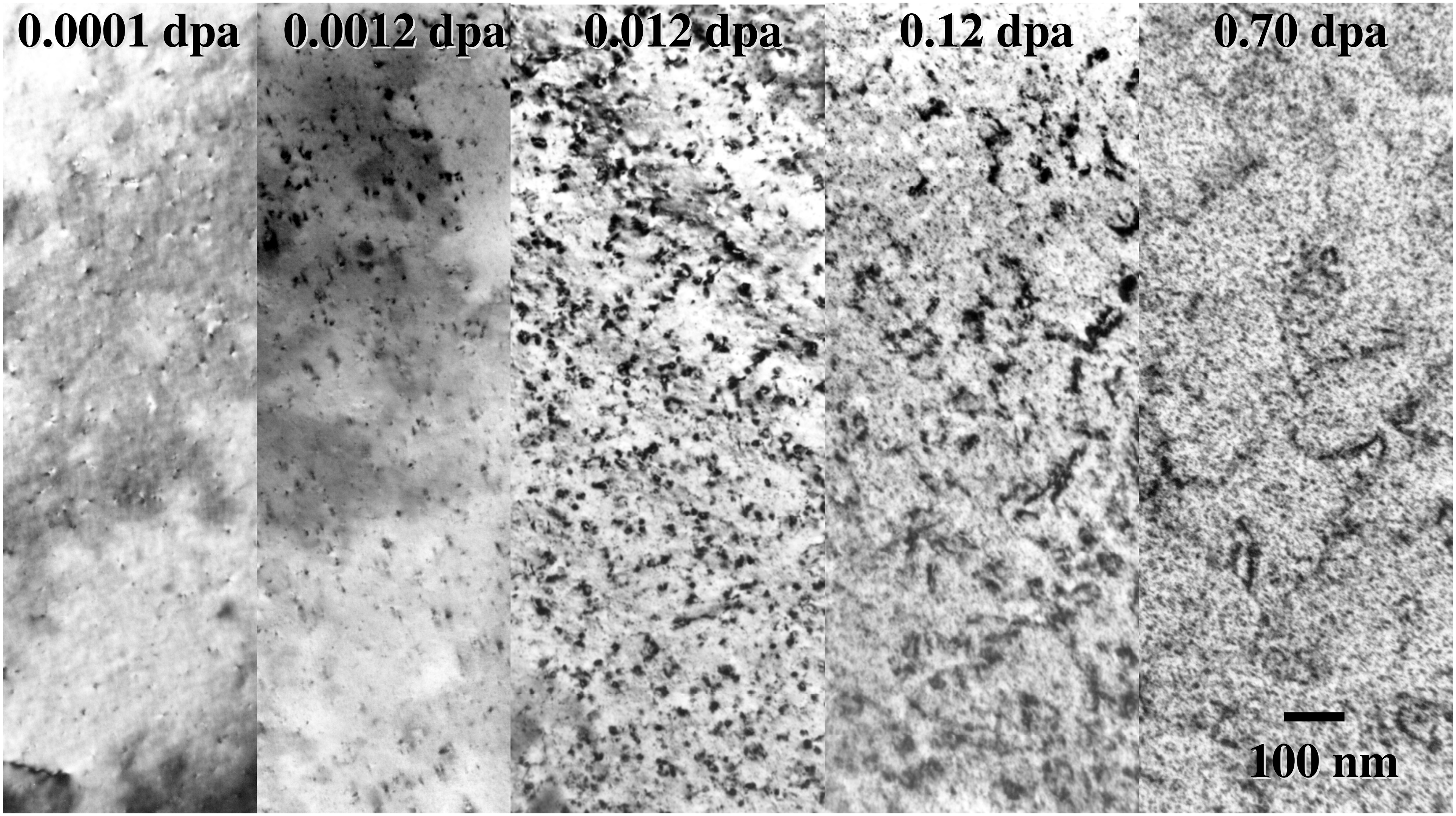

Peak loop density occurs at ~0.01 dpa

Dislocation loop formation is enhanced in Cu alloys irradiated below Stage V

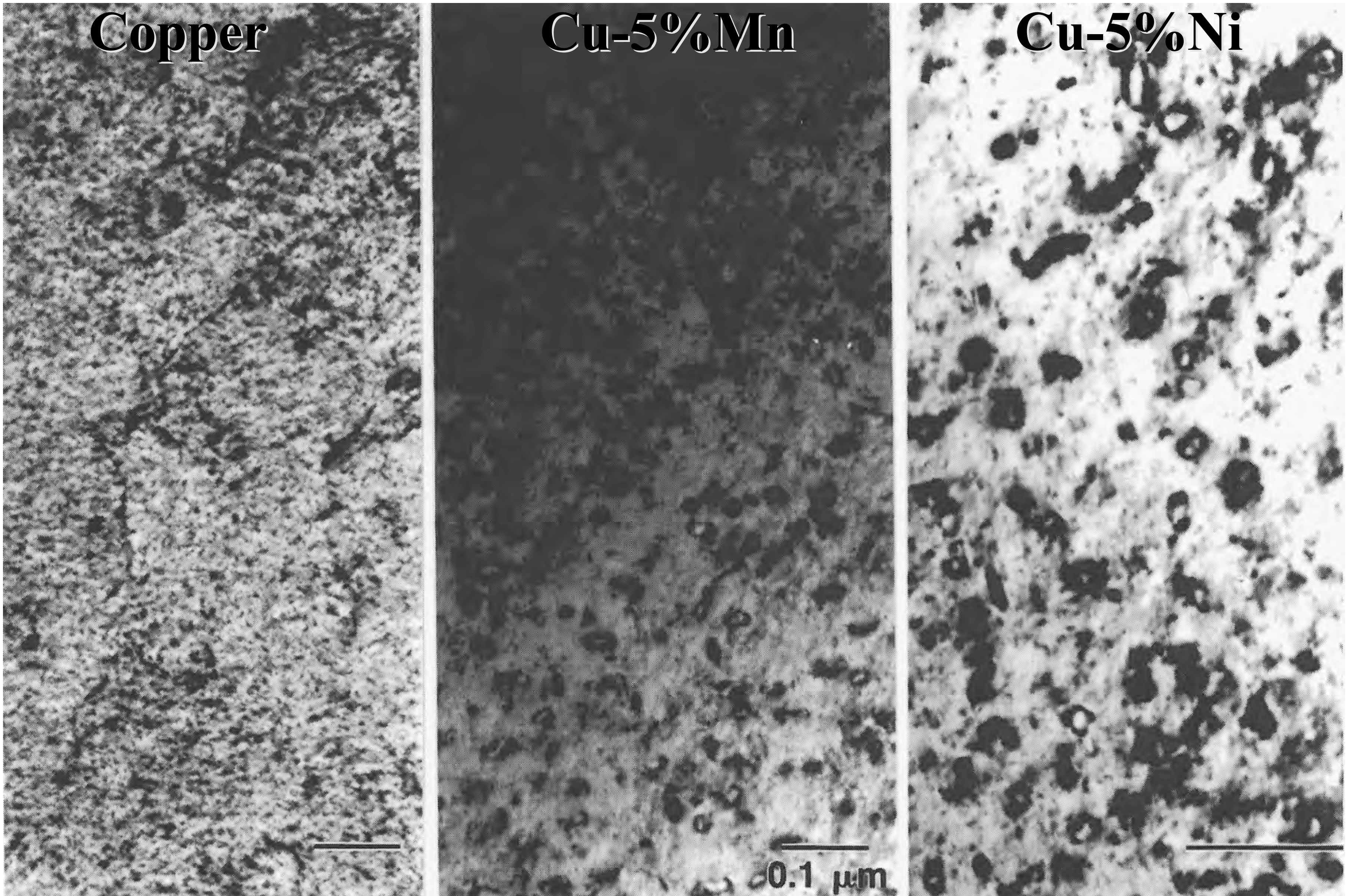

~1 dpa, 100˚C, LAMPF

Dislocation loop formation is enhanced in Cu alloys compared to pure Cu irradiated below Stage V

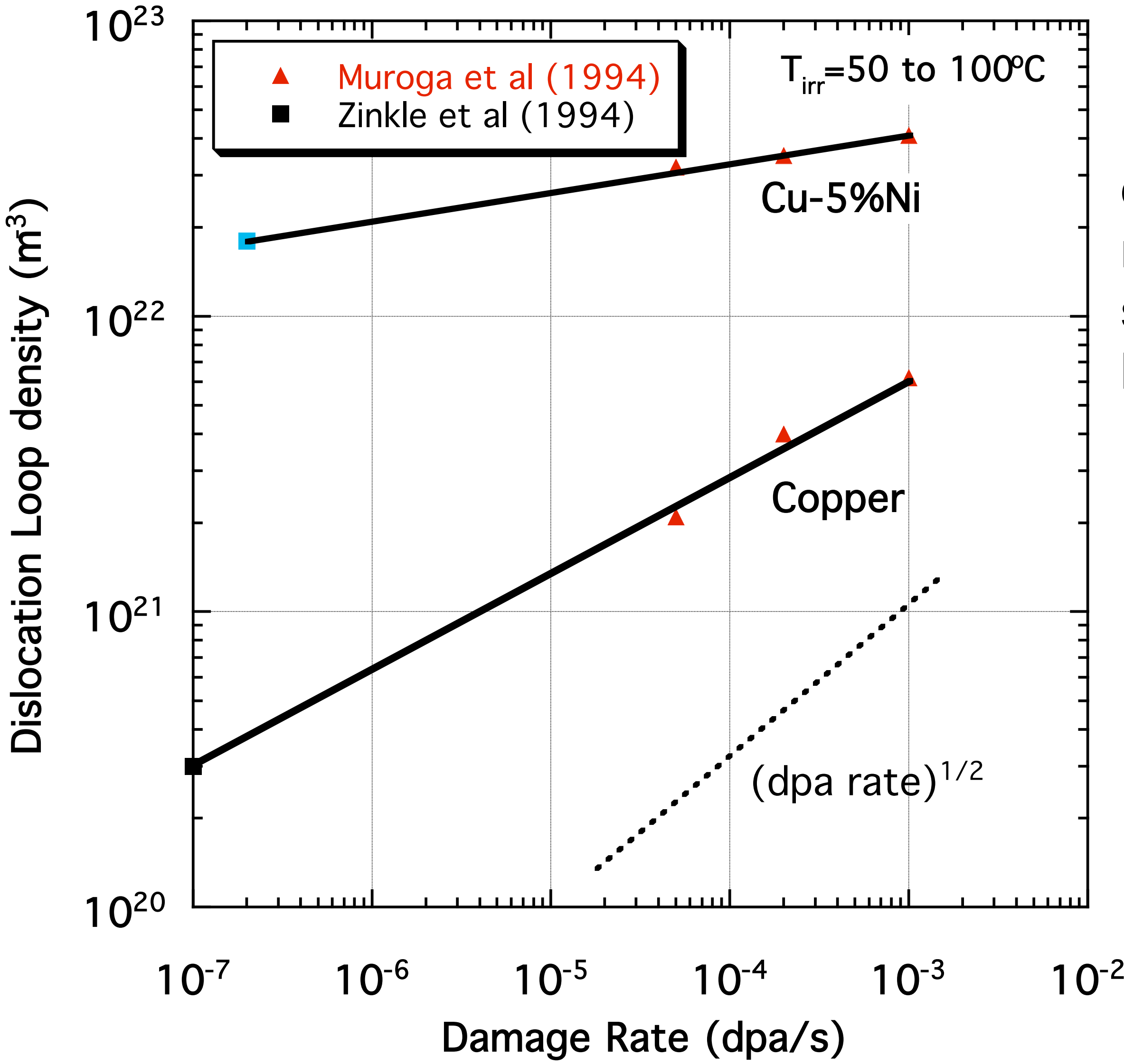

Behavior of alloy is different from pure metal; nearly all computer simulation models are based on pure metals

Formation of dislocation loop rafts in Fe after neutron irradiation to 0.8 dpa at 70˚C

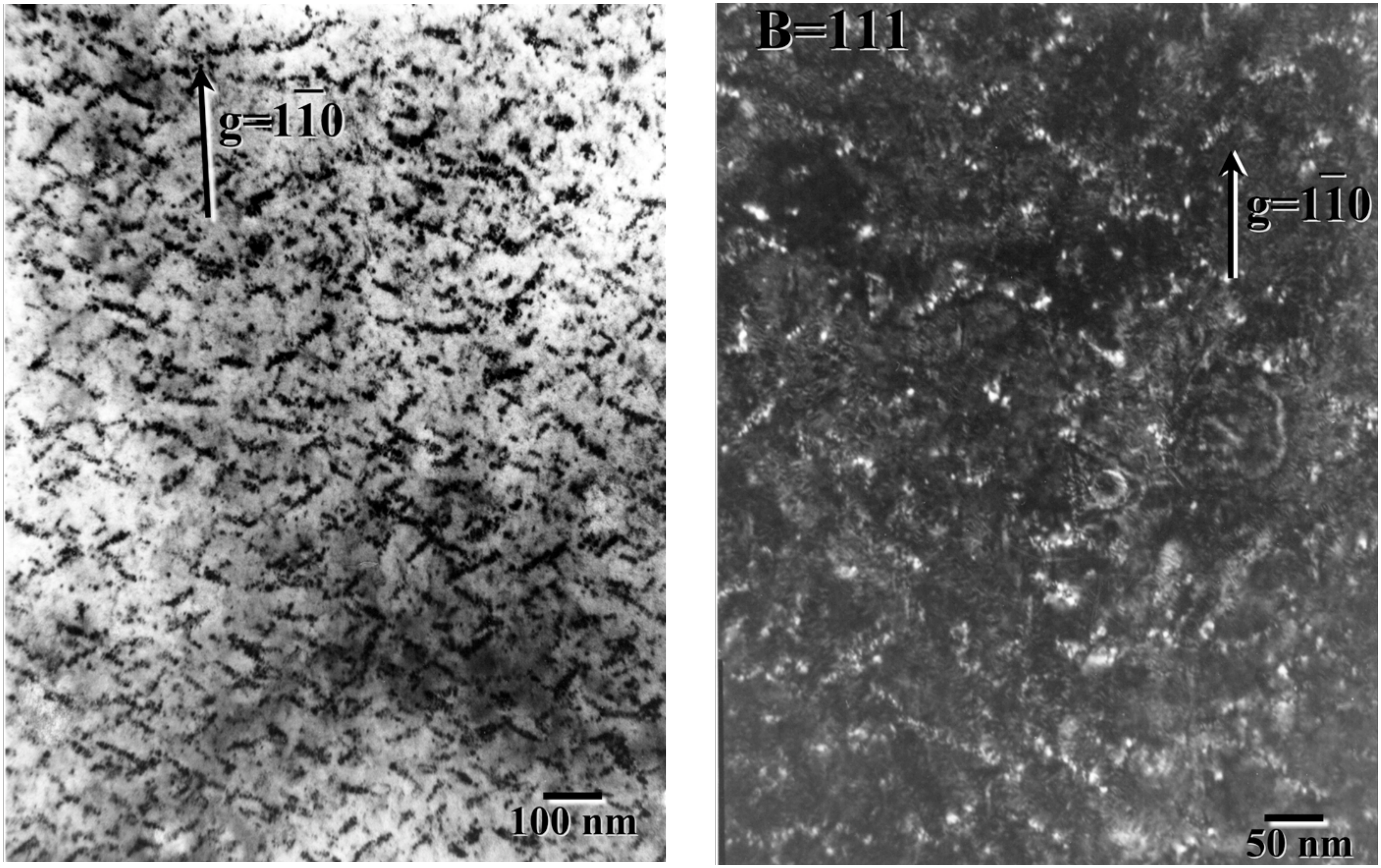

a/2<111>{111} loops form in rafts along <110> directions

S.J. Zinkle and B.N. Singh, J. Nucl. Mater. <u>351</u> (2006) 269

Design of Radiation-Resistant Materials: KMC Modeling of Pinning and Rafting

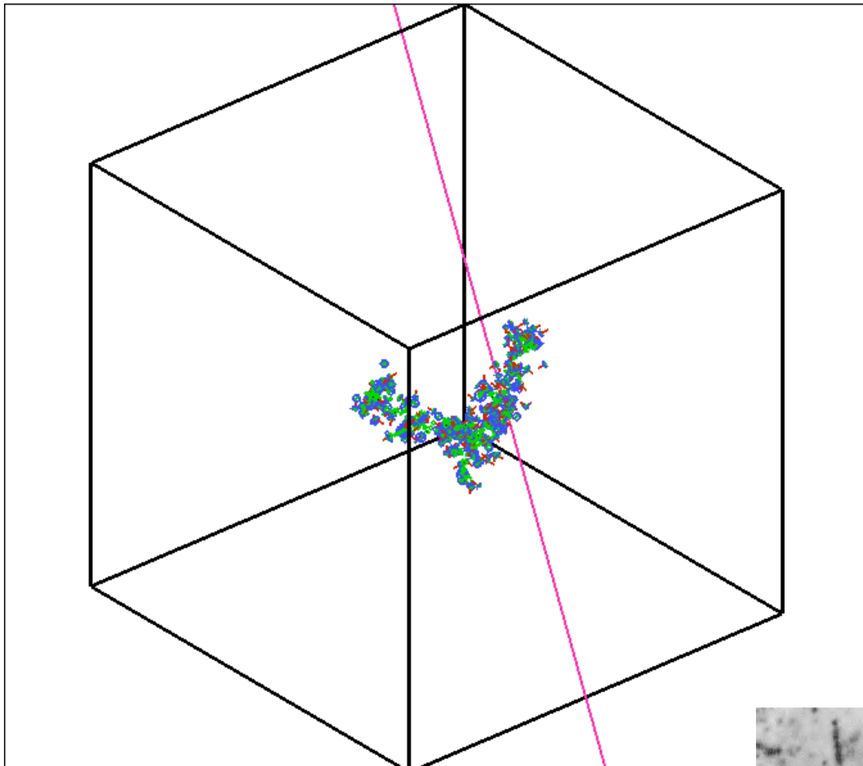

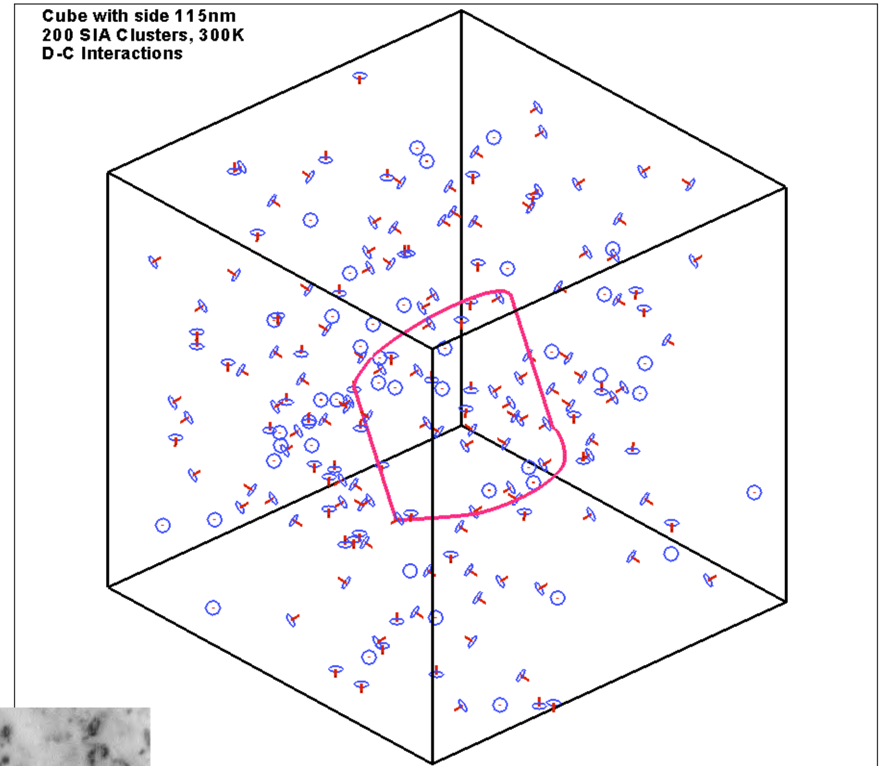

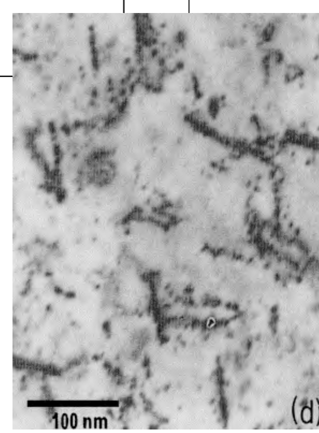

Low tensile ductility in FCC and BCC metals after irradiation at low temperature is due to formation of nanoscale defect clusters

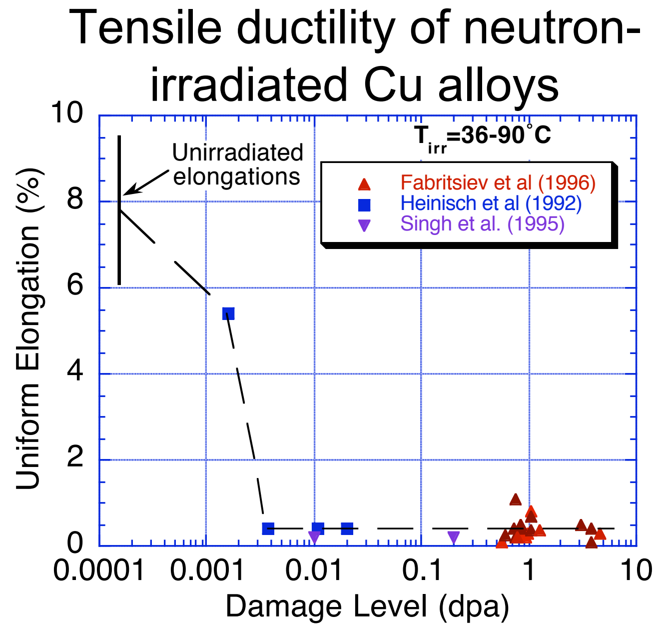

Outstanding questions to be resolved include:

- Can the defect cluster formation be modified by appropriate use of nanoscale 2nd phase features or solute additions?
- Can the poor ductility of the irradiated materials be mitigated by altering the predominant deformation mode? (e.g., twinning vs. dislocation glide)

Oak Ridge National Laboratory

Radiation hardening in V-4Cr-4Ti

High hardening and loss of uniform elongation occurs for irradiation and test temperatures <0.3 T_M

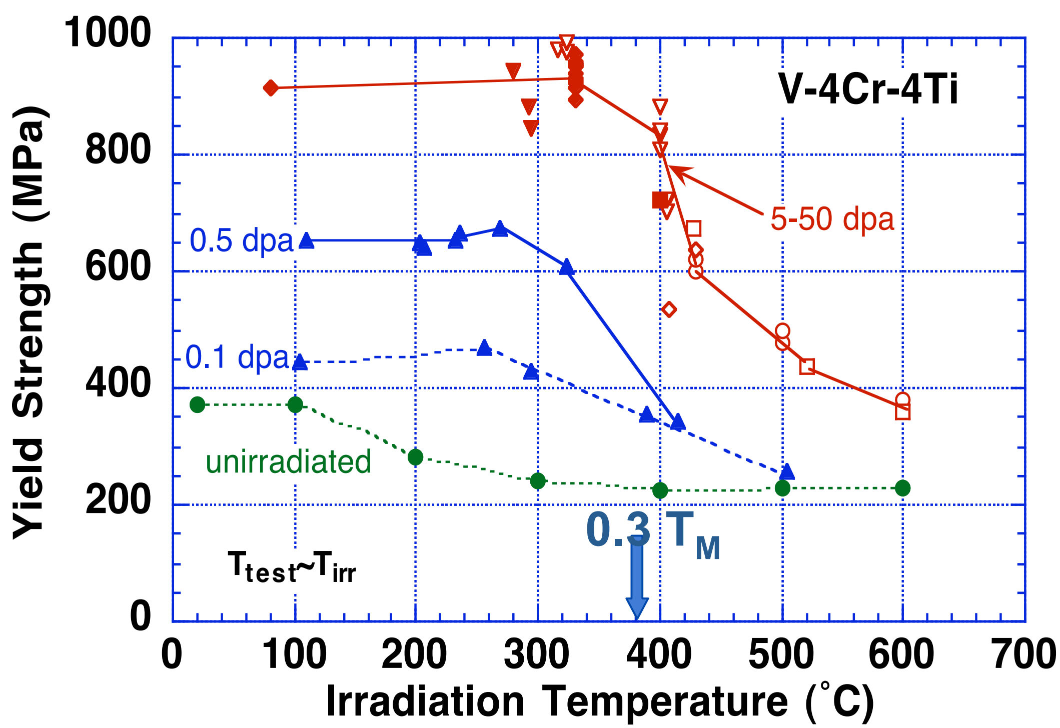

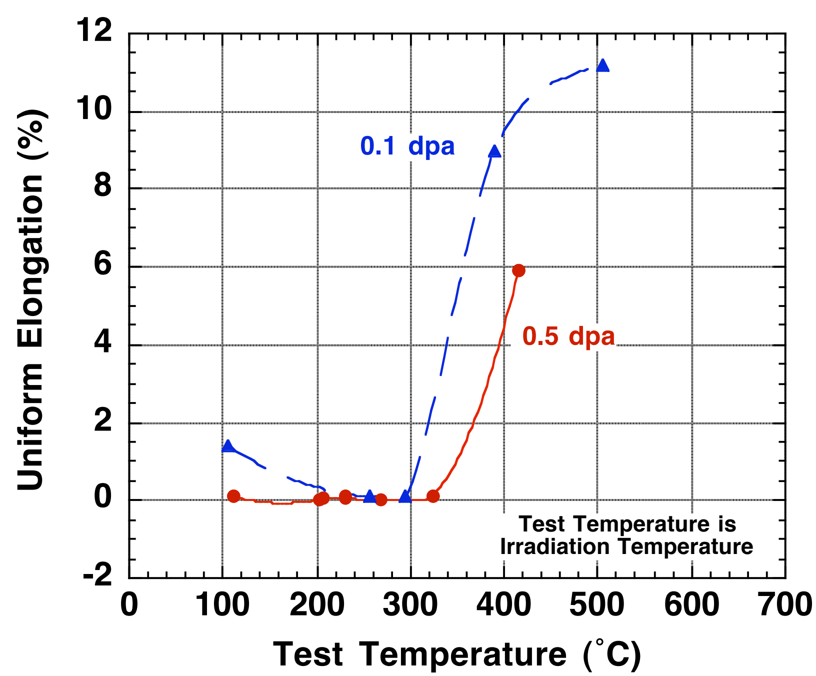

Low tensile ductility in FCC and BCC metals after irradiation at low temperature is due to formation of nanoscale defect clusters

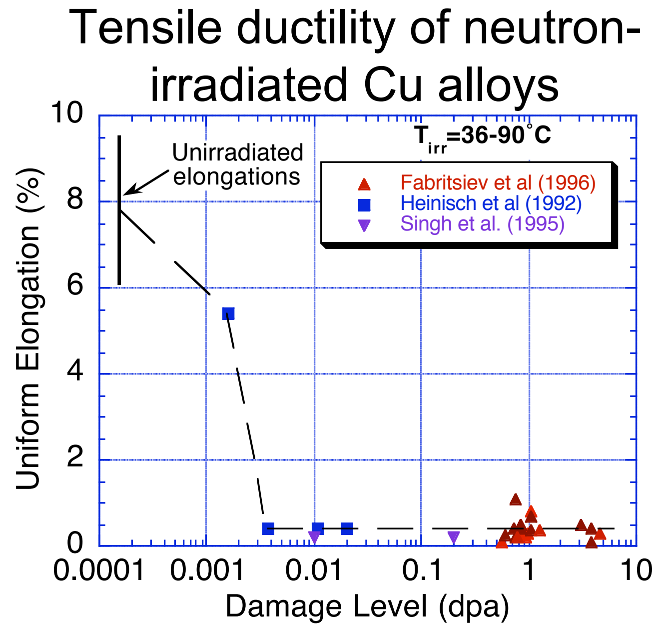

Outstanding questions to be resolved include:

- Can the defect cluster formation be modified by appropriate use of nanoscale 2nd phase features or solute additions?
- Can the poor ductility of the irradiated materials be mitigated by altering the predominant deformation mode? (e.g., twinning vs. dislocation glide)

OAK RIDGE National Laboratory

Fracture surface of Irradiated Nb-1Zr shows ductile behavior, despite low uniform elongation value

Nb-1 Zr

0.22 dpa at ~70°C
[4.5×10^{20} n/cm^2 (>0.1 MeV)]

Tensile Test at ~35°C

0.2 % Uniform Elongation
9.6% Total Elongation

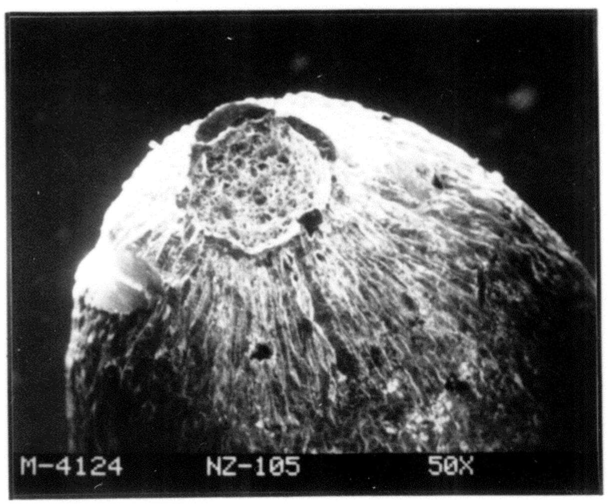

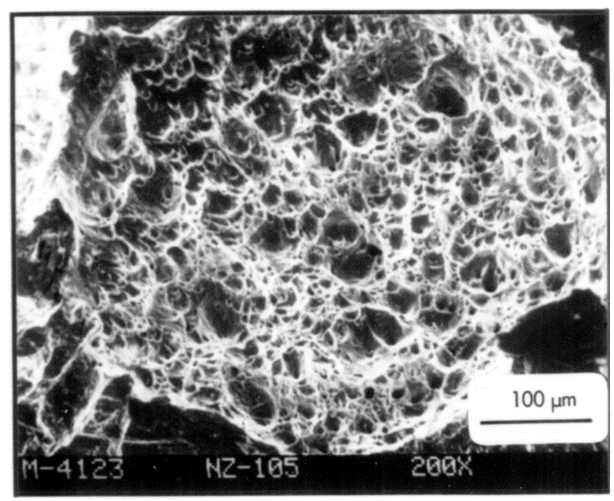

F.W. Wiffen, unpublished results

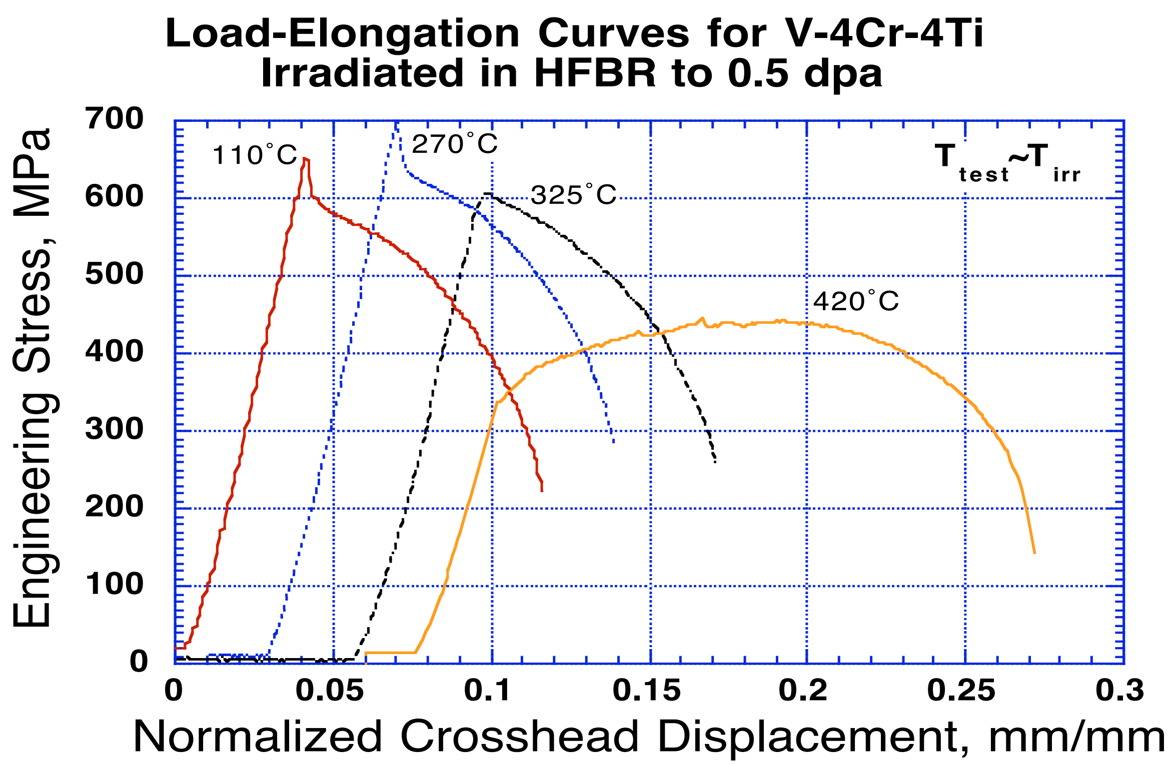

Load-Elongation Curves for V-4Cr-4Ti
Irradiated in HFBR to 0.5 dpa
Engineering Stress, MPa
Normalized Crosshead Displacement, mm/mm
0
100
200
300
400
500
600
700
0.05
0.1
0.15
0.2
0.25
0.3
110˚C
270˚C
325˚C
420˚C
T test~T irr

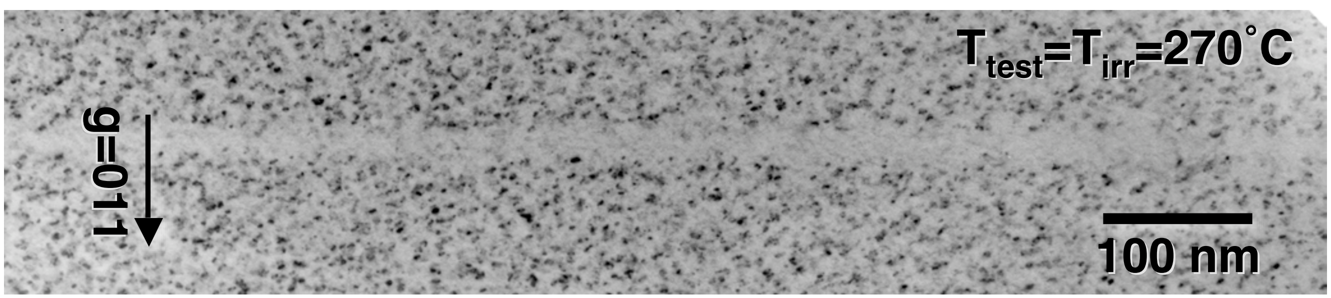

T test=T irr=270˚C
g=011
100 nm

Localized deformation (and dislocation channeling) occurs in many irradiated material systems

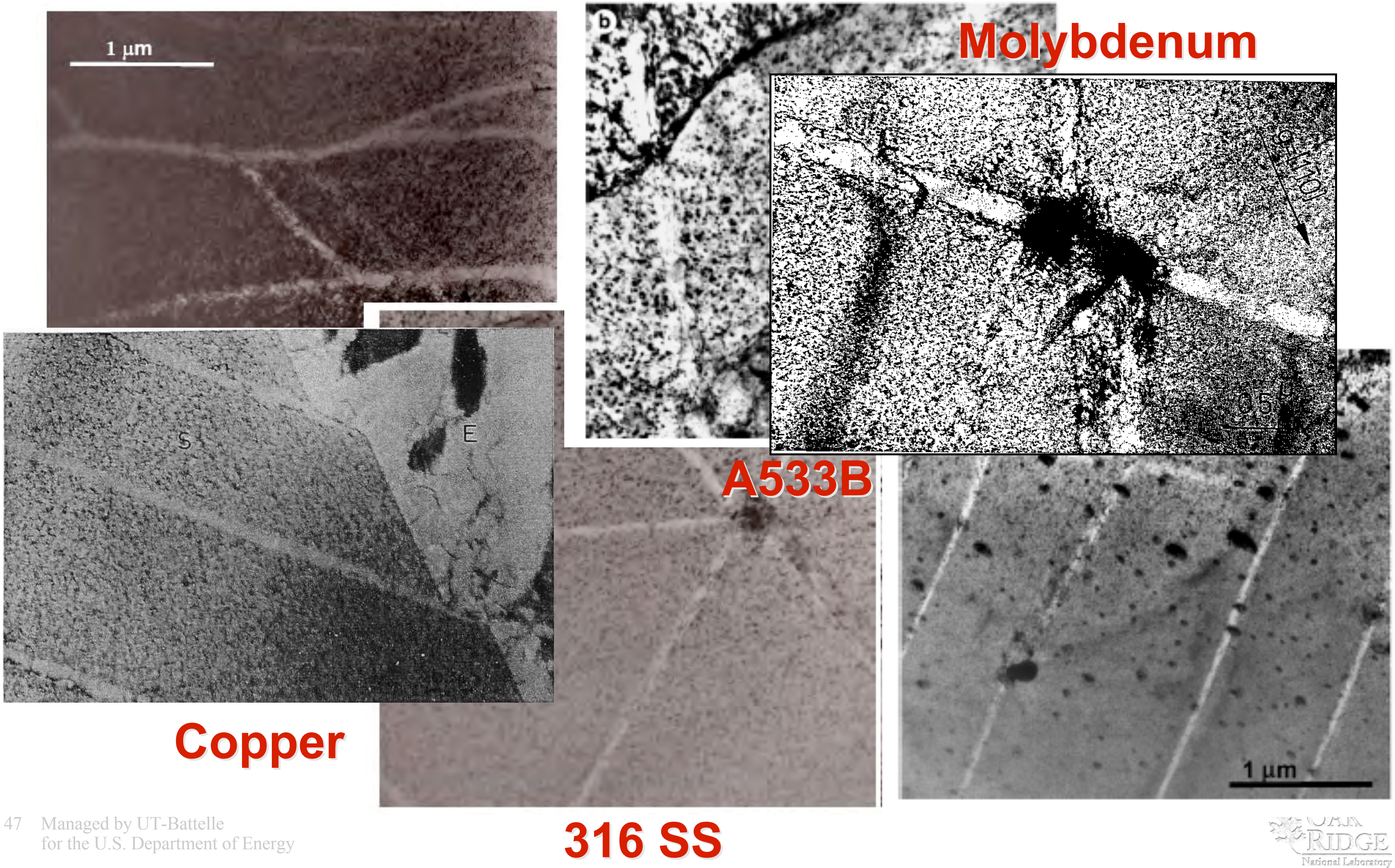

Direct formation of SFTs in Cu displacement cascades based on molecular dynamics simulations

L=1.3 nm

L=2.3 nm

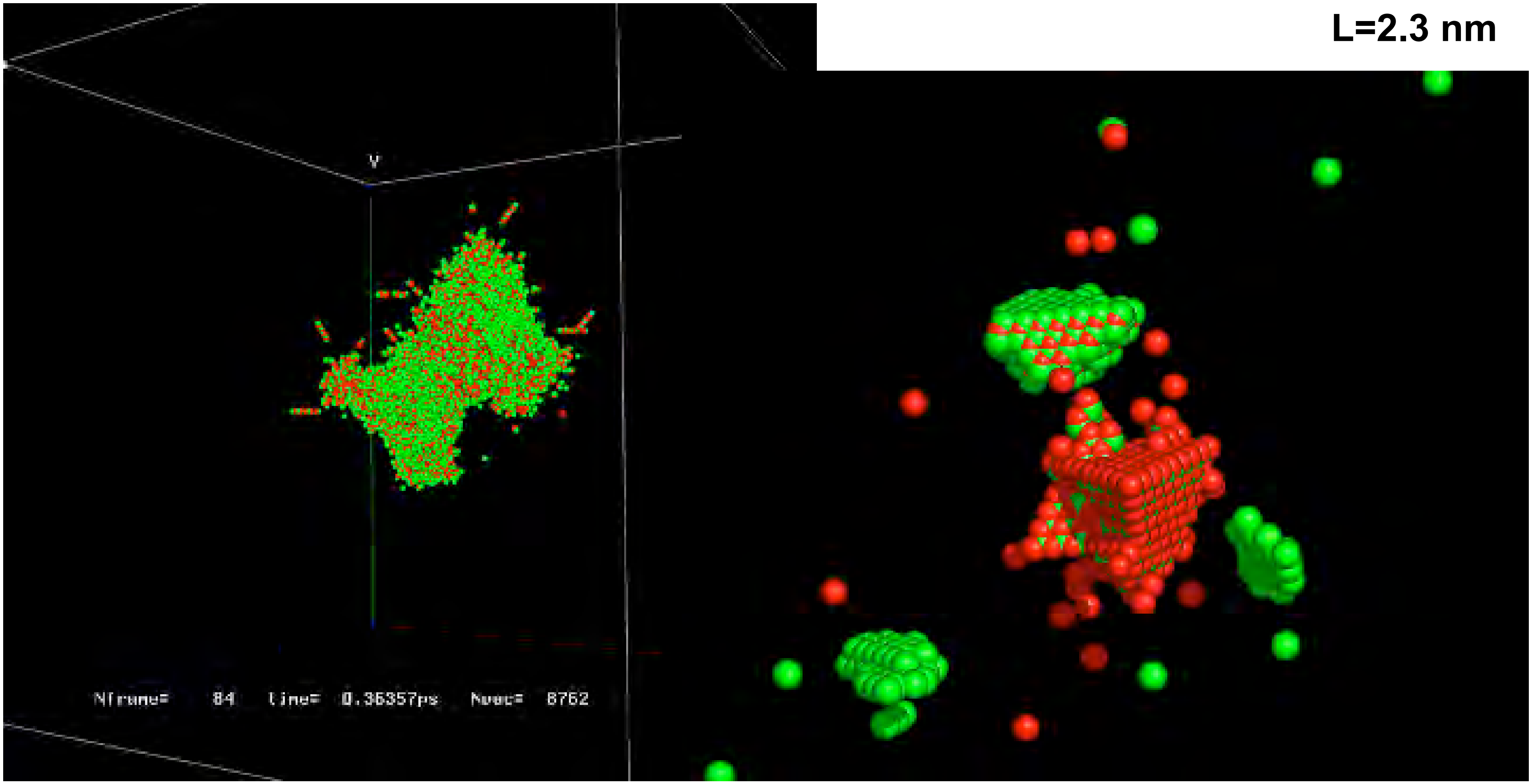

• Nearly perfect SFTs are formed in cascades within ~50 ps

Yu. N. Osetsky

Dislocation channel interactions in Fe deformed following neutron irradiation at 70°C to 0.8 dpa

Zinkle & Singh, J. Nucl. Mater. 351 (2006) 269

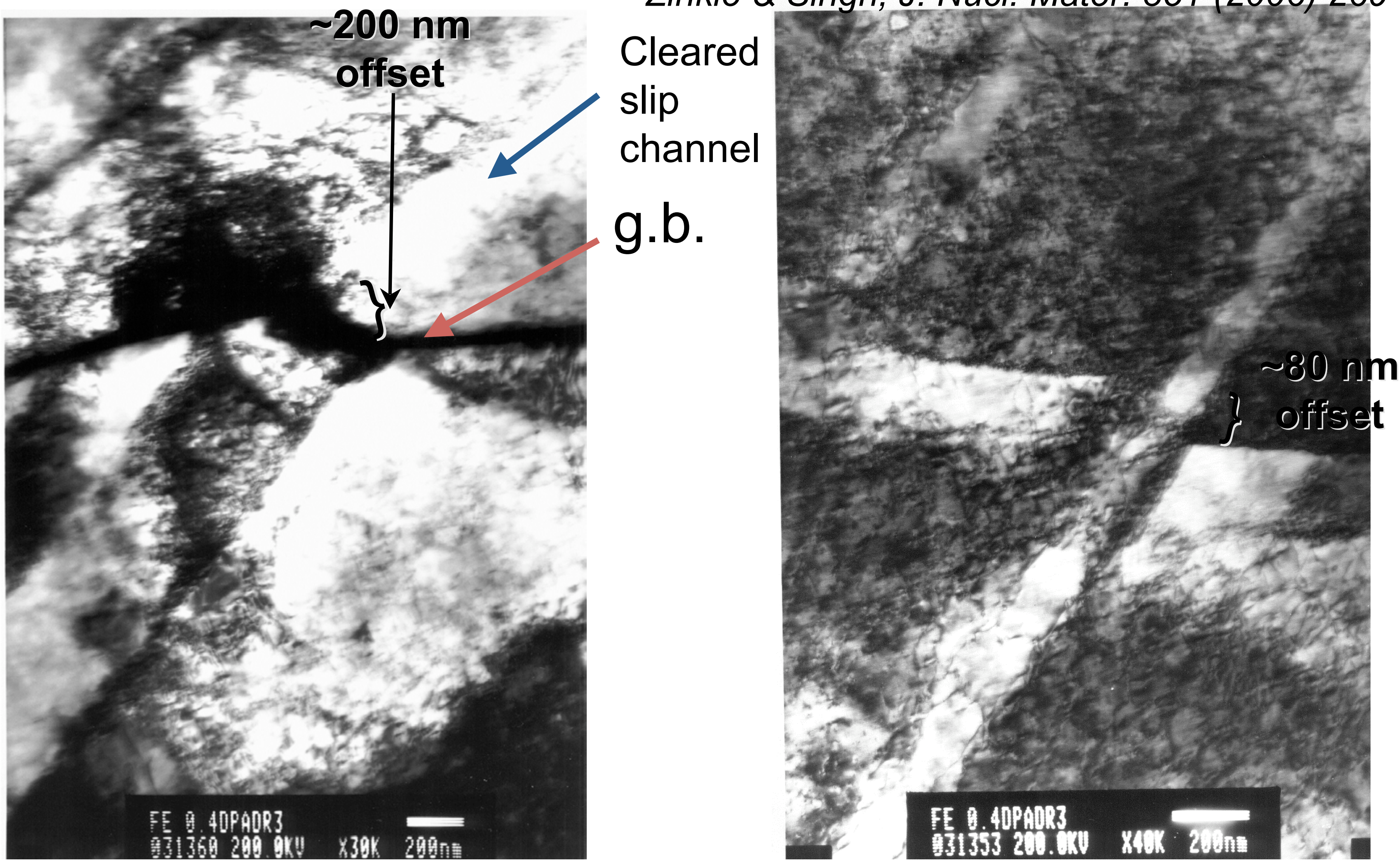

Need well-engineered materials to mitigate neutron radiation effects

Dislocation interaction with SFTs in quenched Au

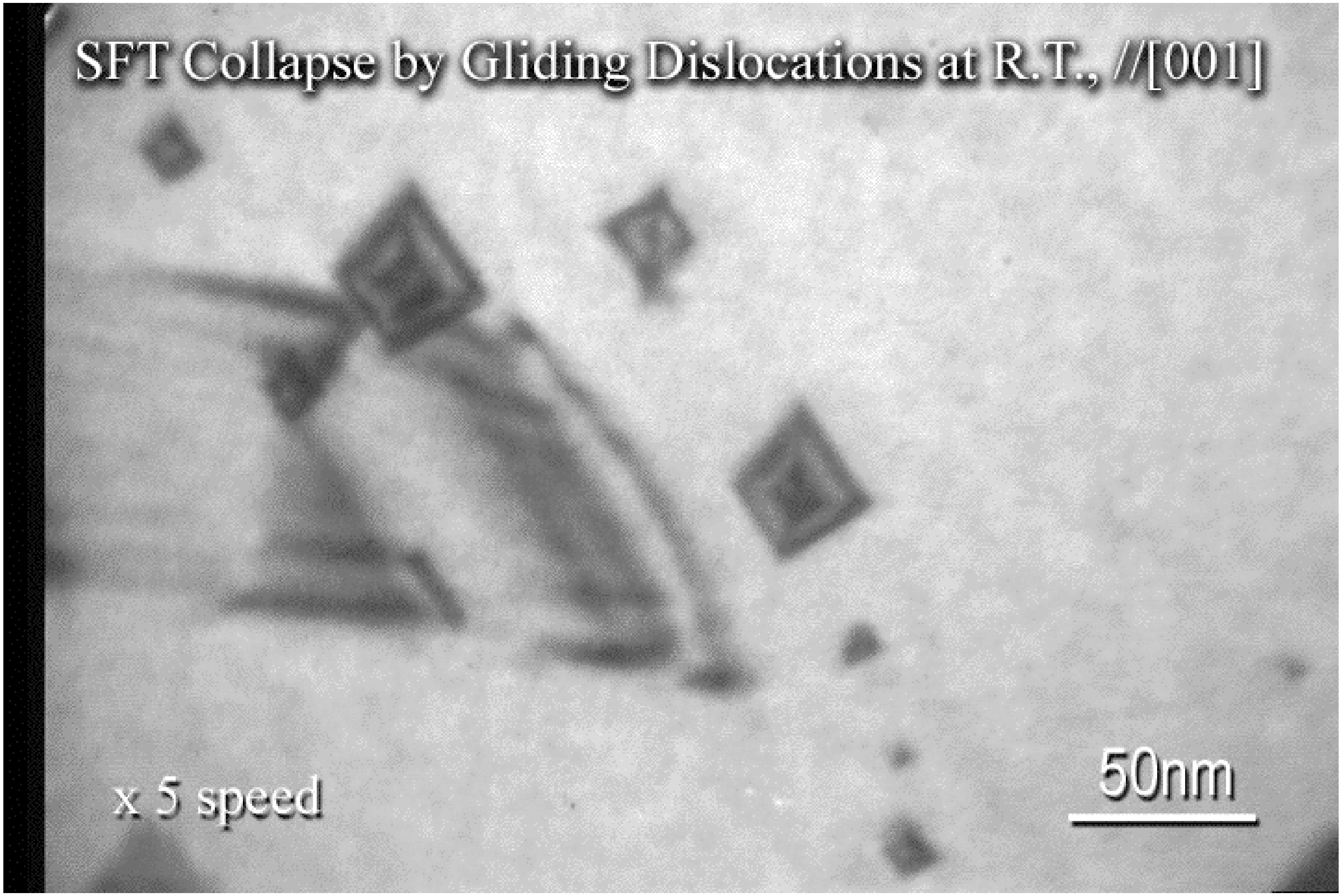

- **Type 1 interaction (Frank loop formation) at room temperature**

Matsukawa, Stoller, Osetsky & Zinkle
J. Nucl. Mater. 351 (2006) 285

Dislocation interaction with SFTs in quenched Au

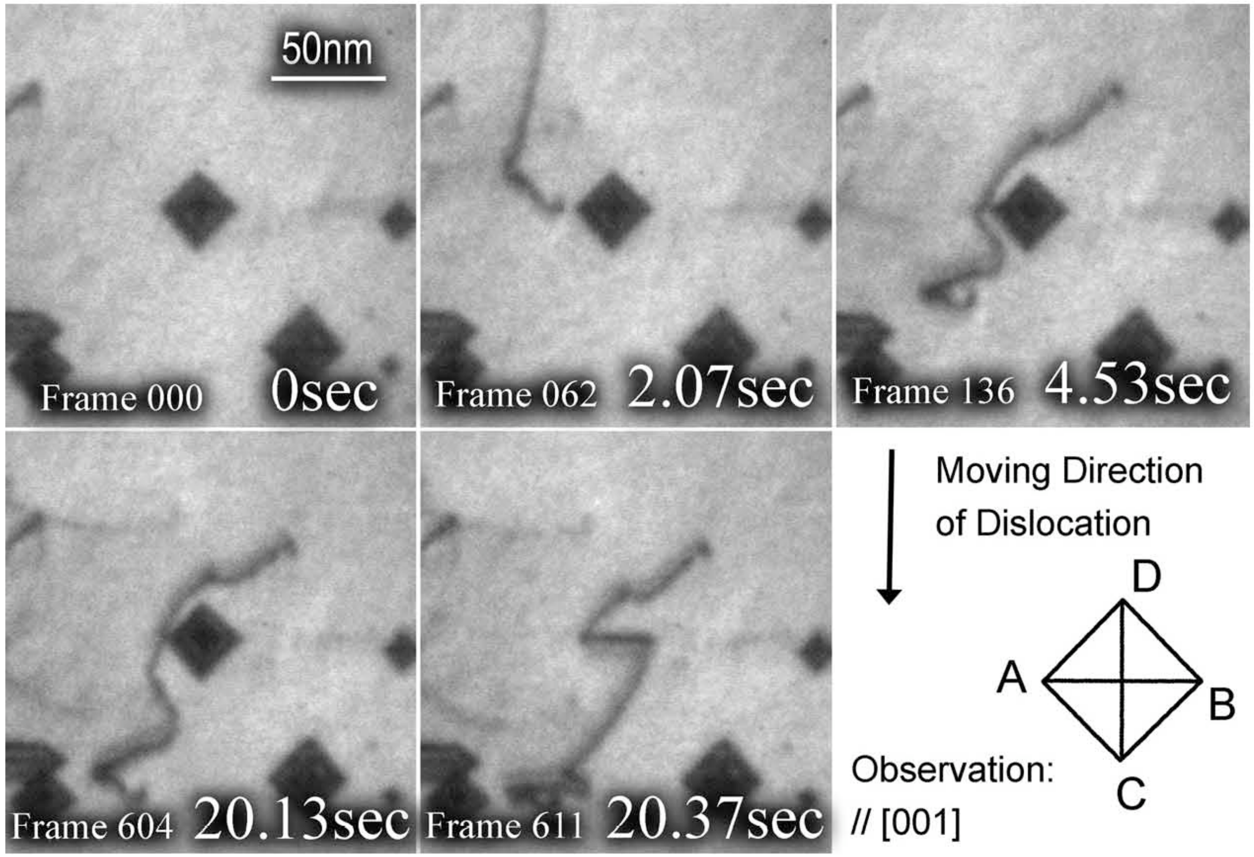

- **Type 2 interaction at room temperature (superjog creation with no SFT remnant)**

Matsukawa, Stoller, Osetsky & Zinkle
J. Nucl. Mater. 351 (2006) 285

Dislocation interaction with SFTs in quenched Au

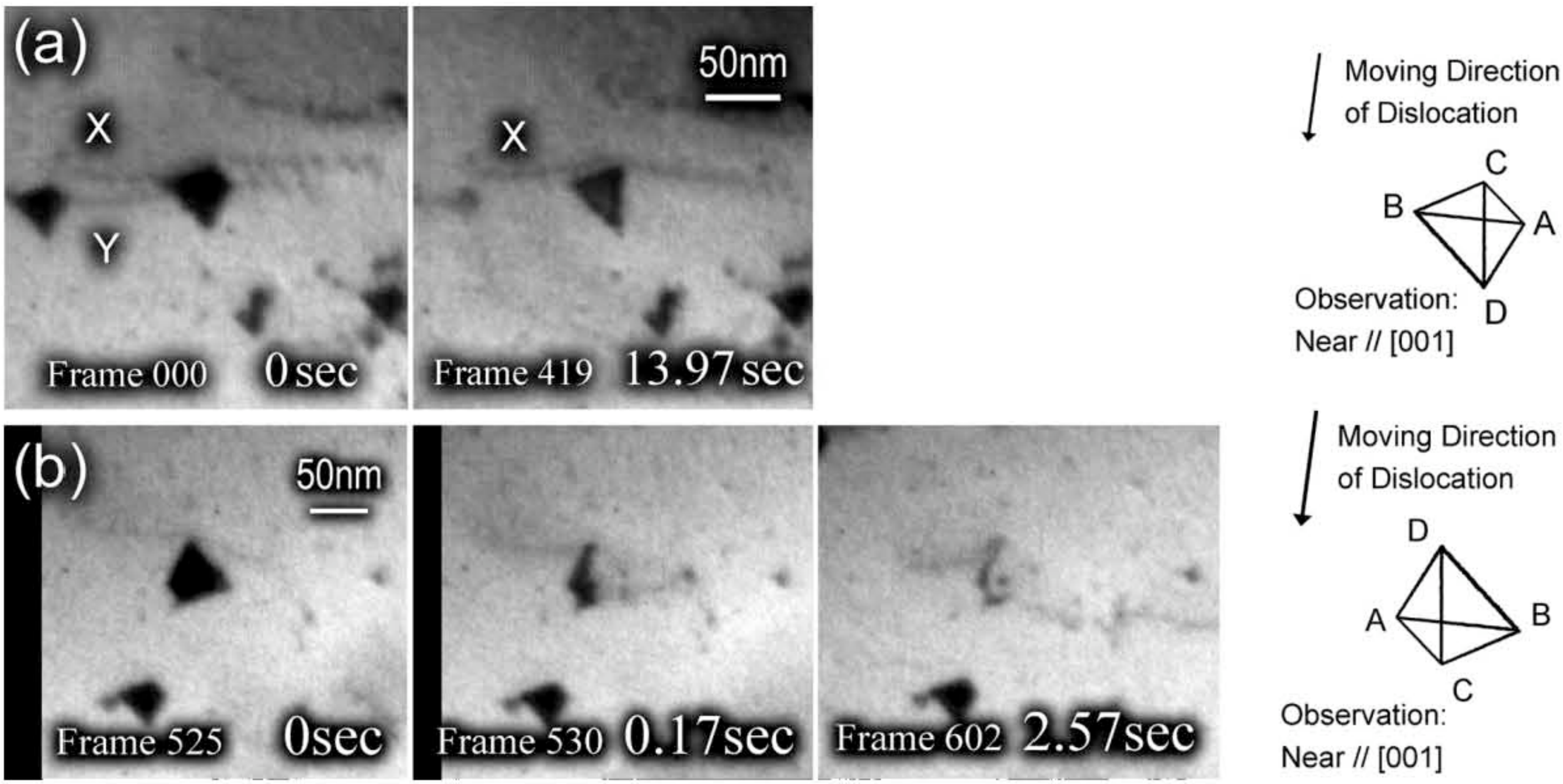

- **Types 1(a) & 2(b) interactions also occur at 100 K (no vacancy migration)**

Matsukawa, Stoller, Osetsky & Zinkle
J. Nucl. Mater. 351 (2006) 285

Dislocation interaction with SFTs in quenched Au

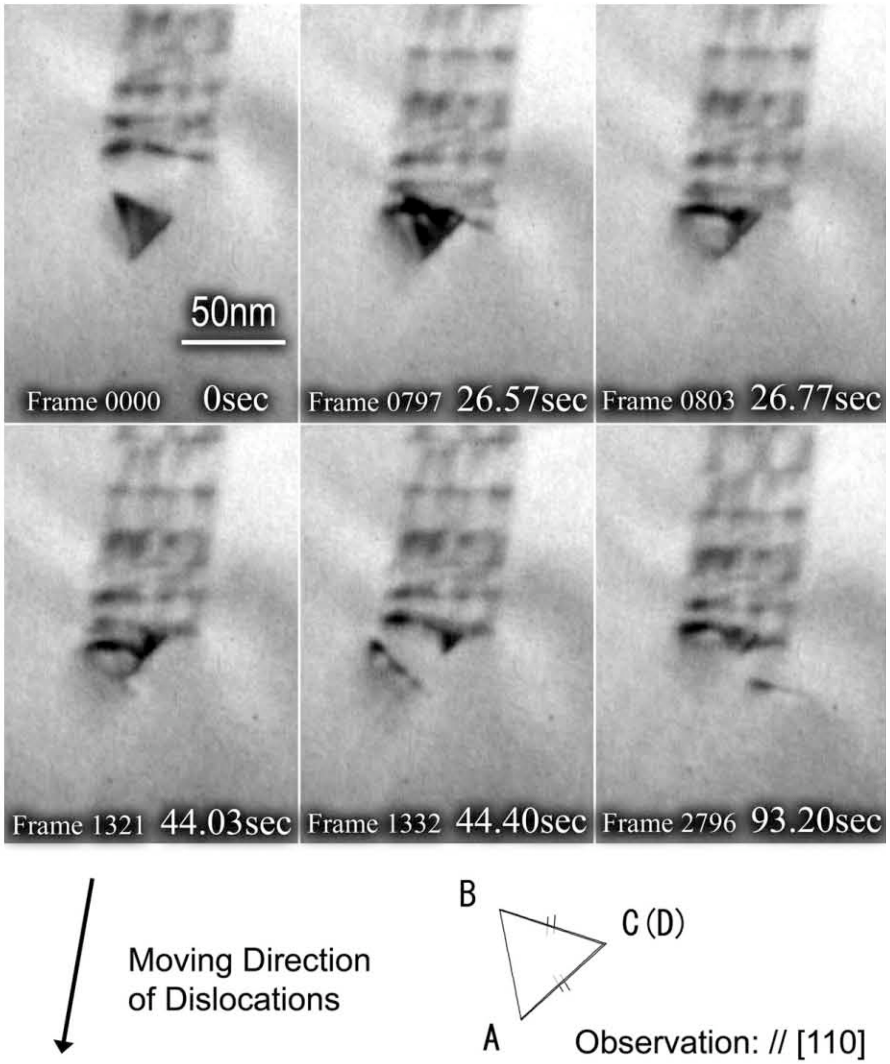

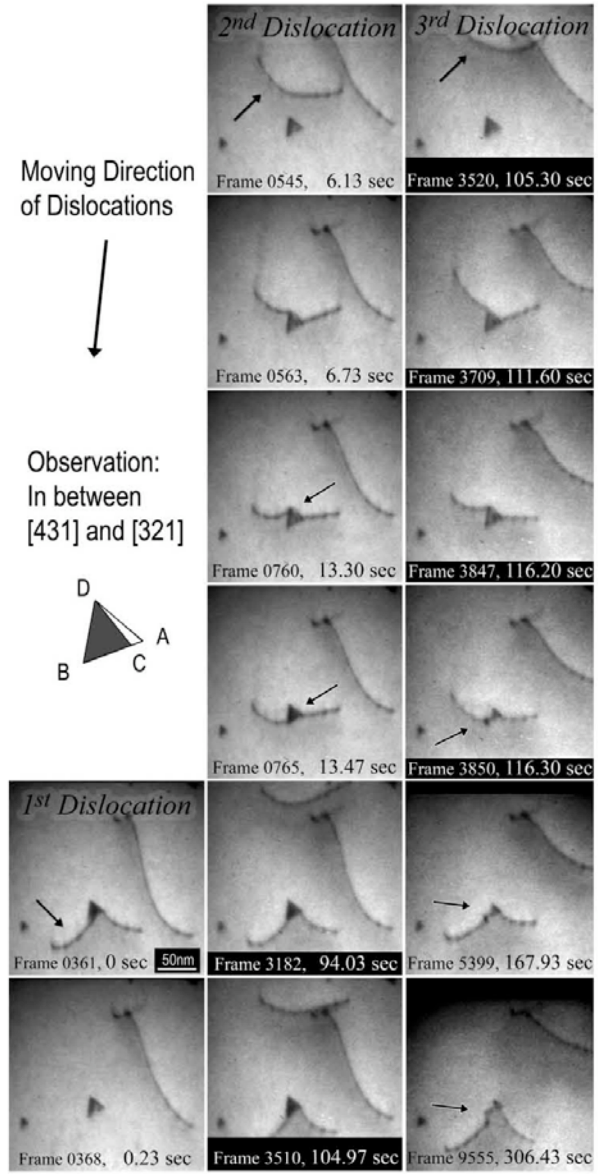

- **Type 3 interactions at room temperature (SFT apex remains); not observed at 100 K**

Matsukawa, Stoller, Osetsky & Zinkle
J. Nucl. Mater. 351 (2006) 285

Effect of temperature on edge dislocation interaction with 136 vacancy SFT in Cu

300 K

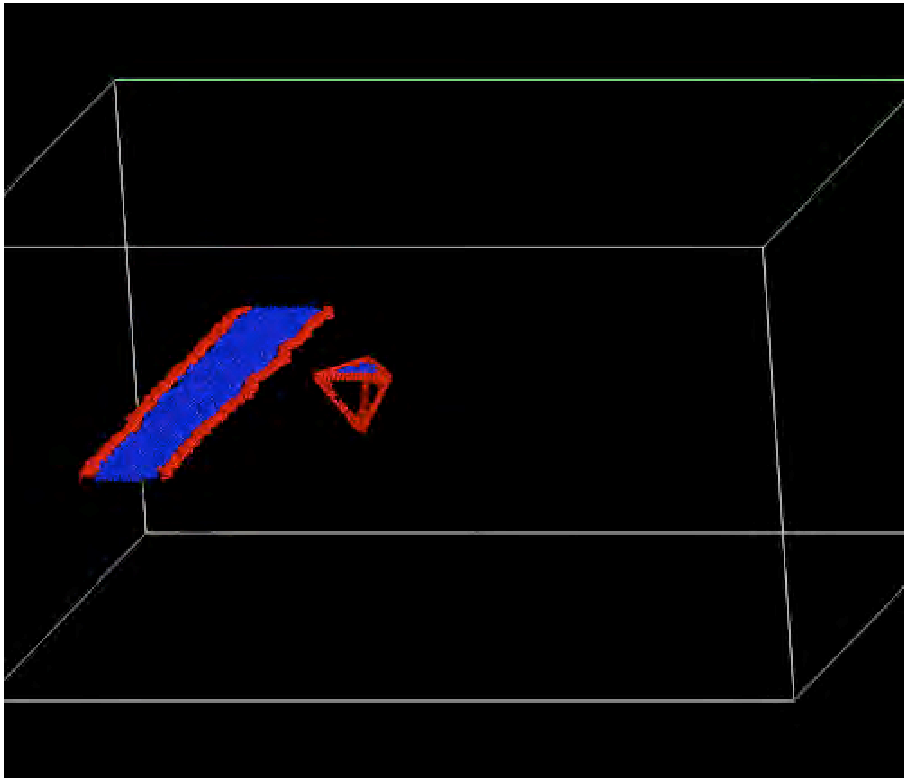

450 K

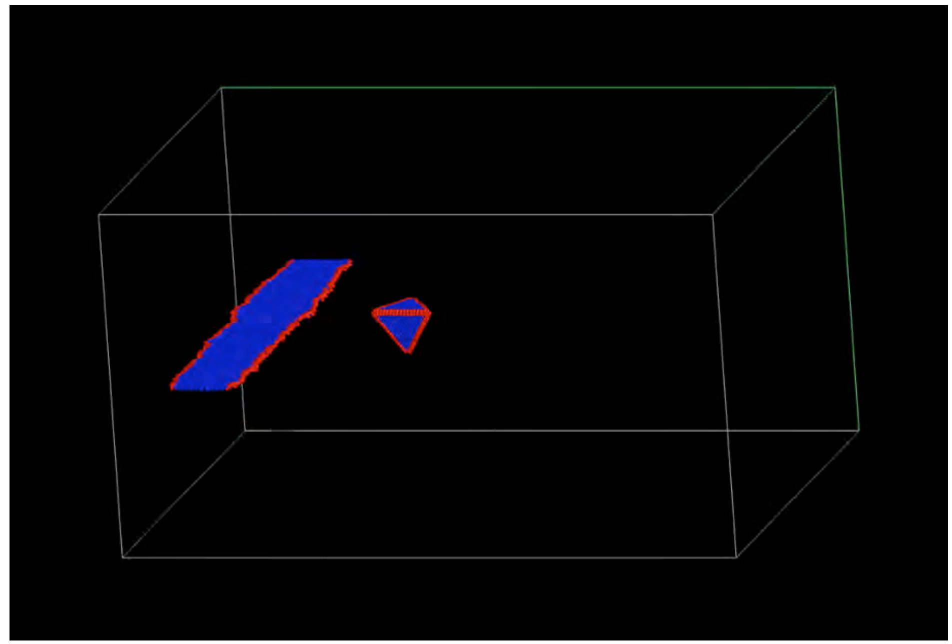

Defect cluster annihilation is enhanced at higher temperatures and slower strain rates (strain rate effect not shown)

- agrees with experimental results

Other parameters such as effect of obstacle size are also under investigation

Y.N. Osetsky

Interaction of a screw dislocation with 78-vacancy SFT and 91-intersitital cluster in Cu thin foil

300 K

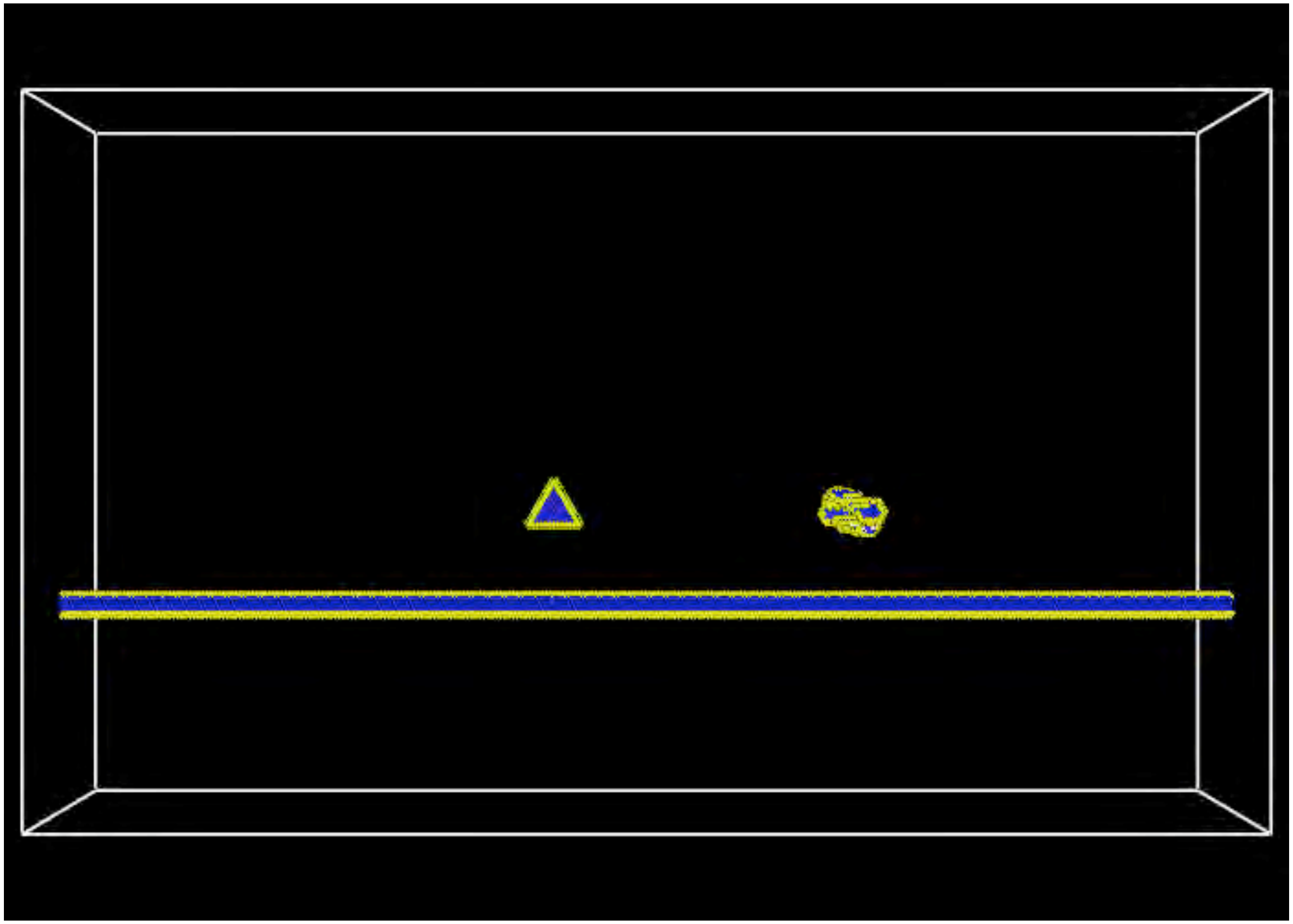

Cooperative effects may be important for annihilation of sessile defect clusters by gliding dislocations during deformation

Yu.N. Osetsky

Engineering and true stress-strain tensile curves for stainless steel before and after spallation irradiation at ~100˚C

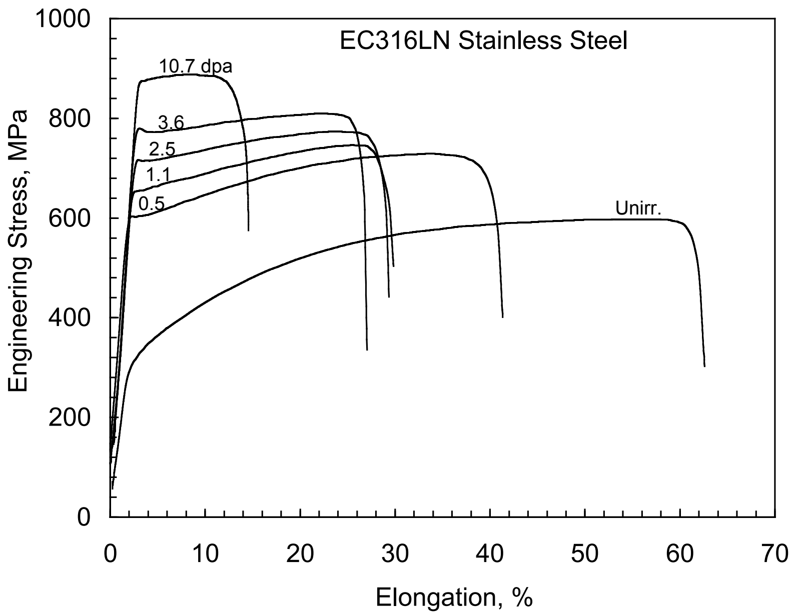

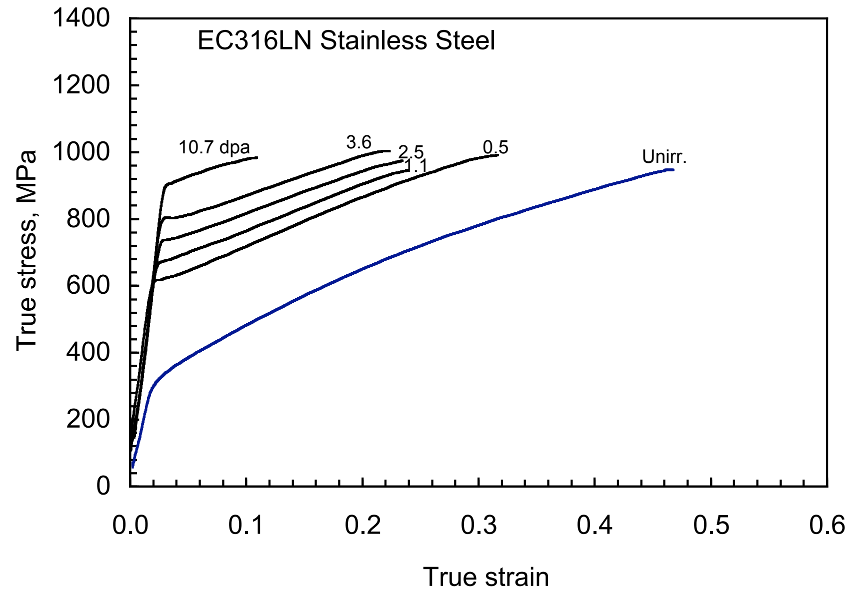

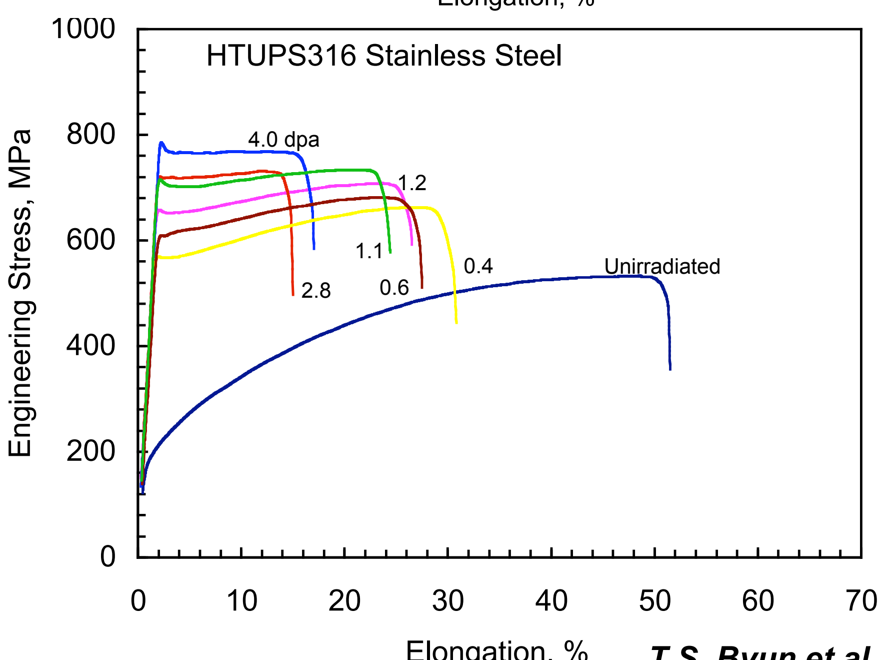

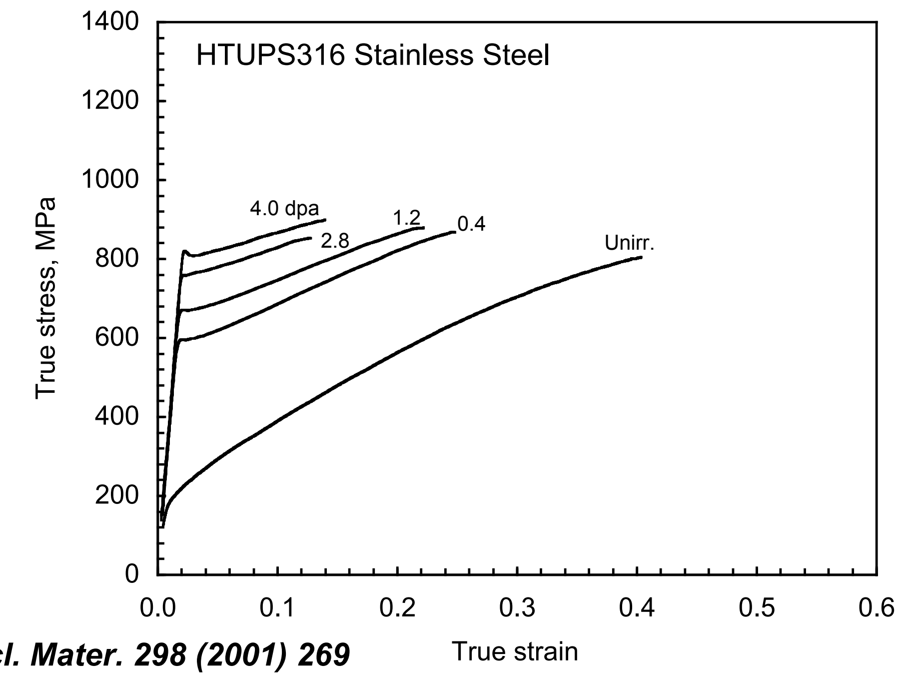

T.S. Byun et al., J. Nucl. Mater. 298 (2001) 269

Plastic Instability Stress (σ_{PI}) of BCC Metals

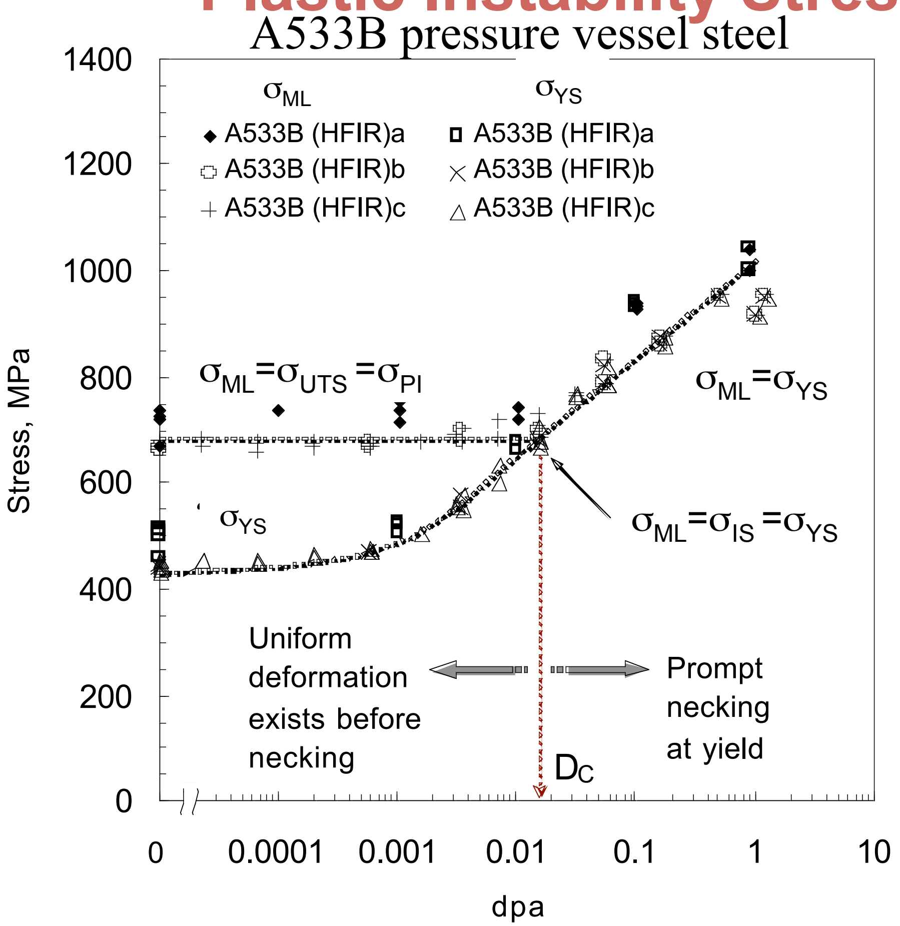

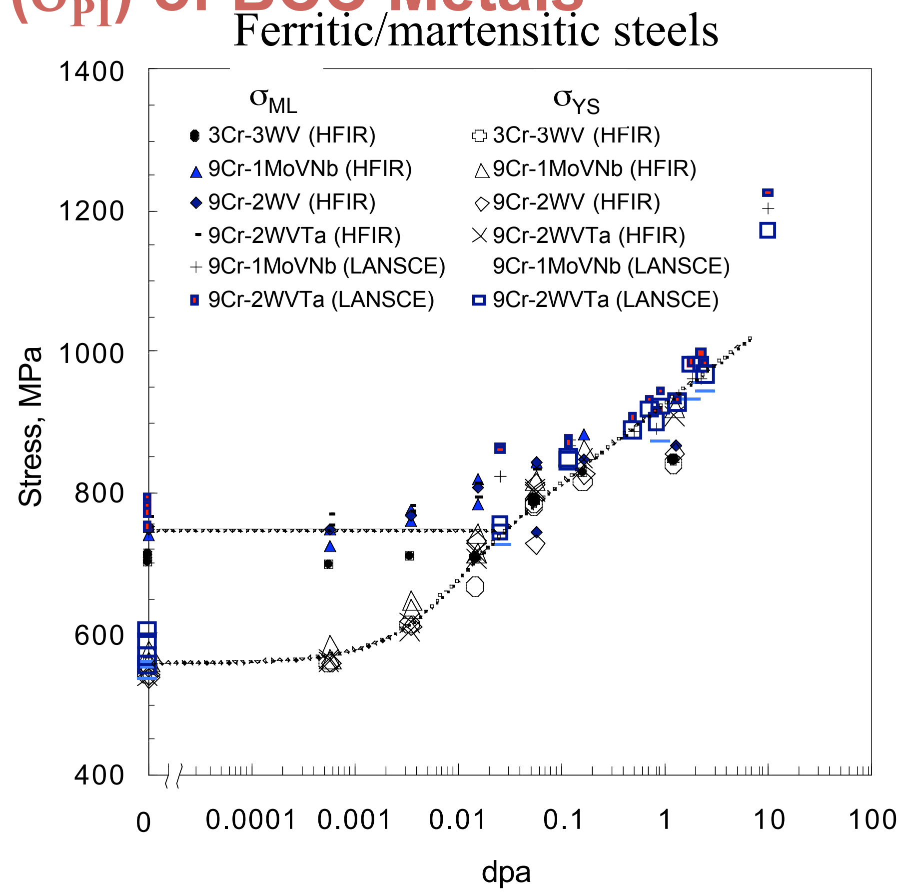

σ_{ML}=true stress at maximum load

- Plastic Instability Stress (σ_{PI}) = the true stress version of Ultimate Tensile Stress
- Plastic Instability Stress is independent of dose when yield stress < σ_{PI}.
- Yield stress can be > σ_{PI}, which is defined only when uniform deformation exists.
- σ_{PI} is considered to be a material constant, independent of initial cold-work or radiation-induced defect clusters

T.S. Byun & K. Farrell,
Acta Mater. 52 (2004) 1597

Deformation mechanisms in stainless steel

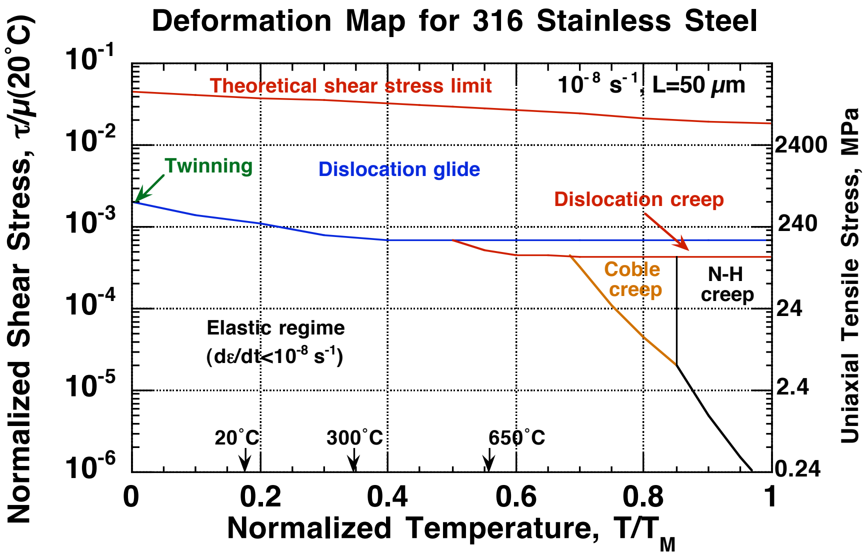

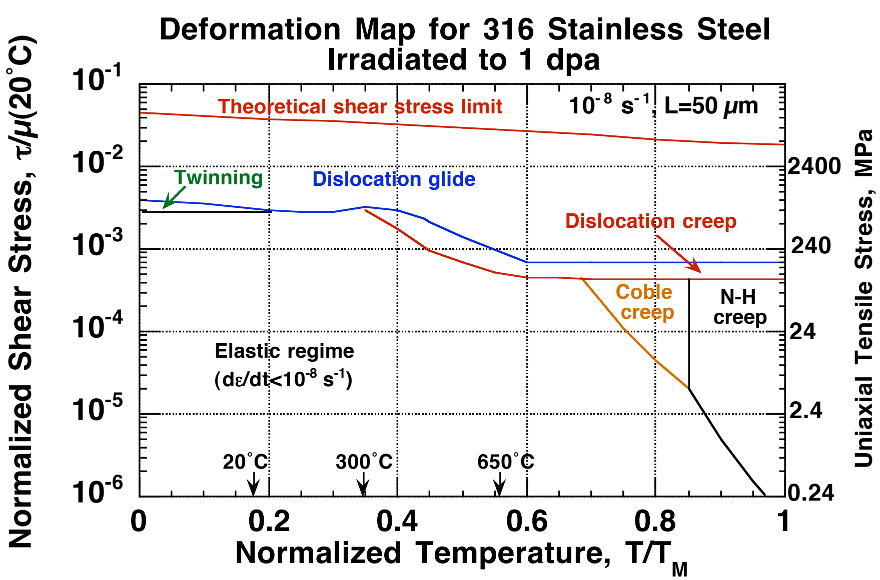

Zinkle and Lucas

Irradiation induces changes in controlling deformation mechanisms

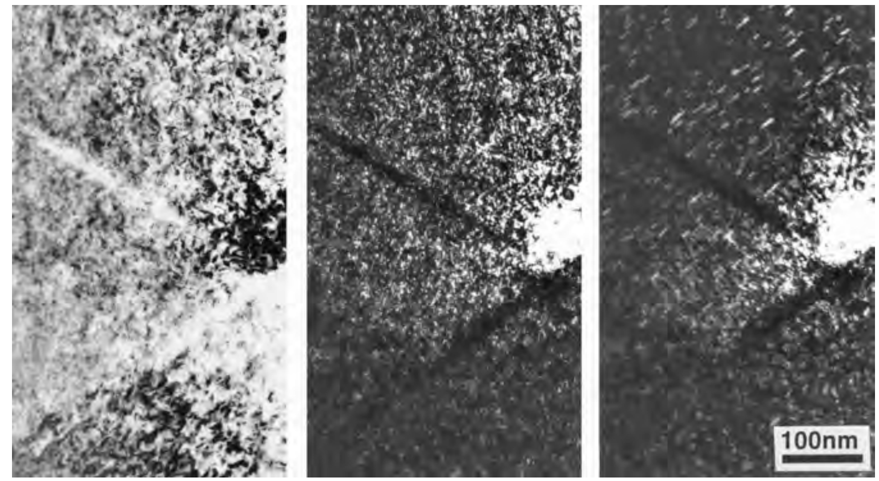

Channeling (Disln glide) occurs at higher temperatures (~300˚C)

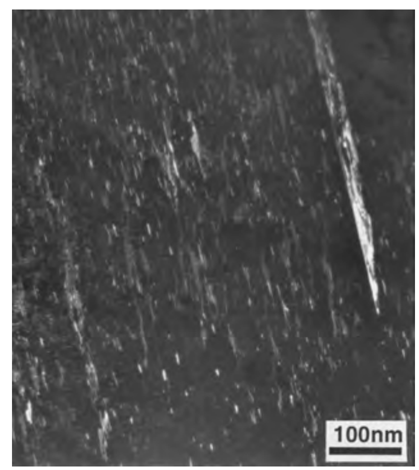

Twinning occurs at lower temperatures (<200˚C) and high strain rates

Hashimoto et al., J. Nucl. Mat. 283-287 (2000) 528

Structural materials involve compromise between strength and ductility

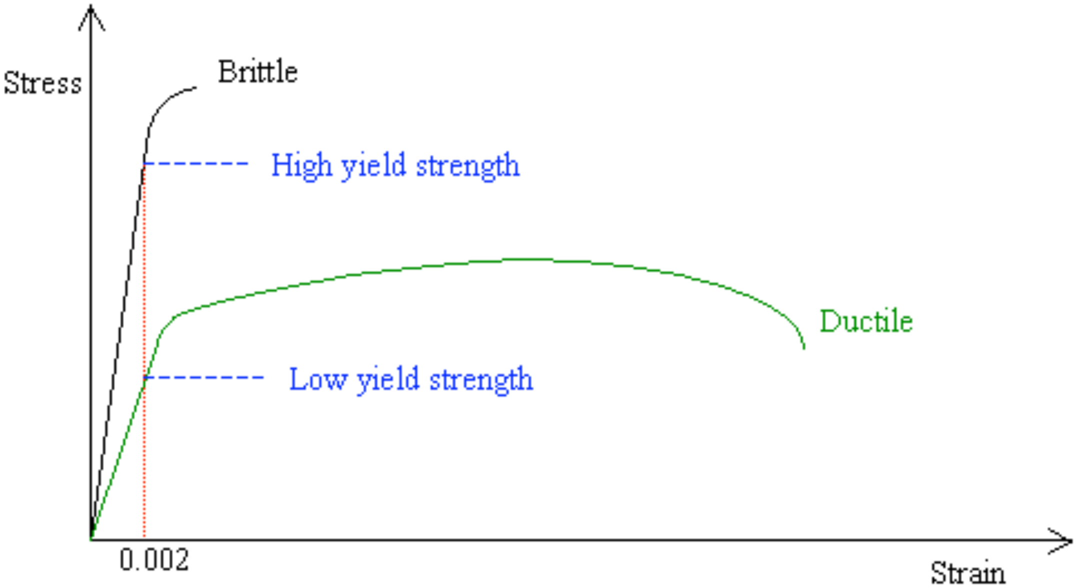

Schenectady Liberty ship, 1943

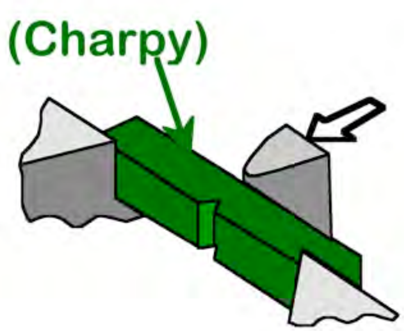

A simple measure of the resistance to brittle cleavage failure is the Charpy notched impact test

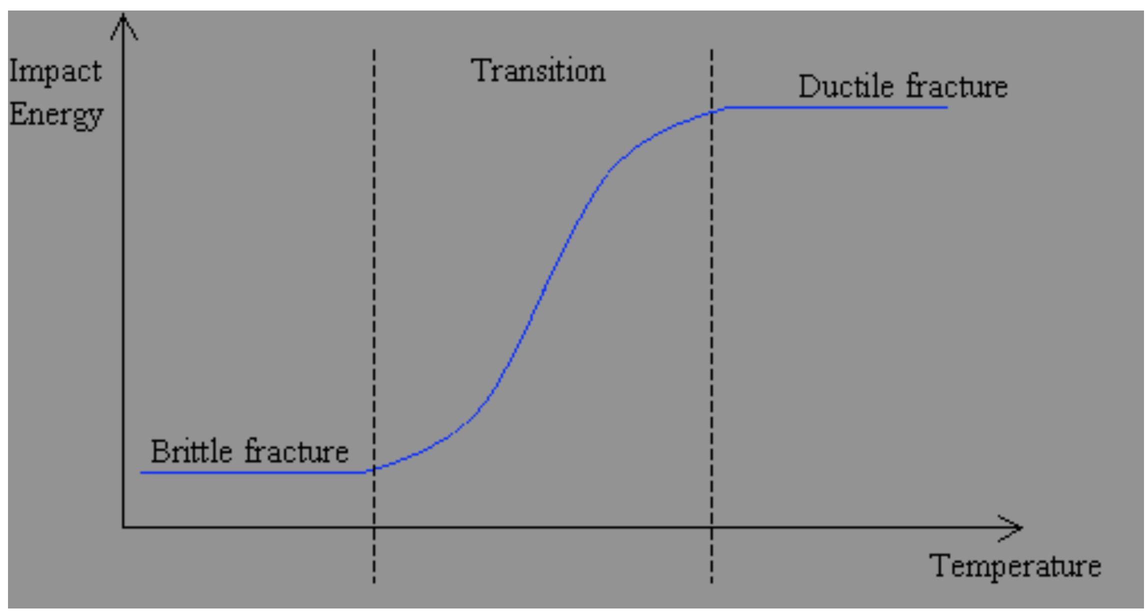

FLAWS ARE STRESS CONCENTRATORS!

- **Elliptical hole in a pl**

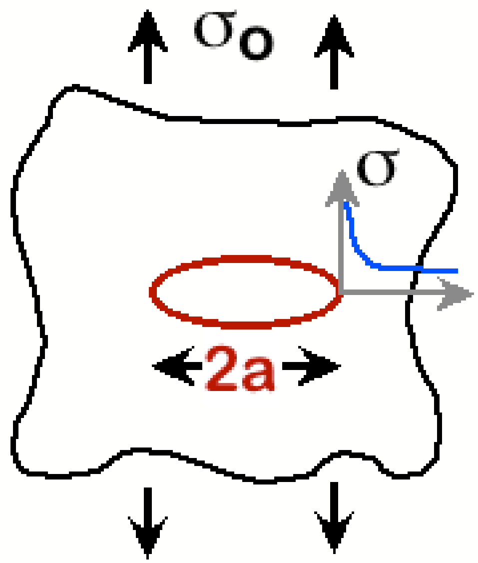

- **Stress distrib. in front of a hole:**

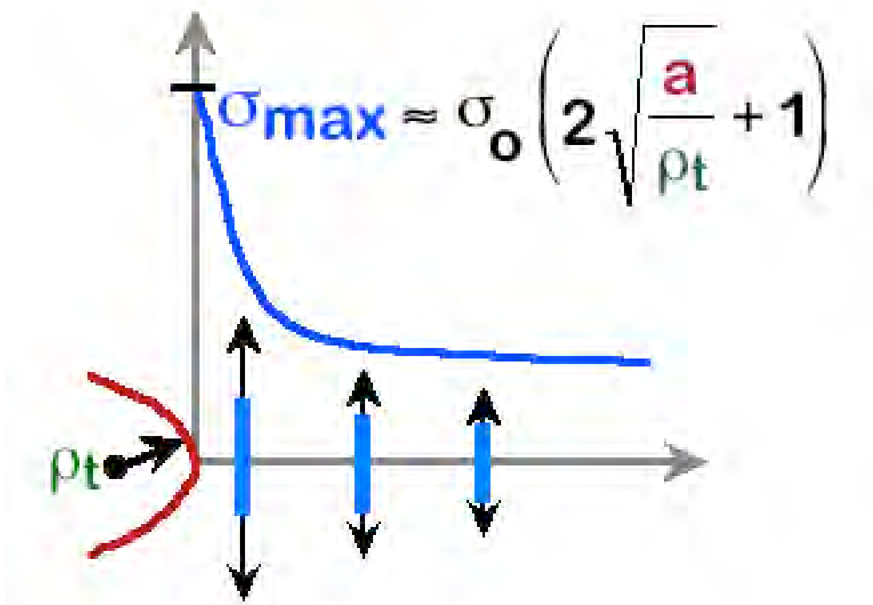

- **Stress conc. factor:** $K_t = \sigma_{max} / \sigma_o$

- **Large K_t promotes failure:**

J. Hayton

Irradiation of Austenitic Stainless Steel in Mixed Spectrum Reactors causes Pronounced Loss in Elongation and Significant Reduction in Fracture Toughness

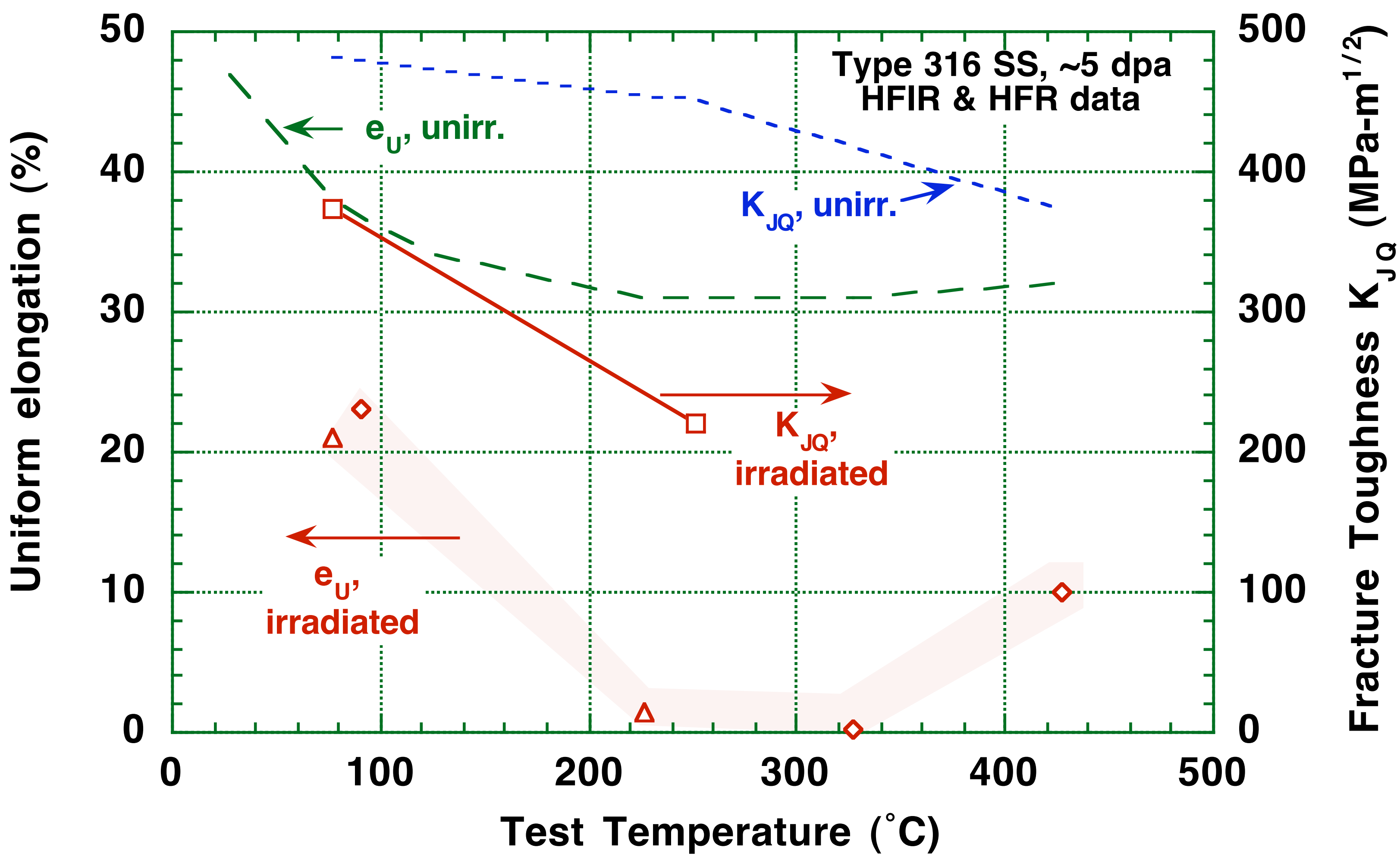

Fracture Toughness of BCC Structural Alloys

- Radiation hardening induces an increase in the ductile-brittle transition temperature (DBTT) in body-centered cubic metals
  - Two approaches to mitigate radiation embrittlement: reduce radiation hardening, or increase critical stress (σ*)

- **Ludwig-Davidenkov relation provides a rough estimation of embrittlement due to radiation hardening**

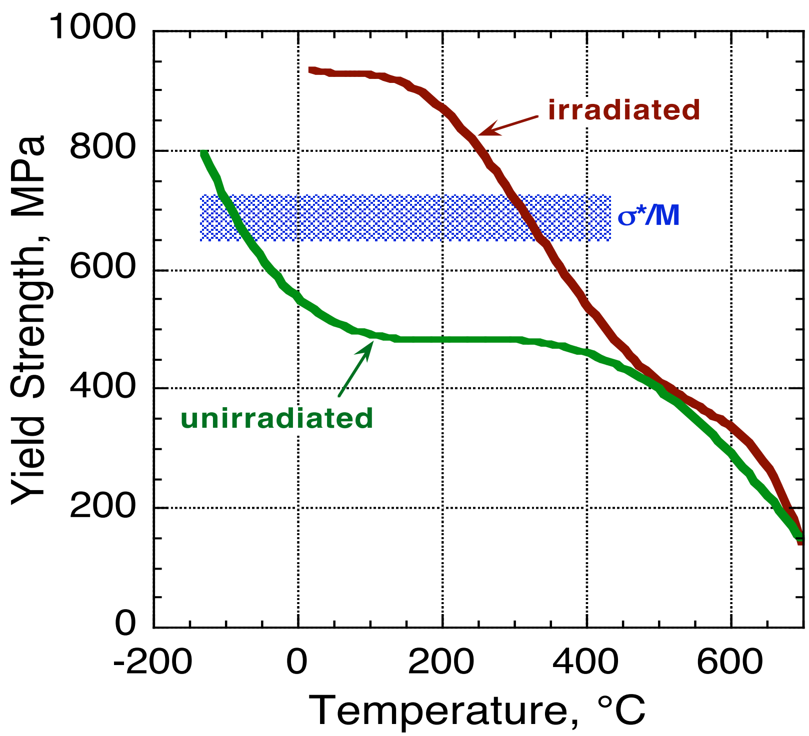

- **Significant improvements in resistance to low temperature radiation embrittlement can be achieved by selective alloying (e.g., reduced Cu in reactor pressure vessel steels)**

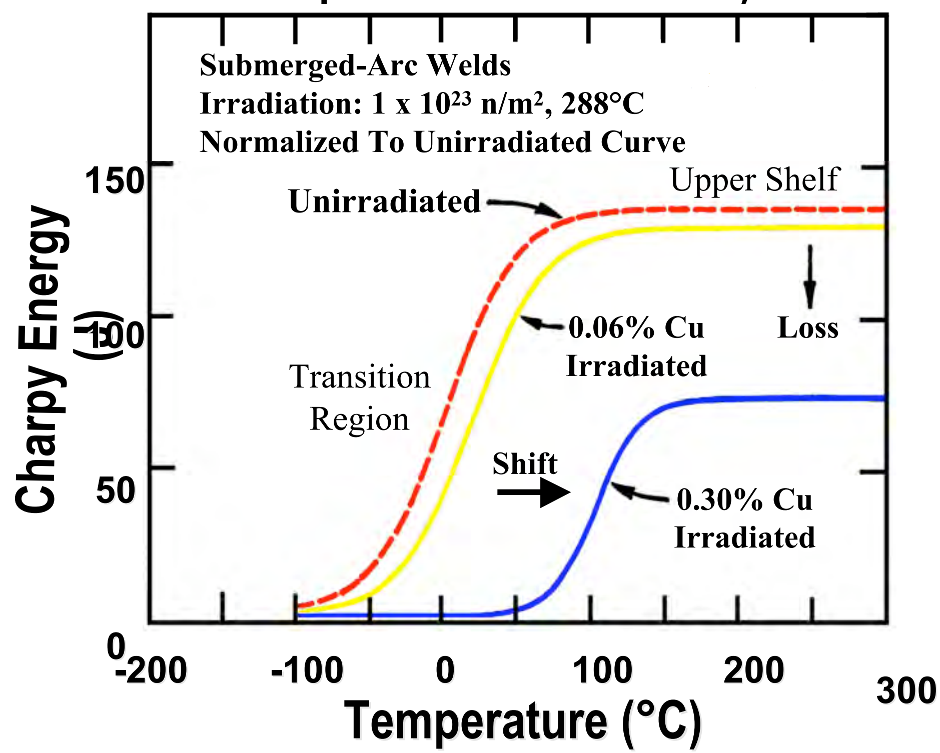

Need specifically designed materials to mitigate neutron radiation effects

TEM in-situ deformation studies can be used to provide insight on fundamental fracture processes

Atomic resolution imaging of ductile crack propagation (plane stress)

- **Macroscopic Mode I fracture is composed of coordinated Mode III shear displacements at the crack tip**

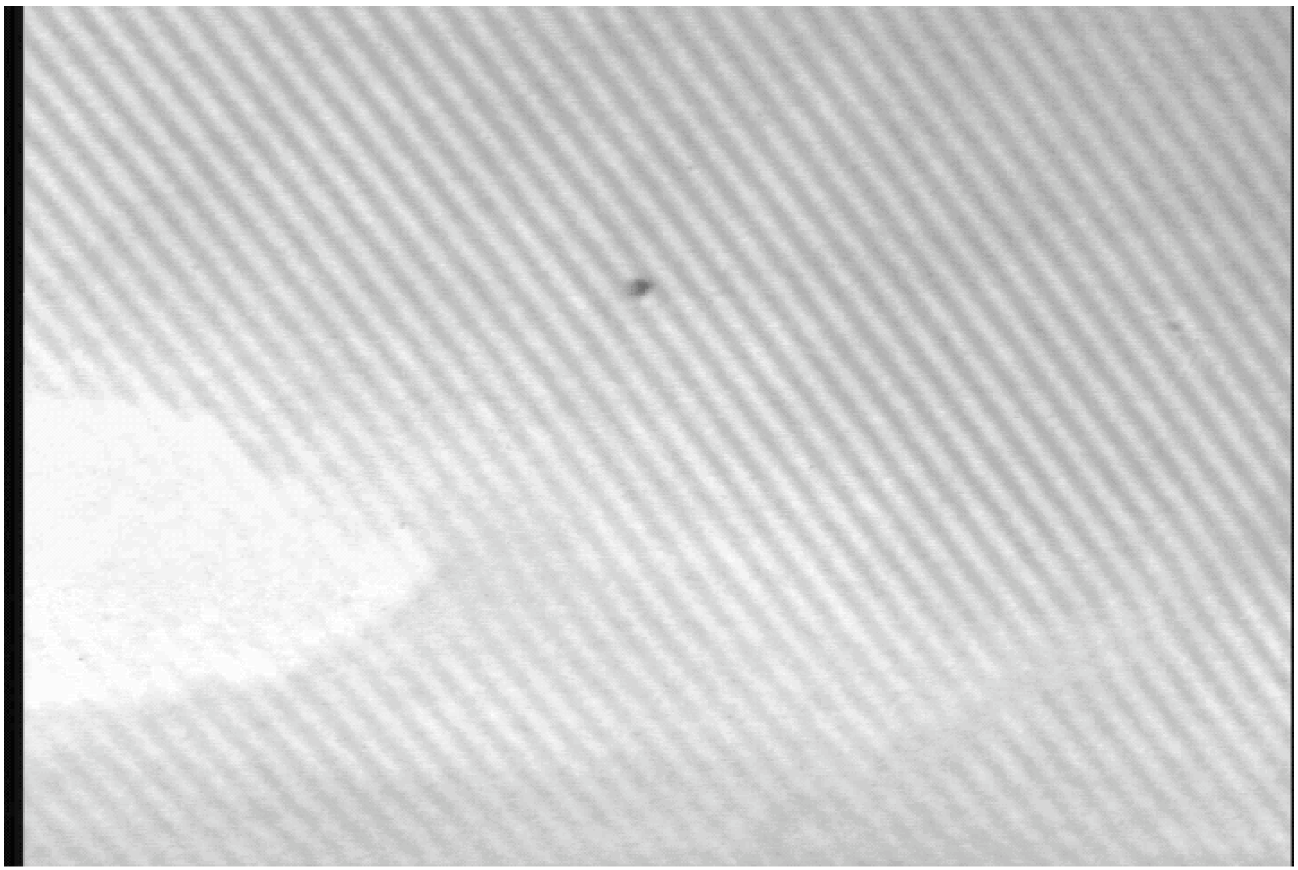

2 nm

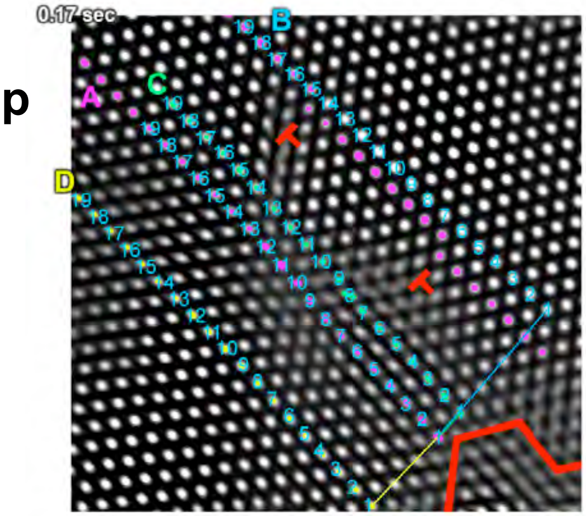

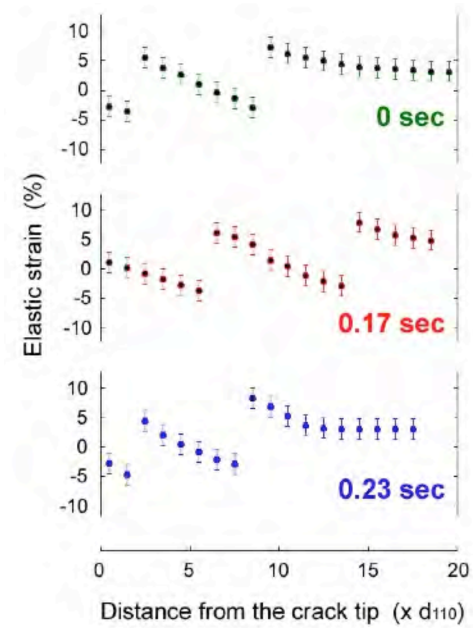

Y. Matsukawa, ORNL

The Operating Window for BCC metals can be Divided into Four Regimes (red values are relevant for Nb1Zr)

I, II: Low Temperature Radiation Embrittlement Regimes

- Fracture toughness (K_J) embrittlement: high radiation hardening causes low resistance to crack propagation (occurs when S_U>500-700 MPa)
  - Regimes which cause K_J<30 MPa-m$^{1/2}$ should be avoided (T_{irr}< ~600 K ?)
- Loss of ductility: localized plastic deformation requires use of more conservative engineering design rules for primary+secondary stress (S_e)

$$S_e = \begin{cases} \frac{1}{3} S_u & \varepsilon_U < 0.02 \\ \frac{1}{3}\left[S_u + \frac{E(\varepsilon_U - 0.02)}{8}\right] & \varepsilon_U > 0.02 \end{cases}$$

(T_{irr}< ~900-1270 K)

where ε_U is uniform elongation, S_U is ultimate tensile strength, E is elastic modulus (additional design rules also need to be considered)

III: Ductile Yield and Ultimate Tensile Strength Regime (e_U>0.02)

- Sets allowable stress at intermediate temperature (very small regime for Nb-1Zr)

IV: High Temperature Thermal Creep Regime (T>~1050 K)

- Deformation limit depends on engineering application (common metrics are 1% deformation and complete rupture)

Stress-Temperature Design Window for Nb-1Zr

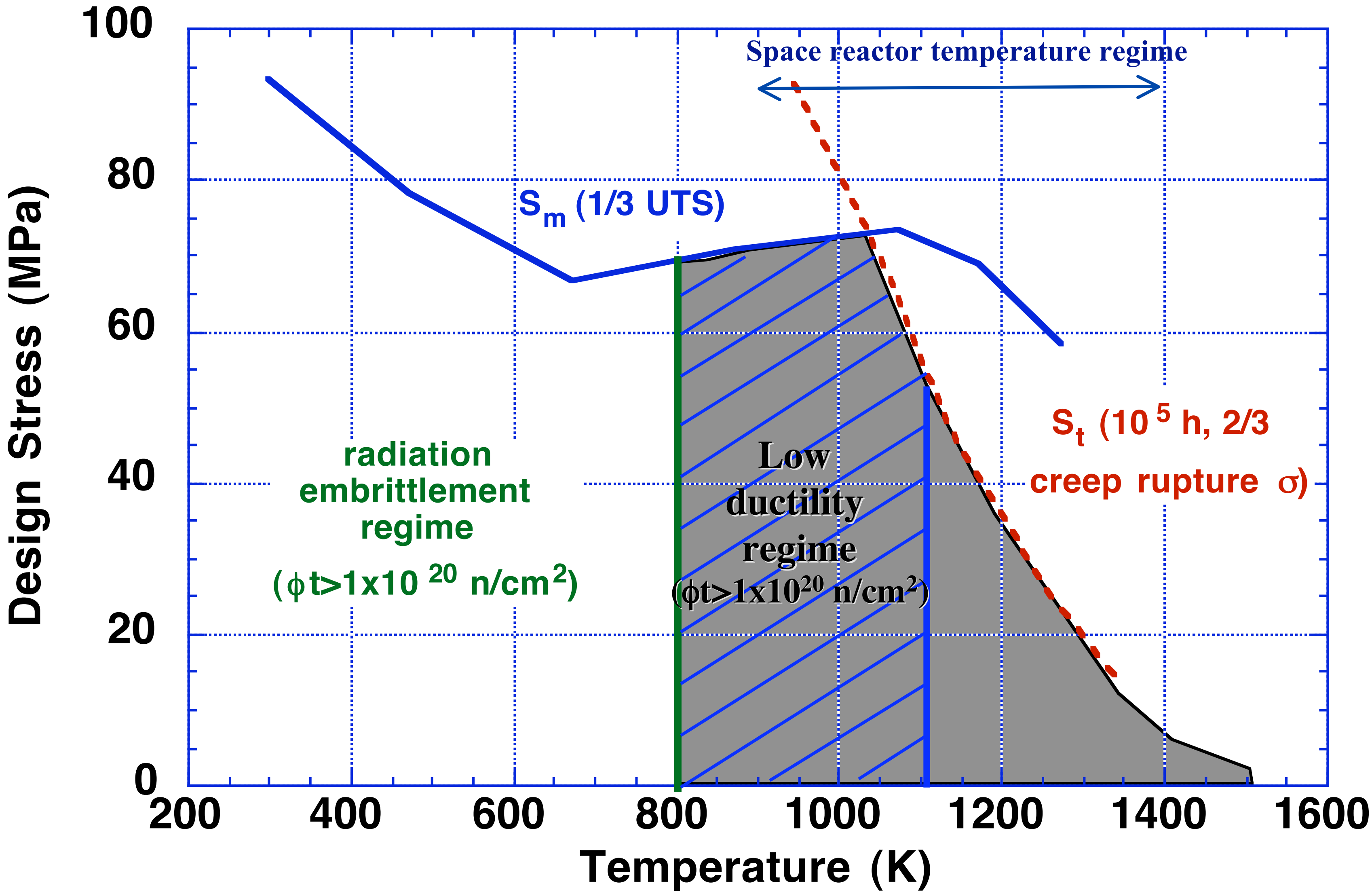

Conventional structural materials are capable of operation within ~300°C temperature window

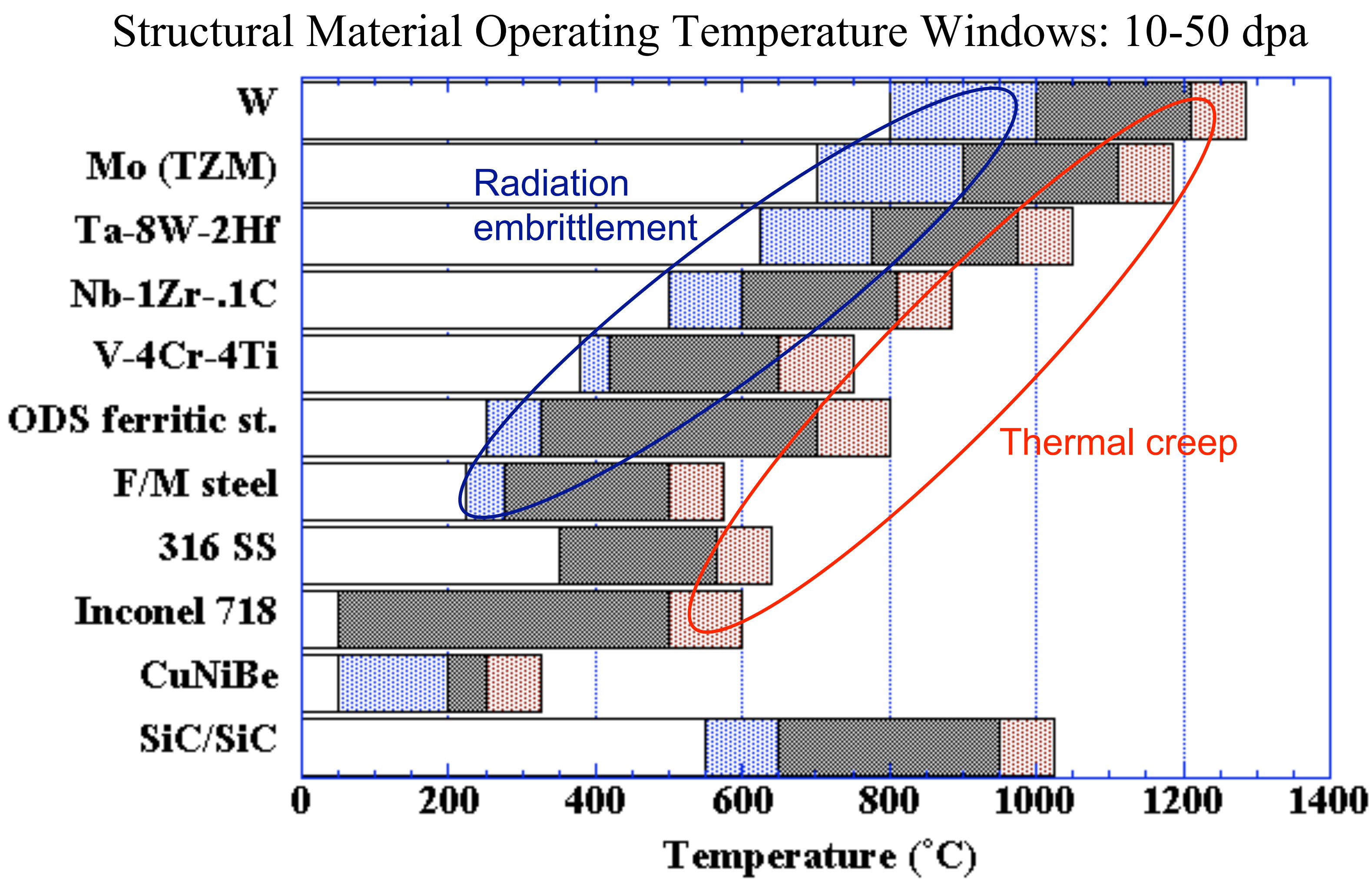

$\eta_{Carnot}=1-T_{reject}/T_{high}$

Low temperature radiation embrittlement typically occurs for damage levels ~0.1 dpa (0.01 MW-yr/m^2)

Zinkle and Ghoniem, Fusion Engr. Des. 51-52 *(2000) 55*

Consideration of Chemical Compatibility can Result in Dramatic Reductions in Temperature Window

Estimated Structural Material Operating Temperature Windows:
Moderately-pure He coolant, 10-50 dpa

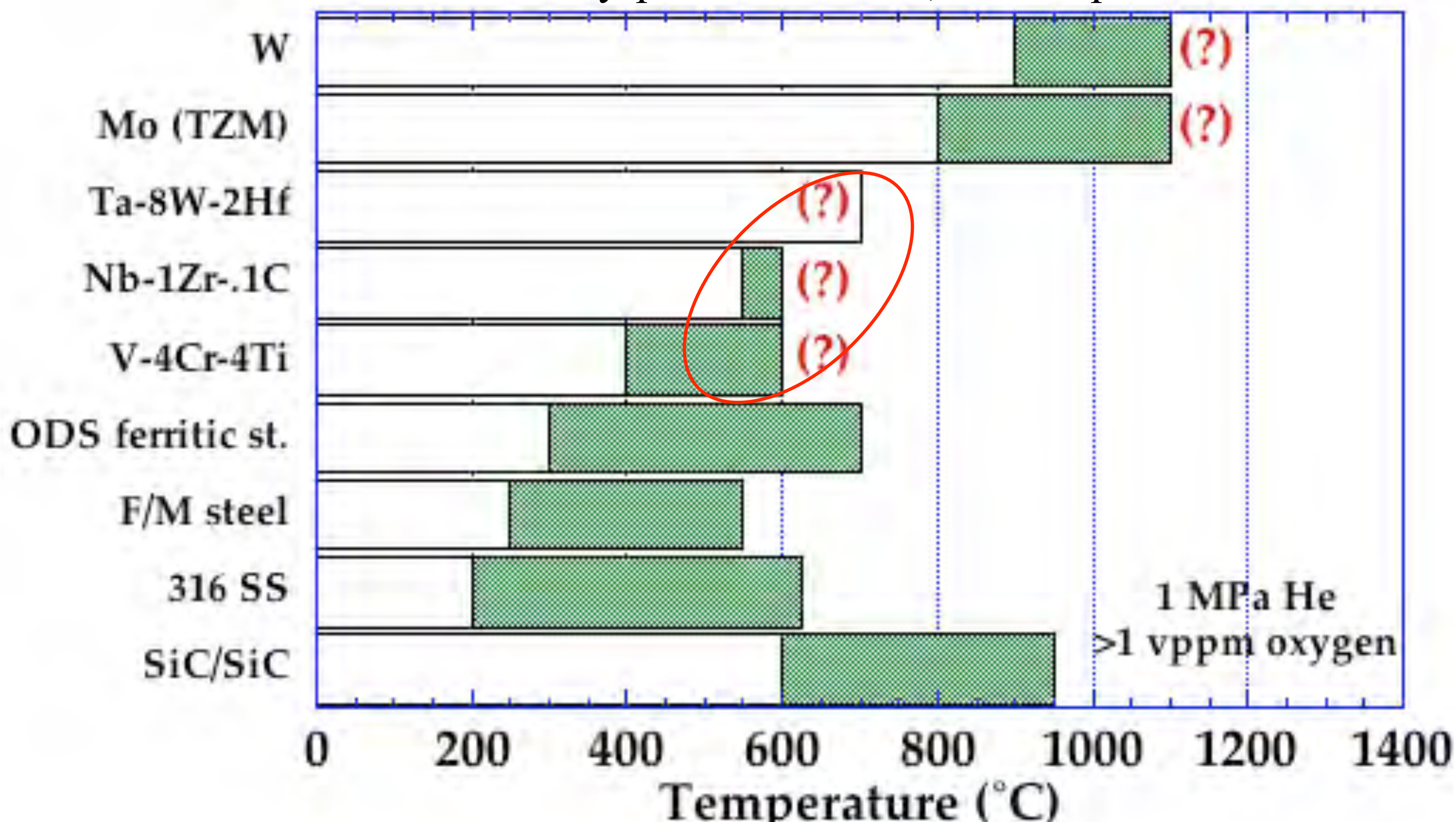

Group V refractory alloys are particularly sensitive to embrittlement from O,C,N solute

Zinkle and Ghoniem, Fusion Engr. Des. 51-52 *(2000) 55*

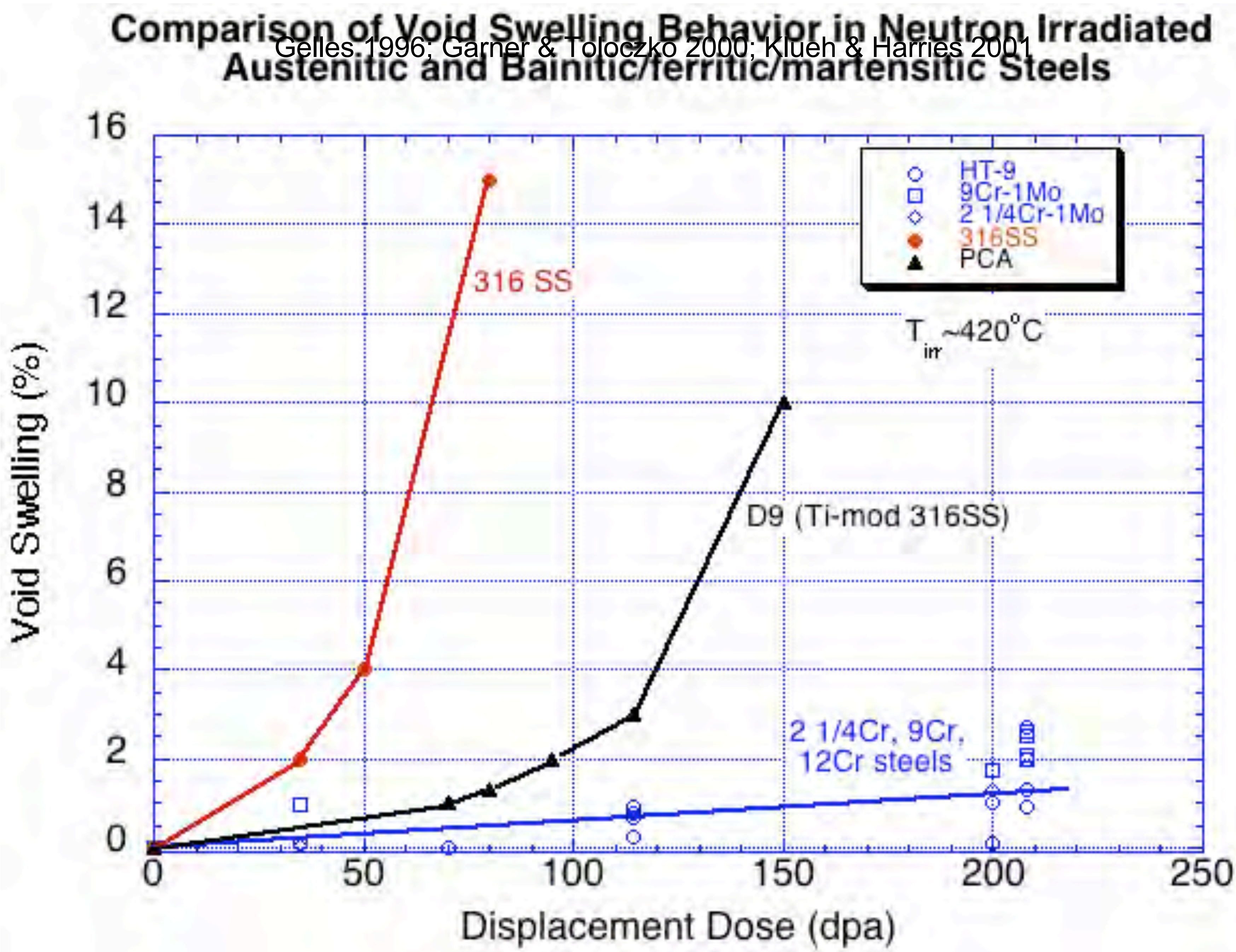
Comparison of Void Swelling Behavior in Neutron Irradiated Austenitic and Bainitic/ferritic/martensitic Steels
Gelles 1996; Garner & Toloczko 2000; Klueh & Harries 2001
Void Swelling (%)
Displacement Dose (dpa)
HT-9
9Cr-1Mo
2 1/4Cr-1Mo
316SS
PCA
316 SS
T irr ~420°C
D9 (Ti-mod 316SS)
2 1/4Cr, 9Cr, 12Cr steels
0
2
4
6
8
10
12
14
16
0
50
100
150
200
250

Swelling Resistant Alloys can be developed by Controlling the He Cavity Trapping at Precipitates

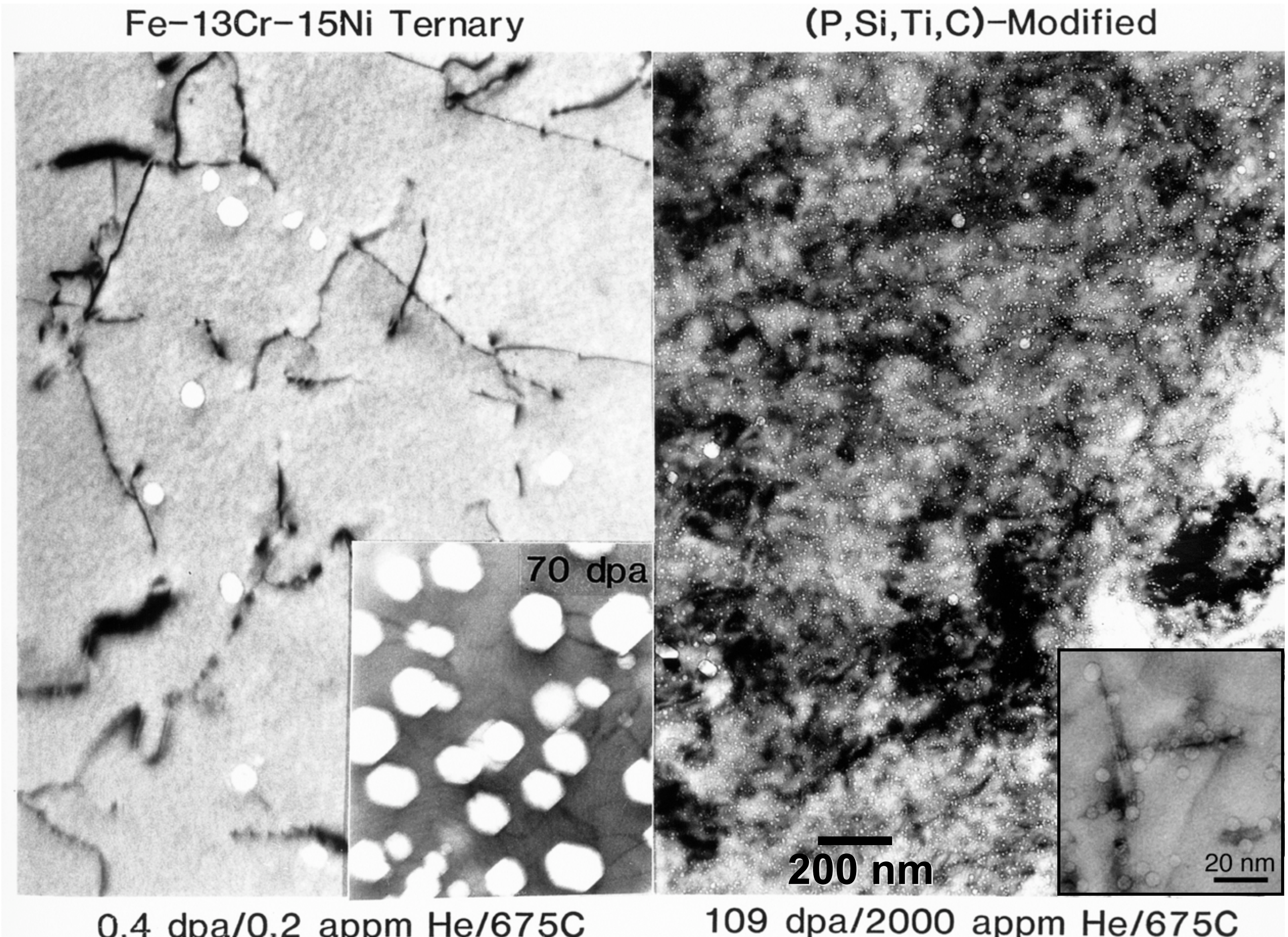

Mansur & Lee
J. Nucl. Mat.
<u>179-181</u>
(1991) 105

These nanoscale precipitates also typically provide improved thermal creep strength

Candidate alloys: nanostructured ferritic alloys (NFA)

- **A high number density of nanoclusters dramatically improve the high temperature strength, including creep performance, and tolerance to neutron irradiation damage of iron alloys**

3-DAP of 12YWT

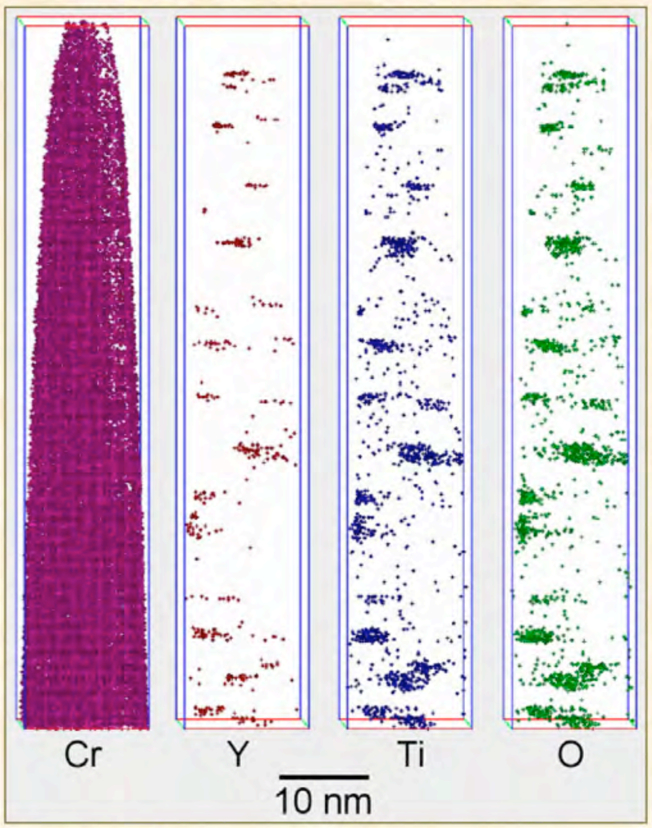

r_g = 2.0 nm N = 1.1×10^{24} m^{-3}

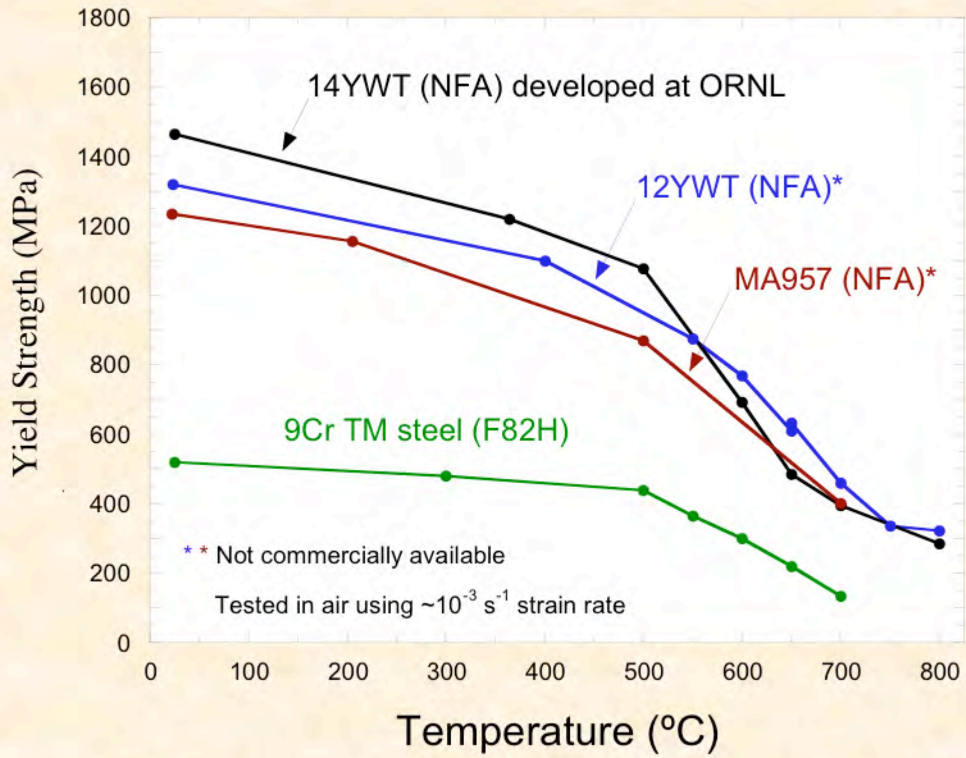

- *The creep rate of NFA is ~6 orders of magnitude lower than conventional steels at 600-900ºC*

NFA Have Remarkable Radiation Damage Tolerance

- **MA957 following neutron irradiation to ~9 dpa at 500°C and implantation of up to ~380 appm He**

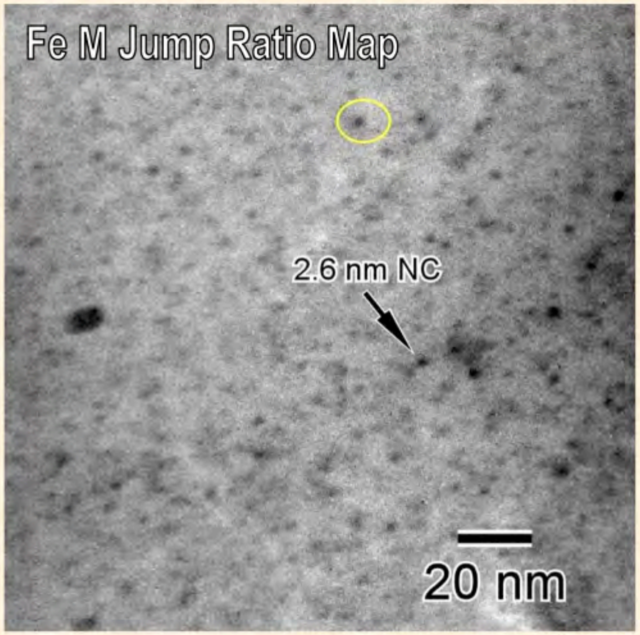

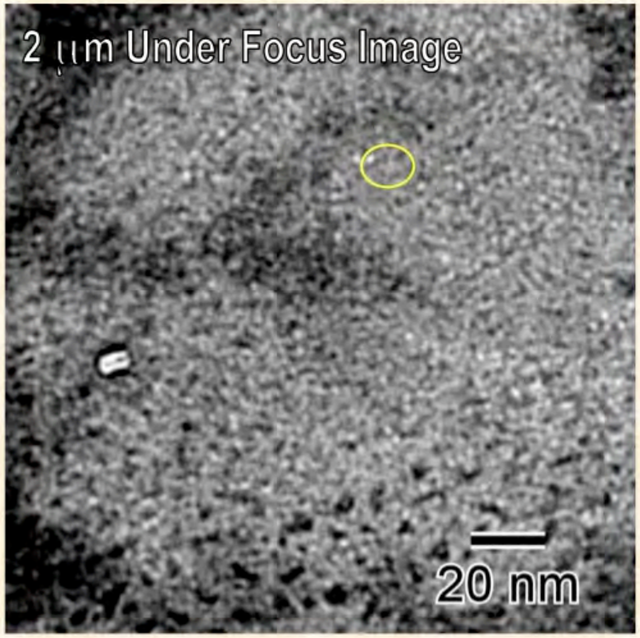

- **Irradiation effects database is not as mature as other alloys (ion irradiation data to ~100 dpa suggests good irradiation stability and tolerance)**
- **Joining and industrial scale up must be demonstrated**
- **Alloy is not ASME code qualified**

The formation of nanoclusters becomes possible in the presence of vacancies

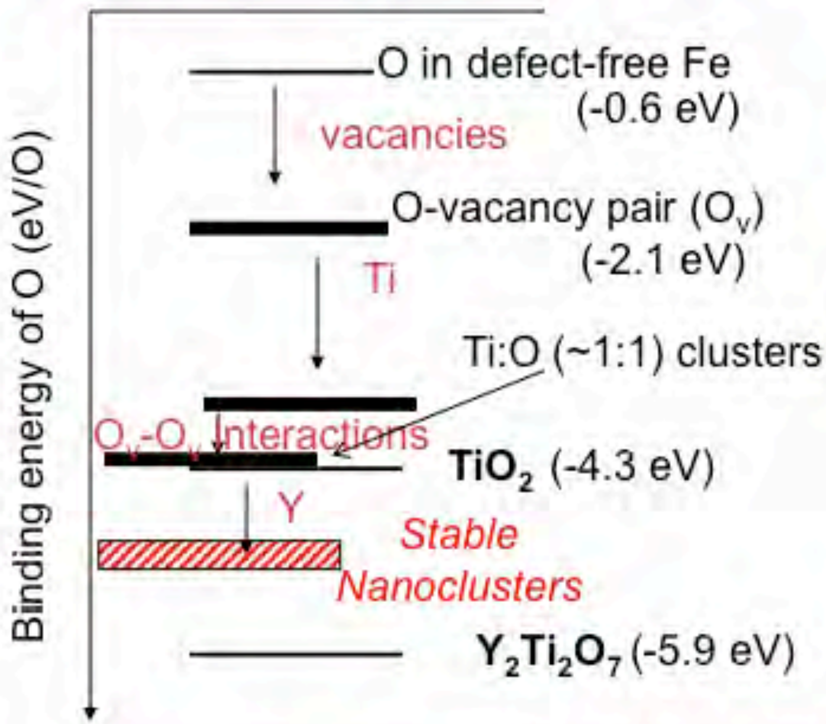

- **Excessive vacancies are *assumed* to exist during mechanical alloying → high solubility of O-vacancy pair**
- **Nanoclusters are modeled as coherent with underlying bcc lattice**
- **Without Y → TiO_2 oxide phase**
- **Too much Y → $Y_2Ti_2O_7$ oxide phase**

Y is pivotal; however, the amount of Y needs to be controlled (Ti >> Y) to avoid the precipitation of $Y_2Ti_2O_7$ oxide phase.

The nanocluster is in a defective, new alloying state

C. L. Fu, M. Krcmar, G. S. Painter, X.-Q. Chen, *Phys. Rev. Lett.* 99, 225502 (2007)

Conceptual view of nanoclusters

precipitate

2 nm

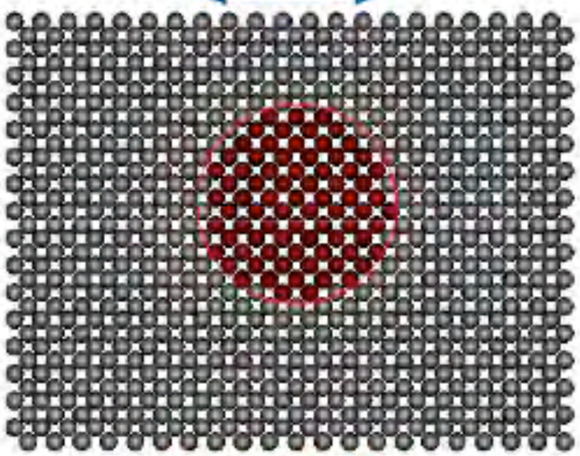

nanocluster

2 nm

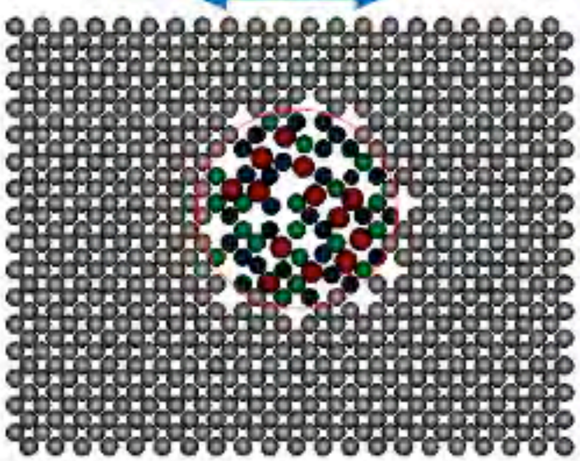

- The structure of the nanoclusters has not been well-established but presumed to be (*coherent*) bcc.
- *high* vacancy concentrations in the form of O-vacancy pairs (vacancies verified by PAC)
- *high* O-vacancy pair solubility in the matrix
- diffuse interface; enriched in Ti, O and Y

Diameter: 2 - 4 nm

Number density: ~10^{24} m^{-3}

Composition: ~ 10 %Y, 40 %Ti, 40% O

What's next?

- Factors controlling size and growth
- More precise structural characterizations: coherence, interface and chemical profile
- Deformation & microstructure stability
- Other metallic systems

C.L. Fu et al.

Conclusions

- Integrated computational modeling and experimental studies can accelerate the development and qualification of high performance materials for nuclear energy systems
- Ongoing radiation materials science research programs span from fundamental studies to targeted alloy development
- Common research themes include:
  - Investigation of fundamental phenomena responsible for materials property changes (degradation) due to irradiation
  - Development of radiation resistant high-performance structural material systems